MECHANISMS OF LEUCYL-TRNA SYNTHETASE DEPENDENT GROUP I INTRON SPLICING

BY

ZHONGYI LI

DISSERTATION

Submitted in partial fulfillment of the requirements
for the degree of Doctor of Philosophy in Biochemistry
in the Graduate College of the
University of Illinois at Urbana-Champaign, 2016

Urbana, Illinois

Doctoral Committee:

Professor Susan A. Martinis, Chair
Associate Professor Raven H. Huang
Assistant Professor Hong Jin
Assistant Professor Auinash Kalsotra

Abstract

Leucyl-tRNA synthetase (LeuRS) plays dual roles within the yeast mitochondria. In addition to protein synthesis, it is also essential to RNA splicing of critical respiratory genes. The LeuRS collaborates with a maturase to excise the bI4 and aI4α introns from the *cob* and *cox1α* genes respectively. The LeuRS-based suppressor mutations have been isolated within the amino acid editing CP1 domain and restore native RNA splicing activity in the presence of an inactive maturase. Mutational analysis of these sites and the regions that surround them demonstrated that certain substitutions can also inactivate LeuRS-dependent splicing activity under *in vivo* and *in vitro* conditions. Binding measurements suggest that these suppressor sites are important in maintaining interaction between LeuRS and the group I intron RNA. Thus, CP1 domain binds specifically to the bI4 and aI4α intron to promote RNA splicing.

In addition to LeuRS from yeast mitochondria (*ym*LeuRS), diverse LeuRSs from varied origins such as *M. tuberculosis* and human mitochondria complement the *ym*LeuRS activities. Similarly, wild-type *E. coli* LeuRS (*Ec*LeuRS) complemented a *ym*LeuRS null strain. Interestingly, at reduced levels of *Ec*LeuRS expression in yeast mitochondria, the heterologous synthetase supported protein synthesis, but not intron splicing. Thus, it is a weak splicing suppressor. Surprisingly, a gain of splicing

activity was exhibited by positive charge substitutions at the Ala293 position, suggesting that this Ala293 can be adapted for alternative activities.

Preliminary footprinting data suggest that LeuRS binds to the P4-P6 core region of the bI4 intron that is cognate to LeuRS. The RNA duplex mimics of the P6 helix were designed and it was shown that LeuRS promotes their annealing in an ATP-independent manner. Domain analysis of LeuRS shows that the C-terminal domain is critical to the RNA annealing activity. Yeast mitochondrial $tRNA^{Leu}$ (*ym*$tRNA^{Leu}$) competitively inhibit annealing. Also, an *ym*$tRNA^{Leu}$ variable-stem-like region was identified on the P6 stem that is important for LeuRS-dependent annealing. These data support that the annealing and tRNA variable arm binding sites overlap on the C-terminal domain of LeuRS. It was shown that the overhang location and length of the duplexes are important features that LeuRS recognizes. It was hypothesized that LeuRS plays a key role in remodeling specific group I intron ribozymes so that they can productively self-splice.

Acknowledgments

First of all, I would like to thank Dr. Susan Martinis for being a wise and trusted advisor. She introduced me to insightful research projects, and has always been a source of guidance, encouragement and support along the way. She has not only taught me scientific critical thinking methods, but also passed me invaluable experience on presentation slides preparation, speech delivery, paper construction, and manners in the academic community. In addition, I am grateful that she gives me freedom to explore my interest in statistics after finishing the research projects. She has always been and will continue to be a role model for me.

I would also like to thank all the Martinis group members for a friendly and learning atmosphere. I benefit a lot from enlightening discussions with all of them. I am particularly grateful to Dr. Michal Boniecki, Dr. Margaret Saks and Dr. Hanchao Zhao. They taught me experimental techniques and are always ready to answer questions and to help with troubleshooting. They along with Aditi Banerjee, Dr. Kiran Poruri in our group and Dillon Cogan from Dr. Satish Nair Group provided a lot of essential reagents for my research, which saved me a huge amount of time. For Doc. Saks, I also appreciate her time in polishing my resume. Finally, I would like to thank Aditi Banerjee for being my closest friend in the lab, with whom I share my happiness and frustration.

I also would like to express thanks to my committee members: Dr. Raven Huang, Dr. Hong Jin and Dr. Auinash Kalsotra. They have given me many advices on experimental techniques and how to become a successful scientist. I appreciate their precious time and sharing.

In addition, I would like to thank my friends in Champaign-Urbana: Bo Liu, Chang Bao, Chang Sun, Xin Ye, Ziqiao Ding, Xinying Zong, Yue Hao. Time spent with them is always joyful, and they have lent helping hands so many times during the time I live alone.

I would like to express my love and thanks to my fiancé Pengfei Yu. His love is always hopeful, endures through every circumstances, and gives me courage and strength to overcome difficulties in research and coursework. Reserved in the end, I would like to thank my parents. Without their support, it is hard to imagine that I can accomplish this Ph.D. degree.

Table of Contents

Abbreviations

AA-AMP	aminoacyl adenylate
AA-tRNA	aminoacyl-tRNA
AARS	aminoacyl-tRNA synthetase
ABD	anticodon binding domain
AMP	adenosine 5´-monophosphate
ArgRS	arginyl-tRNA synthetase
AspRS	aspartyl-tRNA synthetase
ArgRS	arginyl-tRNA synthetase
ATP	adenosine 5´-triphosphate
A76	adenosine at position 76 of tRNA
BME	β-mercaptoethanol
CP1	connective polypeptide 1
CTD	C-terminal domain
CysRS	cysteinyl-tRNA synthetase
D-arm	dihydrouridine arm
DHU	dihydrouridine
DNA	deoxyribonucleic acid
dNTP	deoxynucleotide triphosphate
DTT	dithiothreitol
E. coli	*Escherichia coli*
EDTA	ethylenediaminetetraacetic acid
EF-Tu	elongation factor Tu
GDP	guanosine diphosphate
GMP	guanosine monophosphate
GlnRS	glutaminyl-tRNA synthetase
GluRS	glutamyl-tRNA synthetase
GlyRS	glycyl-tRNA synthetase
GTP	guanosine triphosphate
HEPES	4-(2-hydroxyethyl)-1-piperazineethanesulfonic acid-KOH
HisRS	histidinyl-tRNA synthetase
IleRS	isoleucyl-tRNA synthetase
IPTG	isopropyl β-D-1-thiogalactopyranoside
K_D	equilibrium binding constant
K_I^{app}	Apparent equilibrium dissociation constant for the inhibitor
LB	Luria broth
LeuRS	leucyl-tRNA synthetase
LSD	leucine-specific domain
LysRS	lysyl-tRNA synthetase
MetRS	methionyl-tRNA synthetase
mRNA	messenger RNA
N. crassa	*Neurospora crassa*

OD	optical density
PCR	polymerase chain reaction
PEG	polyethylene glycol
PheRS	phenylalanyl-tRNA synthetase
PPi	pyrophosphate
P. horikoshii	*Pyrococcus horikoshii*
RNA	ribonucleic acid
S. cerevisiae	*Saccharomyces cerevisiae*
SerRS	seryl-tRNA synthetase
SDS	sodium dodecyl sulfate
SDS-PAGE	sodium dodecyl sulfate polyacrylamide gel electrophoresis
T-arm	TψC arm of tRNA
TCA	trichloroacetic acid
ThrRS	threonyl-tRNA synthetase
TLC	thin-layer chromatography
TNFα	tumor necrosis factor α
TOR	target of rapamycin
Tris	tris(hydroxymethyl)aminomethane
tRNA	transfer ribonucleic acid
TrpRS	tryptophanyl-tRNA synthetase
TyrRS	tyrosyl-tRNA synthetase
T. thermophilus	*Thermus thermophilus*
ValRS	valyl-tRNA synthetase
ZBD	zinc-binding domain

Chapter 1. Introduction

1.1 Overview of aminoacyl-tRNA synthetases

Aminoacyl-tRNA synthetases (AARSs) are an ancient family of enzymes catalyzing the first step of protein synthesis (Ibba & Söll, 2000; Pang, Poruri, & Martinis, 2014; Ribas de Pouplana & Schimmel, 2001a). In prokaryotes, there are 20 AARSs for each of the 20 standard amino acids. In eukaryotes, there are two sets of AARSs encoded in the nuclear. One set is targeted to cytoplasm and the other to the mitochondria. In plants and some parasitic species, there is a third set of AARSs for chloroplast and apicoplasts, respectively (Brandao & Silva-Filho, 2011). Each of the amino acids corresponds to one or more cognate transfer RNAs (tRNAs) and is recognized as single AARS (except lysine which is recognized by two AARSs in some species (Leveque, Plateau, Dessen, & Blanquet, 1990).

The AARSs catalyze a reaction called aminoacylation, which covalently attaches amino acids to the cognate tRNA isoacceptors. In addition, during the lengthy evolutionary period of AARSs, they have acquired cellular activities other than aminoacylation and protein synthesis (M. Guo, Schimmel, & Yang, 2010; Martinis, Plateau, Cavarelli, & Florentz, 1999), such as mitochondrial RNA splicing (Lambowitz & Perlman, 1990), transcriptional regulation (Putney & Schimmel, 1981), translational regulation (Romby et al., 1996). They can impact

angiogenesis and the immune response as well as signaling pathways, such as those induced by mTOR (Bonfils et al., 2012; Han et al., 2012), IFN-γ (Wakasugi et al., 2002) and p53 (Sajish et al., 2012).

1.1.1 Classification

The AARSs are categorized into two classes based on sequence, structure and functional properties (Cusack, Berthet-Colominas, Hartlein, Nassar, & Leberman, 1990; Eriani, Delarue, Poch, Gangloff, & Moras, 1990; Ribas de Pouplana & Schimmel, 2001b) (Table 1.1). The classification is consistent among all the living organisms except for LysRS, which is classified into Class I in euryarchaeal species while Class II in others (Ibba et al., 1997). Each class can be further divided into subclasses based on more extensive sequence homology, structural and mechanistic features (Cusack, 1995; Landes et al., 1995; Ribas de Pouplana & Schimmel, 2001b).

Table 1.1 Classification of AARSs based on sequence and structural homology

Class I	Class II
Ia	IIa
LeuRS*	SerRS
IleRS*	ThrRS*
ValRS*	AlaRS*
MetRS*	GlyRS
CysRS	ProRS*
ArgRS	HisRS
Ib	IIb
GlnRS	AspRS
GluRS	AsnRS
LysRS-I	LysRS-II*
Ic	IIc
TyrRS	PheRS*
TrpRS	
	SepRS
	PylRS

* The AARSs possess proofreading activities to clear misactivated and/or mischarged amino acids.

The Class I AARS catalytic core is characterized by a Rossmann ATP binding fold consisting of six parallel β-strands intervened by four α-helices (Irwin, Nyborg, Reid, & Blow, 1976; Rould, Perona, Soll, & Steitz, 1989). In the catalytic core there are two consensus sequences unique in Class I AARSs (Schimmel, 1987): “KMSKS” (Lys-Met-Ser-Lys-Ser) (Brick, Bhat, & Blow, 1989; Hountondji, Dessen, & Blanquet, 1986; Rould et al., 1989; Schmitt, Meinnel, Blanquet, & Mechulam, 1994) and “HIGH” (His-Ile-Gly-His) (Webster, Tsai, Kula, Mackie, & Schimmel, 1984). In the aminoacylation reaction, the “KMSKS” and “HIGH” loops move closer to the catalytic core and help stabilize the substrates, switching the catalytic

core from an “opened” to “closed” conformation (Ilyin et al., 2000; Nakama, Nureki, & Yokoyama, 2001). Distinct from the Class II AARSs introduced below, Class I AARSs bind to an ATP molecule in an extended conformation (Brick et al., 1989; Brick & Blow, 1987; Perona, Rould, & Steitz, 1993; Rould et al., 1989), interact with the minor groove of the tRNA accepter stem (Arnez & Steitz, 1996; Rould et al., 1989), and catalyze the addition of amino acid onto the 2’-OH of the terminal ribose on the tRNA (Perona et al., 1993; Sprinzl & Cramer, 1975).

While the Class I AARSs are typically monomeric, Class II AARSs are dimeric or tetrameric. The aminoacylation core of Class II AARSs is composed of seven antiparallel β-strands surrounded by α-helices (Cusack et al., 1990; Eriani et al., 1990; Rossmann, Moras, & Olsen, 1974). Unlike the Rossmann ATP binding fold in Class I AARSs, this structure is not widely spread in protein structures. Class II AARSs are marked by three consensus motifs. Motif 1 is gϕxxϕxxp$\phi\phi$, motif 2 fRxe-h/rxxxFxxx(d/e), and motif 3 gϕgϕgϕ(d/e)R$\phi\phi\phi\phi$ (x: variant; ϕ: hydrophobic; lower case letter: amino acid partially conserved). Motif 1 is found at dimer interface, and is proposed to help with communication between the two active sites (Arnez et al., 1995). Motif 2 and motif 3 are part of the aminoacylation core (Cusack et al., 1990; Eriani et al., 1990; Ruff et al., 1991). Different from the Class I AARSs, Class II AARSs bind to a bent ATP molecule (Arnez & Moras, 1997; Cavarelli et al., 1994), bind the major groove of

the tRNA accepter stem (Ruff et al., 1991; Sankaranarayanan et al., 1999) and add the amino acid onto the 3’-OH of the terminal ribose on the tRNA (Cavarelli et al., 1994; Sprinzl & Cramer, 1975), with the exception of PheRS, which adds Phe to the 2’-OH of tRNAPhe (Goldgur et al., 1997). Apart from the AARSs named after the 20 standard amino acids, SepRS (O-phosphoserine-RS) and PyrRS (pyrrolysine-RS) have been discovered later and grouped into the Class II AARSs (O'Donoghue, Sethi, Woese, & Luthey-Schulten, 2005; Polycarpo et al., 2004).

1.1.2 Mechanism of aminoacylation reaction

The AARSs-catalyzed aminoacylation reaction can be further dissected into two steps (Figure 1.1): First, the amino acid is activated by ATP, forming aminoacyl-adenylate intermediate (AA-AMP). Although tRNA is not a substrate in the first step, the cognate tRNAs have been reported to function as cofactors for GluRS, GlnRS, ArgRS and LysRS-I. Second, the amino acid is transferred to the 3′-end of the tRNA bound by the AARS, forming aminoacylated tRNA (AA-tRNA^{AA}) (A. P. Mascarenhas, An, Rosen, Martinis, & Musier-Forsyth, 2009; Pang et al., 2014). Then the aminoacyl tRNA is transported to the ribosome by EF-Tu and the aminoacyl group be added to the growing polypeptide chain, directed by the codons in a messenger RNA.

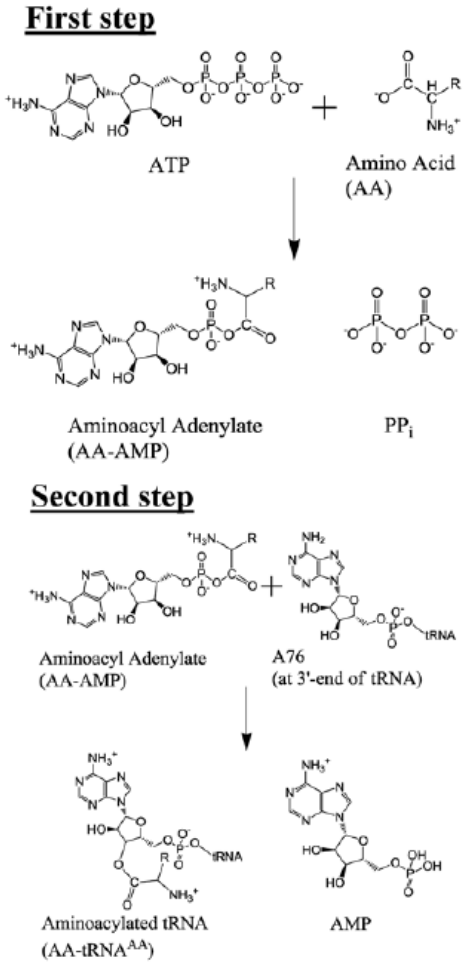

Figure 1.1 Two-step aminoacylation reaction catalyzed by AARSs. Step 1 is ATP-dependent activation of the amino acid (AA), forming the enzyme-bound aminoacyl adenylate (AA-AMP) intermediate at the synthetic active site. The first step involves a nucleophilic attack by the α-carboxyl oxygen of the amino acid at the α-phosphate of ATP. Step 2 is the transfer of the activated amino acid to the 3′-end of the tRNA. In the second step the 2′-OH of the ribose ring of terminal adenosine at the 3′-end of tRNA makes a second nucleophilic attack (for class I AARSs) at the carboxyl carbon of the aminoacyl adenylate intermediate, forming the aminoacylated tRNA.

1.1.3 Proofreading (Editing) pathways in AARSs

Faithful translation of genetic information from mRNAs to proteins is crucial for cells. Errors in translation can lead to accumulation of misfolded proteins which do not function properly, causing cell death in microbes and/or diseases for mammals. In the translation process, “check points” for the translational errors exist at several levels, including AARSs which catalyze charging of tRNAs with amino acids (A. P. Mascarenhas et al., 2009), EF-Tu which transports the charged tRNAs to ribosomes (LaRiviere, Wolfson, & Uhlenbeck, 2001), ribosomes where amino acids on the tRNAs are translocated to the elongating polypeptide (Ogle, Murphy, Tarry, & Ramakrishnan, 2002; Zaher & Green, 2009). Among them, AARSs are the first check point, thus play a very important role in maintaining translation fidelity.

Editing function has been found in almost half of the AARSs (A. P. Mascarenhas et al., 2009). The strategies AARSs use to carry out editing include post-transfer editing and pre-transfer editing (Figure 1.2) (Sarkar & Martinis, 2011; Williams & Martinis, 2006). Post-transfer editing is hydrolysis of the mischarged tRNA. The post-transfer editing sites are usually not located in the aminoacylation catalytic core, but in a separate editing domain. The 3’-end of tRNA is translocated from the synthetic core to the editing domain, positioning the noncogate aminoacyl linkage for hydrolysis, followed by release of the tRNA and amino acid.

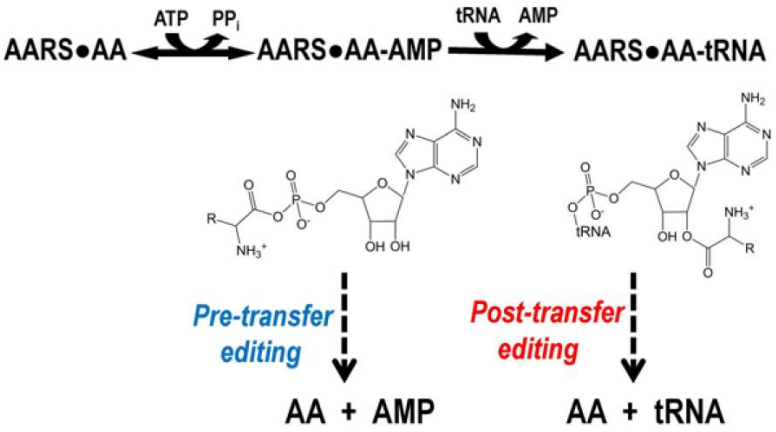

Figure 1.2 Scheme showing pre- and post-transfer editing pathways. The aminoacyl adenylate (AA-AMP) is the substrate for pre-transfer editing, while the mischarged tRNA (AA-tRNA) is the substrate for post-transfer editing.

Pre-transfer editing targets the misactivated aminoacyl-AMP (AA-AMP) for hydrolysis to form AMP and free amino acid (Baldwin & Berg, 1966). The enzyme either catalyzes the AA-AMP cleavage (selective hydrolysis) or release the AA-AMP into the solution for hydrolysis (selective release). Misactivated AA-AMP can be selectively hydrolyzed in a tRNA-independent or -dependent fashion (Minajigi & Francklyn, 2010; Splan, Ignatov, & Musier-Forsyth, 2008). This can occur either in the aminoacylation catalytic core (Gruic-Sovulj, Rokov-Plavec, & Weygand-Durasevic, 2007) or following transfer to the editing domain that is originally proposed for post-transfer editing (M. T. Boniecki, Vu, Betha, & Martinis, 2008; Fukunaga & Yokoyama, 2006; Nomanbhoy, Hendrickson,

& Schimmel, 1999).

Pre- and post-transfer editing can co-exist in one AARS (M. T. Boniecki et al., 2008; Martinis & Boniecki, 2010; Williams & Martinis, 2006). For example, ProRS clears misactivated alanine by both pre-transfer (Beuning & Musier-Forsyth, 2000) and post-transfer editing (Wong, Beuning, Nagan, Shiba, & Musier-Forsyth, 2002) in some bacteria species. The dominance or partitioning of the two strategies in one AARS has been found to be directed by the availability of the active sites and the types of noncognate amino acids (M. T. Boniecki et al., 2008; Martinis & Boniecki, 2010; Sarkar & Martinis, 2011). For example, the pre-transfer editing activity of *E. coli* LeuRS is unmasked when certain post-transfer editing active site residues are mutated or the whole editing domain deleted (X. Chen et al., 2011; Williams & Martinis, 2006). Human cytoplasmic LeuRS clears misactivated amino acid-like synthetic intermediates, α-aminobutyrate and novaline, by pre- and post-transfer editing respectively (X. Chen et al., 2011). The balance between pre-transfer and post-transfer editing redundantly ensures the highest-possible translation fidelity for AARSs.

Paradoxily, there are AARSs that are naturally editing-deficient, which contributes to produce a proteome with more statistical mutations. Examples include the parasite *Mycoplasma mobile* LeuRS which lacks the editing domain in LeuRS (L. Li et al., 2011). The error-prone proteome

should be beneficial for those living organisms in certain environments.

1.1.4 Overview of alternative cellular functions in AARSs

As one of the most ancient protein families, AARSs have acquired a repertoire of non-translational functions that are crucial for cell metabolism during their lengthy evolution (Figure 1.3) (Martinis et al., 1999; Pang et al., 2014). These functions have been found in both lower and higher organisms. Some of the discovered secondary functions capitalize upon nucleic acid binding capability of AARSs. For example, when *E. coli* $tRNA^{Tyr}$ concentration is low, excess tyrosyl-tRNA synthetase binds to a $tRNA^{Tyr}$-like sequence upstream of its translation start site and prevents its own translation. The *E. coli* AlaRS binds to a palindromic sequence in the promoter region of its gene and represses its own transcription (Putney & Schimmel, 1981). In lower eukaryotes, mitochondrial LeuRS in *Saccharomyces cerevisiae* and TyrRS in *Neurospora crassa* bind to certain group I introns to act as splicing factors in processing the pre-mRNAs (Lambowitz & Perlman, 1990).

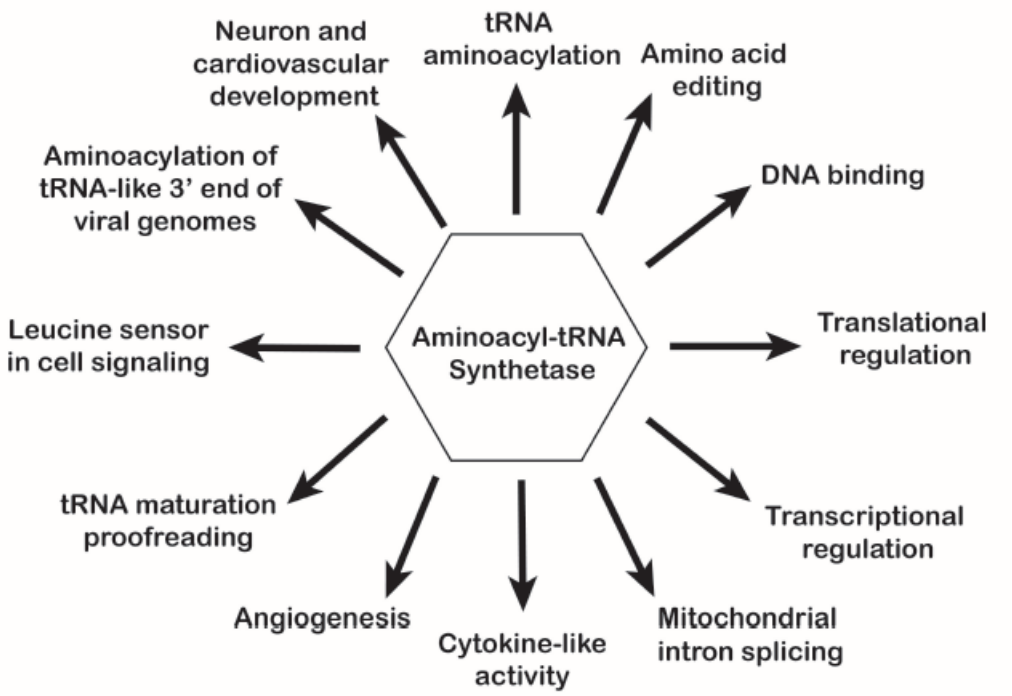

Figure 1.3 Non-canonical functions of AARSs. AARSs adapted to encompass secondary roles in addition to their aminoacylation function.

The amino-acid binding capability of AARSs link them to some signaling pathways that have amino acids and/or their metabolites identified as centrals of the pathways. For instance, human and S. *cerevisiae* cytoplasmic LeuRSs serve as intracellular leucine sensors and signals to TORC1 in the TOR pathway, which is a pathway that regulates nutrition intake and cell growth (Bonfils et al., 2012; Han et al., 2012).

Instead of using the tRNA and amino-acid binding sites, some higher eukaryotes have evolved appended domains that specialize in non-translational functions of AARSs (M. Guo et al., 2010). Interestingly, these appended domains usually emerge at important transition points in

evolution. The number and complexity of these appended domains in AARSs correlate with the complexity of the organism on the tree of evolution. This is not observed in other ancient protein families, such as ribosomal proteins. Many of these appended domains are dispensable for aminoacylation and are specifically evolved for protein-protein interactions.

For example, the WHEP domain of tryptophanyl-tRNA synthetase (TrpRS) emerges in insects and then mere maintained thereafter. The name of WHEP domain comes from 3 of the 5 WHEP containing AARSs: TrpRS (W), HisRS (H) and GluProRS (EP). Deleting the WHEP domain has negligible effects on aminoacylation activity of TrpRS. However, it has been shown that there is a strong correlation between human TrpRS level in nucleus and the mechanics of IFN-γ-induced antiproliferation. In particular, the WHEP domain plays a key role by co-localizing DNA-dependent protein kinase (DNA-PKcs) and poly (ADP-ribose) polymerase 1 (PARP-1) to activate p53 (Wakasugi et al., 2002).

Another example is the UNE-S domain in seryl-tRNA synthetase (SerRS). This 45-residue domain emerges in zebrafish (Xu et al., 2012), which is the transition point in evolution where the open circulation of invertebrates transforms to the closed circulation of vertebrates. It has been found that the UNE-S domain is dispensable for aminoacylation but required for vascular development in zebrafish embryo.

The secondary functions of some tRNA synthetases are revealed after being naturally fragmented by alternative splicing or proteolysis. For example, proteolysis specifically cleaves TyrRS in half. Both fragments then act as distinct cytokines in inflammatory pathways. The full-length TyrRS lacks of this activity (Wakasugi & Schimmel, 1999). Another example is the splice-variant of TrpRS that is missing the WHEP domain has been shown to have angiostatic effects. This activity is absent in the full-length TrpRS (Zhou et al., 2010).

Mutations of tRNA synthetases correlate to many diseases. For example, mutations of different mitochondrial tRNA synthetases (mtAARSs) cause damage to very specific central neural cell types. Each leads to distinct clinical phenotypes (Konovalova & Tyynismaa, 2013). This suggests that each of these mtAARSs harbor important and different nontranslational functions in the neural system. Mutations of GlyRS and TyrRS, LysRS and AlaRS have been causally associated with Charcot-Marie-Tooth (CMT) disease, which is an inheritable disease on the peripheral nerve system (Antonellis & Green, 2008; Zhao et al., 2012).

1.2 Structure overview of leucyl-tRNA synthetase

Several structures of LeuRS have been solved from different species, with different substrates bound, in both aminoacylation and editing conformations (Table 1.2). The architectural characteristics of LeuRS

structure is consistent with other Class I AARSs, of which the main body consists of Rossmann-fold catalytic domain with catalytically important "KMSKS" and "HIGH" conserved sequences, and the Class Ia anticodon–binding domain. The LeuRS also has flexible inserted domains, including the zinc-binding domain, the connective polypeptide 1 (CP1) editing domain, the leucine-specific domain and the C-terminal domain (Figure 1.4). Aminoacylation and editing of LeuRS in all species as well as the group I intron splicing function in S. *cerevisiae* mitochondria LeuRS, involve coordination of the four flexible domains.

The aminoacylation catalytic core of LeuRS is composed of Rossmann adenylate binding fold. Upstream of the Rossmann fold (N-terminal side in sequence) are two inserted zinc binding domains ZBD-1 and ZBD-2. On the C-terminal side of the Rossmann fold is the anticodon binding domain characterized by five α-helices structure seen in Class Ia AARS structures. Further downstream is the C-terminal domain that binds the corner of $tRNA^{Leu}$.

Table 1.2 Compilation of solved crystal structures of LeuRS

PDB ID	Reference	Structure description
1H3N	(Cusack, Yaremchuk, & Tukalo, 2000)	*T. Thermophilus* LeuRS complexed with sulfamoyl ananlog of leucyl-adenylate
1OBH	(Lincecum et al., 2003)	*T. Thermophilus* LeuRS complexed with a pre-transfer editing substrate analogue in both synthetic active site and editing site
2BTE, 2BYT	(Tukalo, Yaremchuk, Fukunaga, Yokoyama, & Cusack, 2005)	*T. Thermophilus* LeuRS complexed with a $tRNA^{Leu}$ transcript in the post-editing conformation and a post-transfer editing substrate analogue
1WZ2	(Fukunaga & Yokoyama, 2005)	*P. horikoshii* LeuRS complexed with a $tRNA^{Leu}$ transcript in the aminoacylation conformation
2V0C, 2V0G	(Rock et al., 2007)	*T. Thermophilus* LeuRS complexed with a sulfamoyl analogue of leucyl-adenylate in the synthetic site and an adduct of AMP with 5-fluoro-1,3-dihydro-1-hydroxy-2,1-benzoxaborole (AN2690) in the editing site
2WFE	(Seiradake et al., 2009)	*C. Albicans* cytosolic LeuRS CP1 editing domain
2WFG	(Seiradake et al., 2009)	*C. Albicans* cytosolic LeuRS CP1 editing domain bound to a benzoxaborole-AMP adduct
2WFD	(Seiradake et al., 2009)	Human cytosolic LeuRS CP1 editing domain
4ARC	(Palencia et al., 2012)	*E. coli* LeuRS complexed with L-leucine in the post-editing conformation
4ARI, 4AS1	(Palencia et al., 2012)	*E. coli* LeuRS complexed with benzoxaborole
4AQ7	(Palencia et al., 2012)	*E. coli* LeuRS complexed with $tRNA^{Leu}$ and Leu-AMS in the aminoacylation conformation

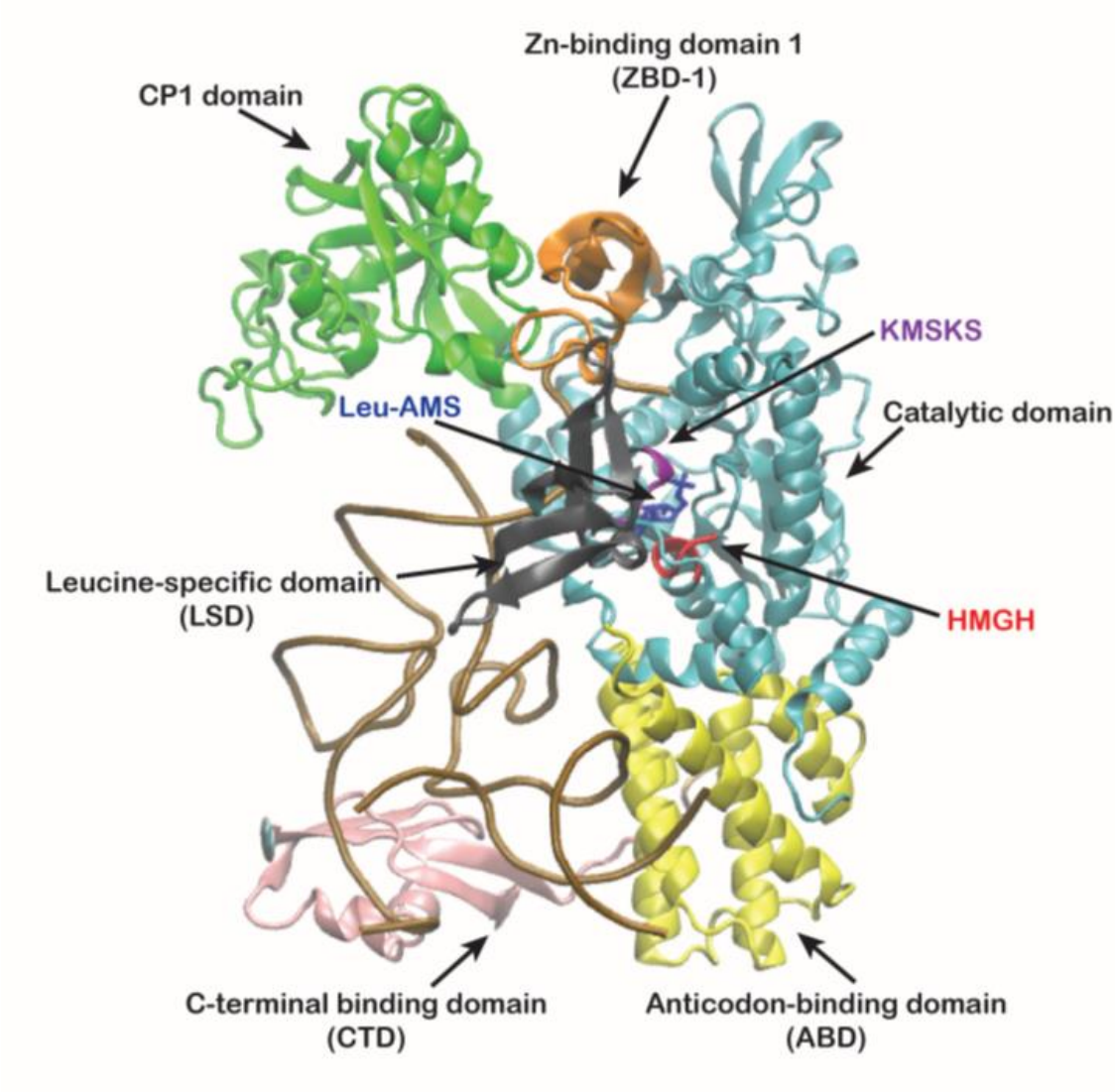

Figure 1.4 Crystal structure of *E. coli* LeuRS complexed with $tRNA^{Leu}$ and Leu-AMS in the aminoacylation conformation. The overall structure is organized into discrete functional domains highlighted with different colors: catalytic domain, cyan; anticodon-binding domain, yellow; C-terminal binding domain, pink; CP1 domain, green; ZBD-1, orange (ZBD-2 not shown); and leucine-specific domain, black (PDB ID: 4AQ7) (Palencia et al., 2012). The $tRNA^{Leu}$ is drawn as a brown tube. Conserved sequences HMGH and KMSKS are highlighted in purple and red, respectively.

1.2.1 The CP1 domain of LeuRS

In the Rossmann fold of LeuRS, there is an inserted large domain (~200 amino acids) called connective polypeptide 1 domain (CP1 domain) (Cusack et al., 2000; Hou, Shiba, Mottes, & Schimmel, 1991; Starzyk, Webster, & Schimmel, 1987). The CP1 domain exists in all of the Class I AARSs. However, only in LeuRS, IleRS and ValRS are the CP1 domains functionally enlarged. The CP1 domain structure is conserved among LeuRS, IleRS and ValRS. The core of the CP1 domain comprises of seven β-strands and four α-helices. Two flanking β-strands connect the core to the main body of LeuRS.

The insertion site of the CP1 domain varies in different AARSs of different species. The archaeal and eukaryotic cytosolic LeuRS as well as all ValRS and IleRS have the CP1 domain inserted between the two halves of the ZBD1 domain, whereas the bacteria and mitochondrial LeuRS have the CP1 domain after the ZBD1 domain. Interestingly, the CP1 domain of archaeal and eukaryotic LeuRS has the same orientation as the bacteria LeuRS, while ~180° rotated in ValRS and IleRS (Fukunaga & Yokoyama, 2005).

The CP1 domain is primarily responsible for the editing function (Mursinna, Lee, Briggs, & Martinis, 2004), as well as required for tRNA specific binding in the aminoacylation conformation (Fukai et al., 2000; Palencia et al., 2012; Silvian, Wang, & Steitz, 1999). A threonine rich

region within the CP1 domain of *E. coli* LeuRS was shown to be important for amino acid editing *in vitro*. T252Y mutation in this region blocks amino acid binding in the active site and abolishes editing activity (Mursinna & Martinis, 2002; Williams & Martinis, 2006). However, a secondary site mutation A293D on the CP1 domain activated a pre-transfer editing pathway when the post-transfer editing pathway is inhibited by T252Y mutation (Williams & Martinis, 2006). Apart from amino acid editing, the *ym*LeuRS CP1 fragment has been shown to facilitate splicing of group I intron in the cytochrome b open reading frame *in vitro* (Sarkar, Poruri, Boniecki, McTavish, & Martinis, 2012).

1.2.2 The C-terminal domain of LeuRS

The C-terminal domain of LeuRS in *E. coli* LeuRS interacts with the D-loop, T-loop and the variable arm of the $tRNA^{Leu}$ in aminoacylation and editing, whereas for other Class I AARSs except LeuRS, the C-terminal domain interacts with the tRNA anticodon region and contributes to the tRNA discrimination. In the transition from aminoacylation to editing conformation, the C-terminal domain moves synchronously with the $tRNA^{Leu}$ to maintain the interaction with the variable arm and T-loop of $tRNA^{Leu}$ (Palencia et al., 2012).

1.3 LeuRS recognition of tRNA

In general, tRNAs have similar secondary and tertiary structures (Figure 1.5). AARSs recognize their respective tRNAs by sequence and structural features on the tRNAs called identity elements, which typically include the discriminator base N73, sequences on the acceptor stem and the anticodon (Giege, Sissler, & Florentz, 1998; Soma, Kumagai, Nishikawa, & Himeno, 1996). For some AARSs, the variable loop and the D arm also contribute to tRNA recognition. Although there are general rules for tRNA recognition, the identity elements vary among different AARS-tRNA pairs in different species.

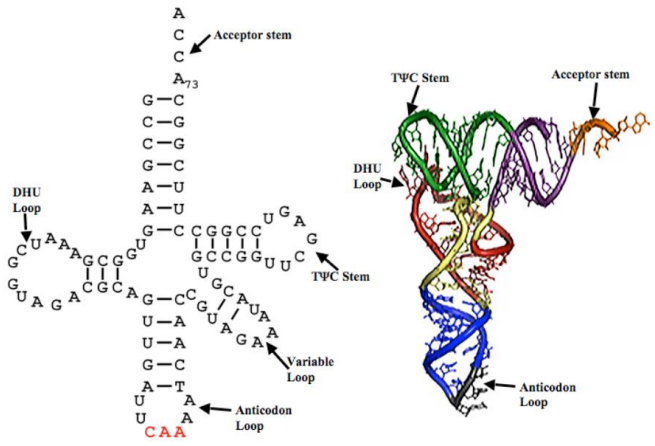

Figure 1.5 Conserved structure of tRNA. The *E. coli* $tRNA^{Leu}_{CAA}$ is shown as an example. On the left is the tRNA secondary structure. The "CAA" anticodon is colored in red. On the right is the tRNA tertiary structure. The stem-loops are highlighted with different colors: acceptor stem, orange; DHU loop, red; anticodon stem, blue; anticodon loop, grey; variable loop, yellow; TΨC stem, green.

Unlike most AARSs, LeuRS, AlaRS (Francklyn & Schimmel, 1989) and SerRS (Biou, Yaremchuk, Tukalo, & Cusack, 1994; Borel, Vincent, Leberman, & Hartlein, 1994) do not use the anticodon loop of their tRNAs as a recognition element as there is too much variation in the anticodons of these isoaccpeters (Asahara et al., 1993; Breitschopf, Achsel, Busch, & Gross, 1995; Larkin, Williams, Martinis, & Fox, 2002). For example, LeuRS recognizes six $tRNA^{Leu}$ isoaccepters, each with a different anticodon. The known exception is S. *cerevisiae* cytoplasmic LeuRS, of which efficient leucylation is dependent on specific sequences of the anticodon loop (Soma et al., 1996). The identity elements in LeuRS:$tRNA^{Leu}$ recognition generally include the discriminator base N73 at the end of the acceptor stem. Specifically, for *E. coli* LeuRS, the identity elements also include a unique structural motif contributed by the triple interaction that is formed between A15:U48 and A20a at the D- and T-arms of tRNA, as well as the invariant G18G19. For archaeal (Fukunaga & Yokoyama, 2005) and human cytoplasmic LeuRS (Breitschopf et al., 1995) but not S. *cerevisiae* cytoplasmic (Soma et al., 1996) or *E.coli* LeuRS (Asahara et al., 1993), the long variable arm of $tRNA^{Leu}$ is an important recognition element.

1.4 Protein-facilitated group I intron splicing

1.4.1 Mechanisms and structures of group I intron splicing

Splicing is a modification of nascent precursor RNAs in which introns removed and exons ligated. Splicing pathways can be categorized into four types with distinct mechanisms: group I and group II intron self-splicing, spliceosomal splicing and tRNA splicing (Irimia & Roy, 2014). The focus here is the group I intron splicing.

Group I introns have been found mostly in organelle genomes as well as some nucleic, bacterial and bacterial-phage genes. In group I intron splicing, the folded RNA structure participate directly in the splicing reaction. Some of them undergo self-splicing in the absence of proteins *in vitro*, while others require proteins to facilitate their splicing but still use the RNA as catalytic center (Burke, 1988; Lambowitz & Perlman, 1990).

Self-splicing of group I intron proceeds via two consecutive transesterification reactions (Cech, 1990). First, an exogenous guanosine or one of its phosphorylated forms (GMP, GDP, GTP) binds to a certain guanosine-binding site on the 3´ region of the intron. The 3´-OH of the guanosine attacks the phosphorus group on the 5´ splice site, forming a 3´, 5´-phosphodiester bond with the first nucleotide of the intron, resulting in excision of the upstream exon (Cech, 1987; Zaug, Grabowski, & Cech, 1983). Then the hydroxyl group on the upstream exon attacks the

phosphorus group on the 3’ splice site, yielding ligated exons and deleted intron.

The group I introns share a conserved secondary structure, made up of a series of base-paired regions (P1-P10) interrupted by extra unpaired sequences (Figure 1.6). The P1 and P10 regions contain the 5′- and 3′-splice site, respectively and are formed by base pairing between an internal guide sequence (IGS) (generally located downstream of the 5′-splice site) (Davies, Waring, Ray, Brown, & Scazzocchio, 1982) and the exon sequences flanking the splice sites (Figure 1.6). The P1 regions of different group I introns vary in sequence, with only one conserved base pair between the U immediately preceding the 5′-splice site and a G in the IGS (Cech, 1990).

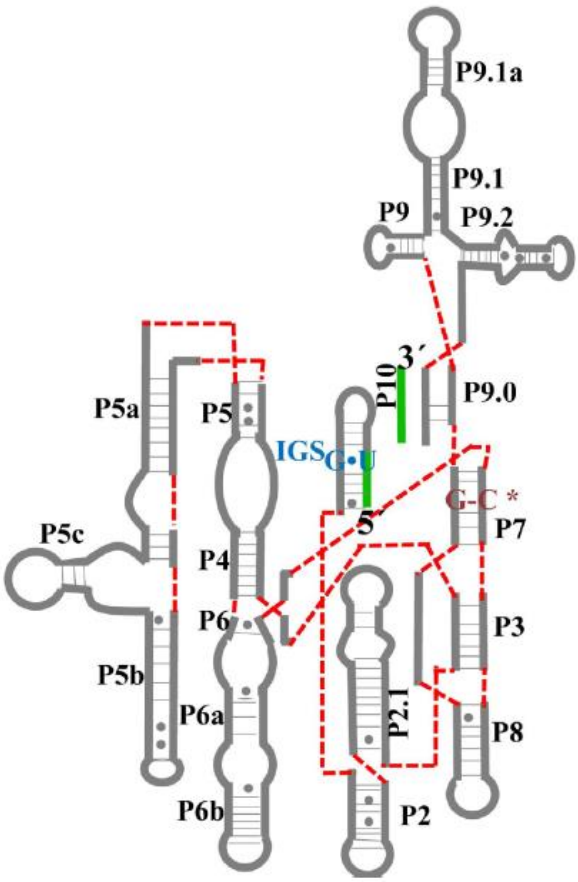

Figure 1.6 Conserved secondary structure of group I intron. The 3´- and 5´-flanking exon sequences are shown in green. Dashes indicate base pairs and dots indicate wobble base pairs. Dashed red lines indicate continuity of intron strand. Tertiary interactions have been omitted for clarity. The conserved U•G base pair in the internal guide sequence (IGS), near the 5´-splice site is highlighted in blue. The guanosine binding site is denoted by asterisk (*). The figure is adapted from (Cech, et al., 1994).

The three-dimensional splicing-competent structure of the group I intron is also conserved, with the catalytic core consisting of two extended RNA domains: P4-P6 and P3-P9. The two domains interact to form the

splicing active site. Folding of the intron into this competent structure brings the guanosine-binding site and the splice sites in close proximity, which are originally at distance in primary structure, so that the two transesterification reactions can take place (Cech, 1988).

1.4.2 Protein facilitation of group I intron splicing

Group I intron splicing is facilitated by protein splicing factors *in vivo* (Burke, 1988; Lambowitz, Caprara, Zimmerly, & Perlman, 1999; Lambowitz & Perlman, 1990). Most of the splicing factors identified so far are proposed to facilitate folding of the intron into the correct catalytic active conformation (Burke, 1988; Cech, 1988, 1990; Tinoco & Bustamante, 1999). One group of the group I intron splicing factors are intron-encoded maturases, which typically only facilitate splicing of their encoding introns (Lazowska, Jacq, & Slonimski, 1980). One exception is the *cob*-I4 (bI4) maturase in yeast mitochondria, which not only aids bI4 intron splicing but also *cox1α*-I4 (aI4α) splicing (De La Salle, Jacq, & Slonimski, 1982; Dhawale, Hanson, Alexander, Perlman, & Mahler, 1981).

The nuclear-encoded protein splicing factors of group I introns include LeuRS (or NAM2) (Herbert, Labouesse, Dujardin, & Slonimski, 1988; Labouesse, 1990) and Mss116p in S. *cerevisiae* mitochondria, TyrRS or (CYT-18) and CTY-19 in *N. crasssa* mitocohondria. The yeast mitochondrial LeuRS (*ym*LeuRS) is required for splicing of bI4 and aI4α

introns (Herbert et al., 1988), while CYT-18 essential for splicing of large rRNA intron as well as intron in the *cob* and ATPase 6 genes (Akins & Lambowitz, 1987; Cherniack, Garriga, Kittle, Akins, & Lambowitz, 1990; Majumder et al., 1989). Other than that, CYT-18 can facilitate splicing of a variety of completely irrelevant group I introns, whereas splicing activity of *ym*LeuRS has not been identified in other RNAs except the two group I introns described above.

Biochemical and footprinting data indicates that CYT-18 promote splicing of group I introns in a two-step sequential manner: it first binds to the P4-P6 region, which serves as a scaffold on which the P3-P9 region assembles (Caprara, Mohr, & Lambowitz, 1996). The solved structure of *N. crasssa* mitocohondria TyrRS bound to a group I intron shows the intron binds across the two subunits of the homodimeric CYT-18 (Figure 1.7) (Paukstelis, Chen, Chase, Lambowitz, & Golden, 2008). Instead of using the $tRNA^{Tyr}$ binding sites, TyrRS evolves distinct RNA-binding surface for the intron. It is proposed that TyrRS acts as an extended scaffold to stabilize the conserved catalytic core of the intron, which explains why it can promote splicing of completely irrelevant group I introns.

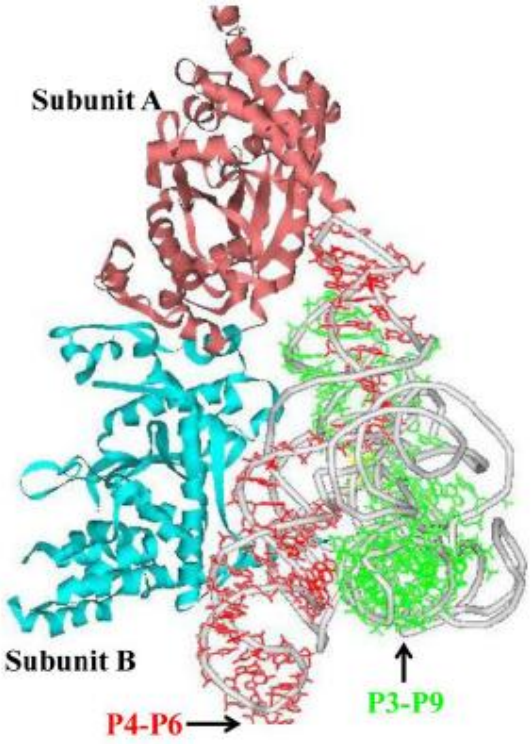

Figure 1.7 Structure of *N. crassa* TyrRS bound to a group I intron RNA. The P4-P6 and the P3-P9 domains of the intron are highlighted in red and green respectively (PDB ID: 2KJ) (Paukstelis et al., 2008).

CYT-19 and Mss116p, from *N. crassa* and *S. cerevisiae*, respectively, stimulate splicing of a variety of group I and II introns, which indicates that they recognize general structural features instead of a specific feature of a single RNA (Halls et al., 2007; S. Mohr, Matsuura, Perlman, & Lambowitz, 2006; S. Mohr, Stryker, & Lambowitz, 2002; Solem, Zingler, & Pyle, 2006; Tijerina, Bhaskaran, & Russell, 2006). CYT-19 has also been shown to work in concert with CYT-18 in splicing of the *N. crassa* mt LSU and *Tetrahymena* AP5abc group I introns *in vitro* (S. Mohr et al., 2002).

1.4.3 Role of LeuRS in group I intron splicing

The *ym*LeuRS encoded by the nuclear gene and transported into mitochondria was first implicated to play a role in splicing by its capability to suppress a splicing-deficient bI4 intron maturase mutation (Labouesse, Herbert, Dujardin, & Slonimski, 1987). Both *ym*LeuRS and bI4 maturase are required for splicing of the bI4 and aI4α introns. It was found that the two proteins bind independently to the bI4 intron and stimulate splicing (Figure 1.8) (Rho & Martinis, 2000).

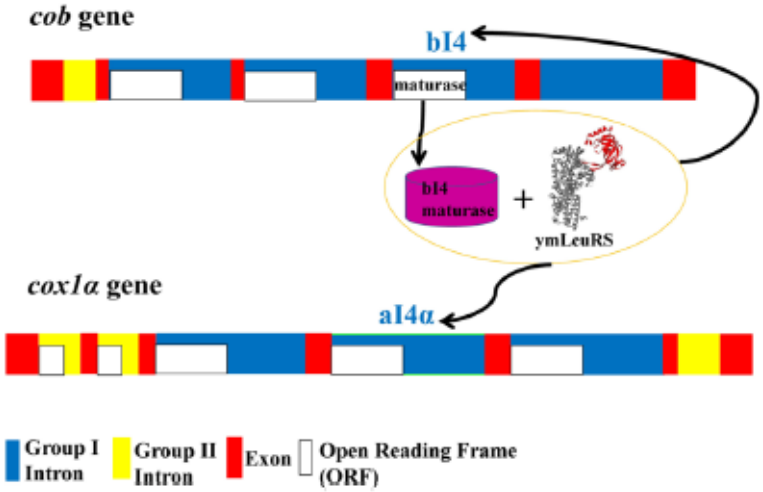

Figure 1.8 Schematic representation of LeuRS-assisted splicing. The yeast mitochondrial LeuRS (*ym*LeuRS) facilitates splicing of two related group I introns, bI4 and aI4α from the yeast mitochondrial *cob* and *cox1α* genes, respectively. The bI4 maturase (encoded by the ORF of intron bI4) and nuclear-encoded *ym*LeuRS act in collaboration to aid in splicing of these two introns. (Color legend: group I intron, blue; group II intron, yellow; exon, red; intron ORFs, white).

Molecular determinants have been identified in LeuRS, although the mechanism of splicing stimulation by LeuRS is still unknown. The CP1 domain of LeuRS is able to suppress the splicing deficiency just like the full-length LeuRS, in which the two β-strands that link the CP1 domain to the main body are essential (Rho, Lincecum, & Martinis, 2002). The N-terminal linking β-strand contains a conserved WIG sequence, in which W273 and G240 identified to be splicing sensitive sites by mutagenesis in the splicing-deficiency suppression experiments (Labouesse, 1990; Labouesse, Dujardin, & Slonimski, 1985; G. Y. Li, Becam, Slonimski, & Herbert, 1996). The role of CP1 domain in splicing has been further confirmed *in vitro* (Sarkar et al., 2012). Apart from the CP1 domain, the C-terminal domain of LeuRS was also involved in splicing and functionally diverged to accommodate both splicing and aminoacylation (Hsu, Rho, Vannella, & Martinis, 2006).

1.4.4 RNA remodeling proteins

Most RNAs must adopt certain competent tertiary structures to be biologically active, such as tRNAs, group I and II self-splicing introns, small ribozymes, long non-coding RNAs and some local untranslated regions on mRNAs. Folding into the correct structures is critical for RNAs to be recognized by their protein partners in ribonucleoproteins (RNPs) and for the RNA ribozymes to be catalytic active (Batey, 2006).

The structured RNA usually include short A-form helices (typically <10 base pairs) as elements of secondary structure that interact with each other to form the overall three-dimensional structure. RNA folding is usually described as a hierarchical process, meaning that the elements of secondary structure are largely stable in the absence of tertiary structure, unchanged when tertiary structures formed, and unaffected when the tertiary structures disturbed (Tinoco & Bustamante, 1999).

In the folding process, there are two problems RNAs can face and RNA remodeling proteins can help with: a thermodynamic one and a kinetic one (Davila-Aponte, Huss, Sogin, & Cech, 1991; Jaeger, Westhof, & Michel, 1991; Michel et al., 1992; Riesner et al., 1979; Szostak & Sekula, 1991; Tanner & Cech, 1985; Walstrum & Uhlenbeck, 1990; Weeks, 1997). The thermodynamic problem is that an RNA has difficulty in specifying the native structure from other similarly stable competing structures. The kinetic problem is that numerous stable misfolded conformations that an RNA can adopt cause the folding process difficult to accomplish on a time-scale (Russell & Herschlag, 2001).

RNA remodeling proteins can be categorized into RNA chaperones including RNA helicases, RNA annealers and specific RNA binding proteins (Table 1.3) (Rajkowitsch et al., 2007). They are reviewed briefly below.

Table 1.3 Definition of terms related to protein-assisted RNA remodeling

RNA chaperone (protein with RNA chaperone activity) A protein that binds non-specifically and transiently to RNA and resolves kinetically trapped, misfolded conformations. RNA chaperone activity entails the disruption of RNA-RNA interactions and the loosening of RNA structures. The interaction with the protein is needed for the unfolding of the RNA but to maintain its structure. The protein does not require ATP-binding or hydrolysis for its activity. Examples: StpA (Müller, Lambert, & Göringer, 2001; O. Mayer, Rajkowitsch, Lorenz, Konrat, & Schroeder, 2007), L1 (Semrad, Green, & Schroeder, 2004), S1 (Bear et al., 1976; O. Mayer et al., 2007; Subramanian, 1983), S12 (Coetzee, Herschlag, & Belfort, 1994)
RNA annealer (protein with RNA annealing activity) A protein that accelerates annealing of complementary RNAs. It can act by binding to one or both RNAs thereby enhancing the local concentration and the probability of RNA-RNA interactions (molecular crowding, Example: Hfq (Rajkowitsch & Schroeder, 2007b)). A protein with matchmaker activity also alters the structure of the RNA upon binding, thereby rendering it annealing-competent (Example: gBP21 (Muller & Goringer, 2002)).
RNA helicase A member of the DExD/H-box protein family that utilizes energy derived from ATP hydrolysis to resolve RNA structures and to displace RNA-bound proteins. Only few are processive, whereas most of the well characterized RNA helicases are non-processive "unwindases" such as DED1, elF4A, CYT-19 and Mss116p (Jankowsky & Fairman, 2007).
Specific RNA-binding protein A protein ligand (protein cofactor) that binds specifically to an RNA and thereby contributes to its native folding and thermodynamic stability. The continuous interaction with the protein is required to maintain the functional RNA structure. Examples: CYT-18 (G. Mohr, Zhang, Gianelos, Belfort, & Lambowitz, 1992; Waldsich, Grossberger, & Schroeder, 2002), CBP2 (Bokinsky et al., 2006; Gampel, Nishikimi, & Tzagoloff, 1989), LtrA (Singh, Saldanha, D'Souza, & Lambowitz, 2002).

1.4.4.1 RNA chaperones

RNA chaperones can help solve the kinetic folding problem by preventing misfolding or by resolving misfolded structures (Clodi, Semrad, & Schroeder, 1999; Herschlag, 1995; Herschlag, Khosla, Tsuchihashi, &

Karpel, 1994; Munroe & Dong, 1992; Phadtare, Inouye, & Severinov, 2002; Schroeder, Barta, & Semrad, 2004; Waldsich et al., 2002). RNA chaperones come from a variety of established protein families that have been assigned with distinct functions, such as regulation of transcription, RNP assembly and stabilization, RNA export, virus replication and histone-like nucleoid structuring. Many of these protein families do not share any common sequence, fold or motif, thus employing different mechanisms when acting as RNA chaperones.

The mechanism of RNA chaperones can be generally categorized into two groups: transient binding and ATP-dependent unwinding. The first group of RNA chaperones bind RNAs weakly and are not required to maintain the native structure after the folding process finished, suggesting that they only act on the RNAs transiently (R. J. Mayer, 1995). Due to their weak and non-specific binding, this group of RNA chaperones usually need to be in excess compared with the RNAs in the *in vitro* folding assays. However, when the protein:RNA ratio exceeds an optimal value, RNA folding is inhibited, probably because protein binding impairs RNA interactions (Cristofari & Darlix, 2002; R. J. Mayer, 1995). Many ribosomal proteins fall into this group of RNA chaperones. Among them, a small subunit protein S12 is one of the most effective one both *in vitro* (Coetzee et al., 1994) and *in vivo* (Coetzee et al., 1994).

The second group of RNA chaperones are also called RNA helicases.

In contrast to the first group of RNA chaperones, RNA helicases are RNA-dependent ATPases that require external energy input to unwind double-stranded RNAs (Henn et al., 2010). They are highly similar to DNA helicases, and most of them belong to the DExD/H-box protein family (Jarmoskaite & Russell, 2014).

Examples of RNA helicases include Mss116p and CYT-19, which stimulate intron splicing in an ATP-dependent manner *in vitro* (Halls et al., 2007). The Mss116p splicing factor also shows RNA annealing activity, like many other DExD/H-box proteins. The annealing activity seems orthogonal to the unwinding activity, for it is ATP-independent and involves a different domain (Halls et al., 2007; Solem et al., 2006; Yang & Jankowsky, 2005).

1.4.4.2 RNA annealers

Complementary RNA oligos can anneal on their own, but this process can be accelerated by RNA annealers up to the diffusion limit (Croitoru et al., 2006; Yang & Jankowsky, 2005). Molecular crowding might be one of the mechanisms RNA annealers employ, which results in increase of local oligo concentration and therefore enhances the possibility of annealing. This can be achieved by simultaneous binding to both of the oligos (R. J. Mayer, 1995; Rajkowitsch & Schroeder, 2007b). Longer RNAs can form stable local mismatched structures, which needs to be broken before

hybridization with the correct complementary sequence (Patzel & Sczakiel, 1999). RNA annealers with matchmaker activity bind and disrupt the incorrect base-pairing and thereby exposing the RNA sequences to the correct intermolecular interactions (Muller, Lambert, & Goringer, 2001).

Similarly, an RNA chaperone can release an RNA sequence from its kinetic trap before the annealing event (You & McHenry, 1994). Nevertheless, RNA annealers differ with RNA chaperones in the mechanism: instead of transient binding, RNA annealers continuously bind to the RNAs until annealing has been accomplished. However, it is usually difficult to distinguish them experimentally (Herschlag, 1995; Muller & Goringer, 2002; Rajkowitsch & Schroeder, 2007a, 2007b).

One of the most thoroughly-studied RNA annealers is the *E. coli* host factor I/Q (Hfq). Electron microscopic and crystalized structures show that Hfq has a haxameric-ring structure and belongs to the large conserved Sm- or Sm-like proteins (Moller et al., 2002; Schumacher, Pearson, Moller, Valentin-Hansen, & Brennan, 2002; Zhang, Wassarman, Ortega, Steven, & Storz, 2002). Most data on Hfq-RNA interaction come from studies on small non-coding RNAs (ncRNAs) interacting with their target mRNAs. The Hfq protein facilitates *in vitro* annealing of spot42 RNA with galK mRNA (Moller et al., 2002), OxyS with fhlA mRNA (Zhang et al., 2002), RyhB with sodB mRNA (Afonyushkin, Vecerek, Moll, Blasi, & Kaberdin, 2005), and SgrS with ptsG mRNA (Kawamoto, Koide, Morita, & Aiba,

2006). Moreover, Hfq was found to harbor ATPase activity, raising the possibility of ATP-fueled activity (Sukhodolets & Garges, 2003). However, ATP is not required for Hfq stimulation of *in vitro* RNA annealing, nor does addition of ATP enables Hfq to non-specifically displace RNA strands (Rajkowitsch & Schroeder, 2007a).

Another well-known group of RNA annealers is the highly-conserved double-stranded RNA binding domain (dsRBD) proteins, RNase III family proteins Drosha and Dicer being two of the most prominent ones. dsRBD proteins can anneal RNA oligos that do not anneal on their own (Hitti, Neunteufl, & Jantsch, 1998).

A third example is the guide RNA targeted RNA annealing. Short RNAs can form complex with proteins and direct the RNPs to their target RNA sequences and anneal with them. RNA-induced silencing complex (RISC) is one of these proteins with an siRNA binding to the argonaute protein (Ameres, Martinez, & Schroeder, 2007). Formation of siRNA-target-RNA complex results in target RNA cleavage and regression of the gene expression.

1.4.4.3 Specific binding proteins

Specific binding proteins recognize and bind to specific conformations in the RNA structures to facilitate RNA folding. They help with formation of functional active sites or intermediate structures (Pontius

& Berg, 1992). Many of those protein-RNA co-crystalized X-ray structures are available, including the ribosome structure (Brodersen, Clemons, Carter, Wimberly, & Ramakrishnan, 2002). Important advances are made by studying folding and assembly of ribosomal RNAs with their specific proteins (Talkington, Siuzdak, & Williamson, 2005). One of the well-studied specific binding proteins is the group I intron splicing factor CYT-18 in *N. crassa*, whose binding to the specific structural element leading to stabilization of the catalytic site of the intron.

Chapter 2. Materials and methods

2.1 Materials

Oligonucleotide primers were synthesized from Integrated DNA Technologies (Coralville, IA). Radiolabeled nucleotides were purchased from Pekin Elmer (Waltham, MA). Cloned *Pfu* DNA polymerase and dNTP mixture were obtained from Agilent Technologies (La Jolla, CA). Restriction endonucleases were purchased from New England Biolabs Inc. (Ipswich, MA) or Promega (Madison, WI). *E. coli* strains DH5α and BL21 (DE3) codon PLUS were obtained from Stratagene (La Jolla, CA). MEGAscript® T7 Transcription Kit was purchased from Thermo Fisher Scientific (Waltham, MA).

2.2 Yeast strains

Complementation assays used three yeast null strains QBY320, HM410 and HM402 [135, 146, 147] that had a defective ymLeuRS. QBY320 (MATa ade2-l ura3-l his3-ll, 15trplA63 leu2-3, 112canl-100 msllA::HIS3 [p+] (pQB223)) has a genomic deletion of the NAM-2 gene encoding ymLeuRS, with an insertion of HIS marker. HM410 (MATa ade2-l his3-ll,15 leu2-3,112 trpl-l ura3-l canl-100 nam2A::LEU2 [WT 777-3A]) and HM402 (MATa ade2-l his3-ll,J5 leu2- 3,112 trpl-l ura3-l canl-100 nam2A::LEU2 [A introns]) strains also contain a genomic disruption of the

*ym*LeuRS gene but have a LEU marker. The *ym*LeuRS fused to a MIS sequence is encoded from the maintenance plasmids pQB223 and YEpGMC063 [146] that also contain a URA3 marker in QBY320 and HM410/402, respectively.

2.3 Site-directed mutagenesis

Mutations were introduced into the template plasmid via polymerase chain reaction (PCR). The 50μl reaction contained 100 ng of template plasmid DNA, 125 ng each of forward and reverse primer, 0.05 mM dNTP mix, and 0.05 units of *Pfu* DNA polymerase in commercial buffer. The final PCR mixture was restriction-digested with 0.8 units of *Dpn*I for 4 h at 37 °C and then used to transform *E. coli* strain DH5α. Plasmid DNA was isolated from a 3 ml overnight culture of a single transformant using the QIAprep Spin Miniprep Kit (Qiagen Inc., Hilden, Germany). Mutations were confirmed by DNA sequencing (UIUC Core Sequencing Facility, Urbana, IL).

2.4 Expression and purification of proteins

N-terminal six-histidine-tagged proteins were expressed from the corresponding plasmids in BL21 (DE3) codon PLUS. A single transformant was used to inoculate 3ml LB media, which was then incubated at 37 °C overnight. The overnight culture was used to inoculate

1L LB culture, which was grown at 37 °C until the OD_{600} reached 0.6 to 0.8. Overexpression of the protein was induced with 1mM IPTG and went on overnight at room temperature. The bacteria was pelleted at 6000 rpm for 10 min at 4 °C by an Avanti J-E (Beckman Coulter, Fullerton, CA) preparative centrifuge.

The bacteria pellet was resuspended with 10 ml HA-I buffer [20 mM Na_2HPO_4, 10 mM Tris (hydroxymethyl) aminomethane (Tris) pH 8.0, 100 mM NaCl and 5% glycerol]. This was followed by addition of PMSF protease inhibitor to around 100 mM final concentration and sonication on ice (Vibra-cell 75185, 9 pulses of 10 s at 30% amplitude). The bacteria lysate was centrifuged at 12,000 rpm for 30 min at 4 °C.

The protein-containing clear supernatant was mixed with 1ml of HIS-Select Nickel Affinity Gel (Sigma-Aldrich) that had been washed three times with 10 mL HA-I buffer each time. The N-terminal His-tagged protein in the supernatant was bound to the resin via gentle rocking at 4 °C for 2 h. Following binding, the resin was washed with 50 mL HA-II buffer [20 mM Na_2HPO_4, 10 mM Tris pH 7.0, 500 mM NaCl, and 5% glycerol] at 4 °C. The bound proteins were eluted from the resin using an imidazole gradient from 2mM to 500mM in the HA-I buffer.

Depending on the purity, the eluted fractions that contained the target protein were further purified using size-exclusion chromatography. The eluted target protein was dialyzed into the storage buffer (50 mM KPi pH

7.6, 5 mM MgCl2, 25 mM KCl, 0.1mM EDTA, 5 mM β-mercaptoethanol, 5mM DTT, 50% glycerol). The final protein concentration was determined spectrophotometrically at 280 nm using the corresponding extinction coefficient, estimated by the ExPASy Protparam tool (http://ca.expasy.org/tools/protparam.html).

2.5 Transcription of tRNAs *in vitro*

The templates for *in vitro* transcription were prepared via PCR amplification. The PCR reaction contained 200 μM dNTPs, 2 μM primers, 5 μl BSA, 40 ng plasmid that contains the corresponding tRNA gene, 20 U Vent polymerase (New England Biolabs Inc., Beverly, MA) in commercial buffer at 1 ml total volume. The PCR products were digested with 400 U *Bst*NI at 65 °C for 2 hr and then purified using QIAquick PCR purification kit. The *in vitro* transcription reactions contained 40 mM Tris-HCl (pH 8.3), 20 mM $MgCl_2$, 5 mM dithiothreitol (DTT), 1 mM spermidine, 4 mM each NTP (pH 8.0), 0.05 mg/ml BSA, 0.002 units/ml inorganic pyrophosphatase, 150 ng/μl affinity-purified T7 RNA polymerase (gift from Dr. M. Saks and Dr. C. Weitzel, University of Illinois), and 18 ng/μl DNA template. The reaction mixtures were incubated for four hours at 40 °C, stopped by adjusting the reactions to a final concentration of 25 mM EDTA and 300 mM sodium acetate (pH 5.3).

Transcribed tRNAs were precipitated from the reaction for 30 min at -

20 °C by adding twice the volume of 100% cold ethanol, pelleted at maximum speed at 4 °C and resuspended in 50 µl water. The tRNA products were purified to single nucleotide resolution by electrophoresis on a denaturing 8% polyacrylamide gel, containing 8 M urea. Electrophoresis was carried out in 1 X Tris-Borate-EDTA (TBE) buffer (90 mM Tris, 90 mM boric acid and 2 mM EDTA, pH 8.0) for 6 – 8 hr at 40 mA [lowered in later stage of electrophoresis to avoid gel overheating]. The tRNA bands were visualized via UV shadowing and the bands excised from the gel. For every 500 µl *in vitro* transcription reaction, the tRNAs were eluted from the gels at 4 °C in 10 ml elution buffer (200 mM potassium acetate, 10 mM EDTA, pH 5.4) with rotation overnight. After the eluted tRNA was recovered from the gel fragments using a clinical centrifuge, a second 5ml aliquot of the same elution buffer was added to elute any tRNA left in the gels for 2 hr. The two elutions were combined, and tRNAs were precipitated from the elutions for two days at -20 °C by adding 2× volume of 100% cold ethanol. The pellets were then washed with 5 ml 75% ethanol, dried and resuspended in NaCl solution with final 1 M NaCl concentration. An equivalent volume of 100% ethanol was added to the resuspended tRNA, which was loaded on a spin cartridge (ThermoFisher Scientific, Waltham, MA) and centrifuged at 10,000 g for 2 min. A 100 µl elution buffer (10 mM Tris pH 7.5, 0.1 mM EDTA) that had been pre-heated to 95 °C was added, and centrifuged at 10,000 g for 1

min to elute the bound tRNA. The elution procedure was repeated with another 100 µl elution buffer and the two elutions were combined to yield the final tRNA stock.

Chapter 3. Characterization of bI4 intron splicing-sensitive regions in leucyl-tRNA synthetase

3.1 Introduction

During their lengthy evolutionary pathway, aaRSs have evolved a wide variety of secondary functions (Lambowitz & Perlman, 1990; Martinis et al., 1999) in addition to their housekeeping function in protein synthesis (Ibba & Söll, 2000). Among them, two fungal mitochondrial synthetases, leucyl-tRNA synthetase (*ym*LeuRS or NAM2p) in *Saccharomyces cerevisiae* (Herbert et al., 1988; Labouesse, 1990; Labouesse et al., 1985) and tyrosyl-tRNA synthetase (TyrRS or CYT-18) in *Neurospora crassa* (Akins & Lambowitz, 1987; Paukstelis & Lambowitz, 2008) aid splicing of group I introns from essential respiratory genes.

The *ym*LeuRS collaborates with the bI4 maturase for the excision of the bI4 and aI4α introns from the *cob* and *coxIα* genes respectively (Labouesse et al., 1987; Rho & Martinis, 2000). The *ym*LeuRS gene was implicated in intron splicing in yeast complementation experiments when a LeuRS missense mutation G240S partially suppressed a splicing deficiency caused by a non-functional bI4 maturase mutant (Labouesse et al., 1987). More recently, it was shown that *ym*LeuRS independently

stimulates splicing activity of the bI4 intron, even in the absence of the bI4 maturase (Rho & Martinis, 2000).

The *ym*LeuRS editing domain (connective polypeptide 1 or CP1 domain) and the C-terminal domain that binds the tRNA elbow were identified to contribute to splicing activity (Hsu et al., 2006; Rho et al., 2002; Sarkar et al., 2012). The CP1 domain independently binds to the bI4 group I intron to support splicing of the bI4 intron in the absence of the full-length protein (Sarkar et al., 2012). The isolated CP1 domain also rescued a *ym*LeuRS deletion yeast strain (Rho et al., 2002). This domain contains a hydrolytic active site for amino acid editing (Betha, Williams, & Martinis, 2007; M. T. Boniecki et al., 2008). The 3' end of the mischarged tRNA binds to this threonine-rich area to hydrolyze the mischarged amino acid on the tRNA (Lincecum et al., 2003). A splicing-sensitive site at Trp238 was discovered on the β-strands that connect the CP1 domain to the main body of *ym*LeuRS and was characterized both *in vivo* and *in vitro* (Labouesse et al., 1987; Sarkar et al., 2012). Since Trp238 interacts with the tRNA during the editing reaction (Nawaz, Pang, & Martinis, 2007), it was hypothesized that other splicing sensitive sites should be identified within or in proximity to the editing active site on the CP1 domain.

3.2 Experimental procedures

3.2.1 Strains and strain constructions.

A suppressor mutation called *NAM2-B2* was isolated that rescues splicing activity and respiration in a yeast strain that expressed a bI4 maturase which has been inactivated by the bI4 PZ16 mutation (a frameshift mutation in the middle of the intron reading frame). Strain PZ16 is a respiration-deficient (gly-) mutant derived from strain ID41-6/161 (*MAT**a** ade1 lys1*) (Anziano, Hanson, Mahler, & Perlman, 1982). Like the *NAM2-1* mutation of the LeuRS gene (Dujardin, Pajot, Groudinsky, & Slonimski, 1980), it partially restores bI4 and aI4 splicing, is dominant or semi-dominant and is linked to the *URA4* gene. The mutation in the *NAM2-B2* allele of the *ym*LeuRS gene was defined by sequencing the gene following PCR amplification and cloning of a *Bam*HI fragment containing the reading frame. A single genetic mutation (A818G) was found, which changes Gln273 (CAG) to arginine (CGG) in *ym*LeuRS.

Plasmid pBLSMSL contains the wild-type *NAM2* 1.1 kb *Bam*HI fragment from strain 161 (above) cloned into the pBLSK+ vector (Stratagene Corp., San Diego, CA). Site-directed mutagenesis was used to introduce the A818G mutation into plasmid pBLSMSL to generate plasmid pBSB2. pBSB2 DNA was digested with *Bam*HI and the fragment containing the *NAM2* gene was isolated, mixed with a PCR product

containing the *URA3* gene and used to co-transform a ρ^o derivative of strain a161U7 (*MAT**a** ade1 lys1 ura3*). Uracil prototrophs were selected and screened for the presence of the gene carrying the *NAM2-B2* mutation by mating to strain αMCC109/(*MATαkar1-1 ade2 ura3*) with CI34-PZ25 mtDNA (Henke, Butow, & Perlman, 1995) and testing for haploid cells that can grow on glycerol medium. One of those strains, 161-NAM2-B2/CI34-PZ25 was isolated and used here; the PZ25 mutation is an in-frame stop codon near the beginning of mature bI4 maturase. DNA sequencing following PCR amplification confirmed the presence of the *NAM2-B2* mutation in that strain. Strain 161-NAM2-1/CI34-PZ25 was constructed analogously, starting with a site-directed mutation of the cloned wild-type LeuRS gene. The 161-NAM2-B2/CI34-PZ25, 161-NAM2-1/CI34-PZ25 and 161/CI34 ρ^+ strains all grow comparably well on glycerol medium.

3.2.2 Plasmid construction and mutagenesis for protein purification

The plasmid p14MB-*ym*LeuRS-WT (M.T. Boniecki, 2007) was used to express wild-type *ym*LeuRS. This plasmid was also used as the template to introduce point mutations at Gln273 with primers *ym*-Fwd-(Q273A) (5'-CCGGAAACTCTTTTTGCTGTAGCGTATGTTGCTCTCGCATTAG-3'), *ym*-Fwd-(Q273R) (5'-CGGAAACTCTTTTTGCTGTACGTTATGTTGCTCTCGCATTAGAC-3'), *ym*-Fwd-(L277A) (5'-GCTGTACAGTAT

GTTGCTGCGGCATTAGACCACCCAATTG-3'), to generate plasmids encoding the *ym*LeuRS that contained Q273A, Q273R, L277A mutations respectively via PCR reactions. Mutations were confirmed by DNA sequencing (UIUC Core Sequencing Facility, Urbana, IL).

3.2.3 Complementation of yeast mitochondrial LeuRS null strains.

Mutations were introduced via PCR into plasmid pQB184 for complementation assays with QBY320 (*MAT**a** ade2-1 ura3-1 his 3-11,15, trp1Δ63 leu2-3, 112 an1-100 msl1Δ::HIS3 [ρ+] (pQB223)*. For complementation experiments with HM402 (*MAT ade2-1 his3-11,15 leu2-3,112 trp1-1 ura3-1 can1-100 nam2Δ::LEU2* [introns]), HM410 (*MATα ade2-1 his3-11,15 leu2-3,112 trp1-1 ura3-1 can1-100 nam2Δ::LEU2* [wt 777-3A], and HM411 (*MATΔade2-1 his3-11,15 leu2-3,112 trp1-1 ura3-1 can1-100 nam2Δ::LEU2* [*box7* mutant (V328)] (G. Y. Li et al., 1996; Seraphin, Boulet, Simon, & Faye, 1987), a derivative of the plasmid pQB184/Trp was used which contained either wild-type or mutant LeuRS genes. The pQB184/Trp plasmid was obtained by excising the *LEU2* marker from a pQB184 derivative (containing either the wild-type or mutant LeuRS gene) by a restriction digest with *Sca*I and *Nsi*I and subsequently introducing a *TRP1* marker. The *TRP1* gene was obtained from Yeplac112 (Sugino & Gietz, 1988) via the same restriction digestion

with *Sca*I and *Nsi*I. Details of the complementation experiments for each set of strains and plasmids have been described previously (Houman et al., 2000).

3.2.4 Expression and purification of proteins

Wild-type or mutant *ym*LeuRS proteins were expressed from the respective plasmids in BL21 (DE3) codonPLUS competent cells (Agilent Technologies, Santa Clara, CA) as described in Chapter 2, except that the HA-I and HA-II buffers were supplemented with 50 mM and 250 mM KCl respectively.

3.2.5 Precursor RNA Transcription

Plasmid pM96Δhj1-3 encodes the gene for the shortest bI4 intron deletion mutant bI4Δ1168 precursor RNA (pre-RNA) that has been shown to be catalytically active *in vitro* (M. T. Boniecki et al., 2009). A custom made RNA ladder ranging from 50 to 250 base pairs was used for analyzing the splicing products by gel electrophoresis. Plasmids pUC8MB-250, pUC8MB-200, pUC8MB-150, pUC8MB-100, and pUC8MB-50 (M. T. Boniecki et al., 2009) encode specific RNAs ranging from 250 to 50 base pairs. Each plasmid was isolated from *E. coli* strain DH5α using a Qiagen Plasmid MegaPrep kit-25 (Qiagen, Hilden, Germany). This is followed by restriction digest with either *Bam*HI for the bI4Δ1168 RNA or *Sal*I for the

ladder RNAs. RNA was transcribed using a T7 MEGAscript kit (Thermo Fisher Scientific, Waltham, MA) and 1 μg DNA template at 37 °C for 6 h in a 20 μl reaction. Radiolabeled RNA was obtained by incorporating 10 μCi of [α-^{32}P]-UTP. The bI4Δ1168 pre-RNA was isolated using Chroma Spin-200 + DEPC-H2O columns (Clontech Laboratories, Inc., Mountain View, CA). RNA concentration was estimated optically, based on its extinction coefficient, calculated by the online ambion oligonucleotide calculator. The bI4Δ1168 pre-RNA was folded *in vitro* at 50 °C for 2 min followed by cooling at 37 °C for 10 min. The ladder RNA fragments were isolated by phenol:chloroform:isomyl alcohol [125:24:1] extraction followed by ethanol precipitation. The recovered RNA pellet was washed with 70% ethanol, vacuum-dried, and then dissolved in 50–100 μl of nuclease-free water (Invitrogen Corp., Carlsbad, CA).

3.2.6 LeuRS-dependent *in vitro* splicing assay

The *in vitro* splicing reaction included 1 μM [^{32}P]-labeled bI4Δ1168 pre-RNA (0.13 μCi/μl), 1 μM LeuRS, 150 mM KCl, Stop RNase inhibitor (5 Prime, Inc., Gaithersburg, MD) in 1× splicing buffer (10 mM Tris, pH 7.5, 100 mM NaCl, 5 mM $MgCl_2$, 1 mM EDTA, and 10% glycerol). The reaction was carried out at 37 °C and initiated with 1 mM guanosine. Aliquots of 10 μl were quenched in 10 μl of 5 M urea, 30 mM EDTA, and mixed with 5 μl of RNA loading dye. The mixture was incubated for 10

min at 65 °C and then electrophoresed on a 6% denaturing polyacrylamide gel overnight at 10 mA in 1×Tris/Borate/EDTA (TBE) buffer. The gel was dried and phosphorimaged using a FUJIFILM BAS Cassette 2040 (FUJIFILM Medical Systems, CT).

Products were visualized by scanning the images using a STORM 840 Molecular Dynamics scanner (Amersham Biosciences). Images were quantified with ImageQuant software. Bands representing the precursor RNA, excised intron, and ligated exons were normalized for each time point by determining the fraction of each band relative to the sum intensity of the three bands. In addition, background was subtracted based on the zero time point. Extent of reaction (product/total bands in each lane) was calculated using GraphPad Prism 5 via its single exponential function as described previously (M. T. Boniecki et al., 2009).

3.2.7 Protein-RNA binding assay

Nitrocellulose membranes (0.45 μM), nylon membranes (0.45μM) and blotting papers were pre-incubated in binding buffer (10 mM Tris-HCl pH 7.5, 100 mM NaCl, 5 mM $MgCl_2$, 5 mM DTT, 1 mM EDTA, 100 μg/ml BSA, 10% glycerol). Each 250 μl binding reaction contained 100 nM [α-^{32}P]-UTP labeled RNA, increasing concentrations of 0 to 500 nM WT or mutant LeuRS, and small amounts of heparin (10 μg/ml). The reactions were incubated in binding buffer for 1 h at 37 °C. Solutions were filtered

through nitrocellulose membrane and nylon membrane under vacuum pressure, air dried and then visualized using a phosphorimager as described. Dots on the nitrocellulose membrane represent protein-RNA complex, while dots on the nylon membrane represent unbound RNAs. The K_D was calculated by fitting the data as follows:

$$Y = \frac{K_D + B_{max} + X - \sqrt{(K_D + B_{max} + X)^2 - 4 \times B_{max} \times X}}{2} \times B_{max}$$

where B_{max} is the maximal binding (GraphPad Prism 5, San Diego, CA).

3.3 Results

3.3.1 Characterization of a CP1-based splicing sensitive site

The LeuRS house keeping protein was first identified for its role in group I intron splicing, when a G240S LeuRS mutation *NAM2-1* was found to rescue a bI4 maturase deficiency (Dujardin et al., 1980). However, we wondered if there are other regions of LeuRS that are important to its splicing activity. As such, we screened for suppressor mutations of a bI4 maturase-deficient strain. One mutation called *NAM2-B2*, exhibited somewhat different properties from the *NAM2-1* suppressor. In particular, the strain containing *NAM2-B2* is temperature-sensitive for glycerol growth (data not shown) while the *NAM2-1* strain was temperature resistant, suggesting that the B2 mutation was a novel suppressor. Linkage to *URA4* and 2/2 segregation of glycerol growth from a B2/*Δmsl* PZ25

diploid established that the B2 mutation was an allele of the *NAM2* gene.

Sequencing the gene from the mutant strain revealed a single DNA point mutation, A818G, that changes Gln273 in LeuRS to arginine. We introduced A818G mutation into the wild-type gene by site-directed mutagenesis followed by transformation and confirmed that it suppresses the gly$^-$ phenotype of a strain carrying the PZ25 bI4 maturase mutation. For comparison, we also constructed a related strain with the *NAM2-1* mutation (G240S LeuRS). Both the Q273R and G240S mutant LeuRS suppressed strains grown similarly on glycerol medium. Northern blot analysis shows that the *NAM2-B2* and *NAM2-1* mutations rescue the bI4 maturase defect similarly, splicing approximately 30% of the *coxI* transcripts to yield a 1.9 kb mature *coxI* transcript (Figure 3.1).

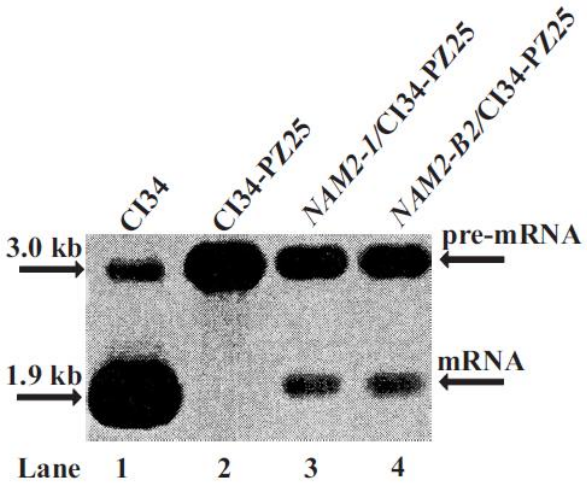

Figure 3.1 Northern blot analysis of *NAM2* mutant suppression of bI4 maturase-based splicing defects. Total cellular RNA was isolated from each yeast strain and separated on a 1.2% denaturing agarose gel. The RNA was transferred for Northern blot analysis, probed with an exon 4-specific oligonucleotide, and quantitated using a Molecular Dynamics phosphorimager. Pre-mRNA and processed mRNA with the bI4 intron excised are marked with arrows respectively at 3.0 kb (upper band) and 1.9 kb (lower band). Lane 1 contains spliced and unspliced RNA from yeast strain CI34, a wild-type control. Lane 2 shows only unspliced pre-RNA from a mitochondrial splicing-defective yeast strain CI34-PZ25 that contains a mutation in the bI4 maturase. Lane 3 demonstrates rescue of the CI34-PZ25 splicing defect by *NAM2-1*. Lane 4 shows suppression of the CI34-PZ25 splicing defect by *NAM2-B2*. This figure is cited from (Henke, 2000).

3.3.2 Mutational characterization of the Gln273 suppressor site.

In previous experiments, we showed that mutation of Gln273 to alanine inactivated CP1-dependent splicing (Rho et al., 2002). Herein, we mutationally analyzed the Gln273 site within wild-type (WT) *ym*LeuRS defined by the *NAM2-B2* mutation by introducing other charged residues including lysine and glutamic acid. Growth tests in a strain that is disrupted for the mitochondrial LeuRS gene (*msl1)* (Houman et al., 2000), but has WT mtDNA showed that mutations of Gln273 to a charged residue support splicing and mitochondrial translation (based on growth on glycerol) while the Q273A allele is defective for one or both functions (Figure 3.2).

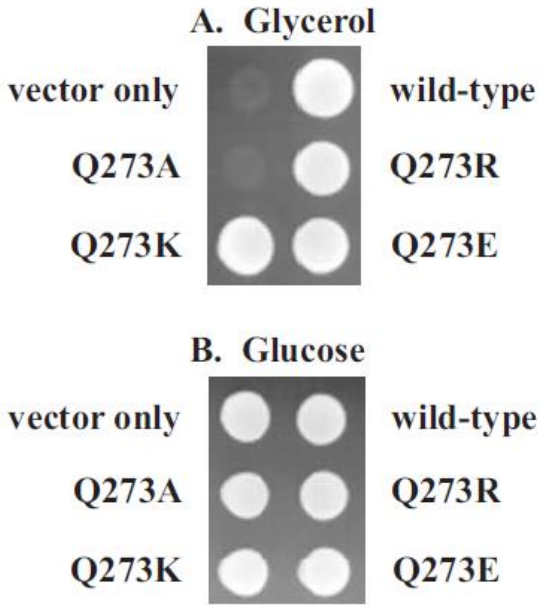

Figure 3.2 Complementation of a yeast strain that contains a null allele of the gene encoding LeuRS. Strain QBY320 was transformed with plasmids that expressed wild-type or various mutant LeuRS genes that contained a substitution at the Gln273 position as indicated. Transformants were purified on 5-fluororotic acid to remove the maintenance plasmid pQB223. The null strain was then tested for grown on glycerol (A.) or glucose (B.) media as described previously. Growth on glycerol medium (white circles) demonstrates that mitochondrial function has been complemented. This work was carried out by S.B. Rho.

We also investigated each of the four Gln273 LeuRS mutations using a series of Δ*msl1* yeast null strains with diagnostic mitochondrial genotypes. Similar to QBY320, HM410 is a wild-type strain. However, its derivative strain HM402 has no introns in its mtDNA and thus does not

rely on RNA splicing for respiratory growth. A third related strain HM411 contains a bI4 maturase mutation that blocks bI4 and aI4α intron splicing. Because some reported LeuRS mutations are temperature sensitive for complementation activity, growth was tested at both 28 ºC and 36 ºC. Both the Q273R LeuRS suppressor mutant (*NAM2-B2*) and the original G240S LeuRS suppressor mutant (*NAM2-1*) complemented the strain lacking the bI4 maturase (HM411) strain at both temperatures demonstrating that they compensate for a defective maturase. Neither the lysine, nor the glutamic acid substitutions suppress the bI4 maturase defect (Figure 3.3). However, the Q273K and Q273E mutant LeuRSs support glycerol growth of the wild-type, intron-containing strain HM410 showing that they effectively collaborate with the bI4 maturase splicing function. As would be expected, these alleles support glycerol growth of the intronless strain, demonstrating that they support LeuRS aminoacylation activity.

Previously, we used three-hybrid assays to determine that the Q273A LeuRS mutant does not bind to the bI4 intron, and thus fails to facilitate the essential splicing activity (Rho et al., 2002). Surprisingly, the Q273A mutant allele does not complement the HM402 intronless strain (Figure 3.3), showing that the mutation not only impedes splicing activity, but also strongly inhibits its function in translation. Thus, the Gln273 site is critical to the enzyme's protein synthesis activity in the yeast mitochondria as well as the RNA splicing activity.

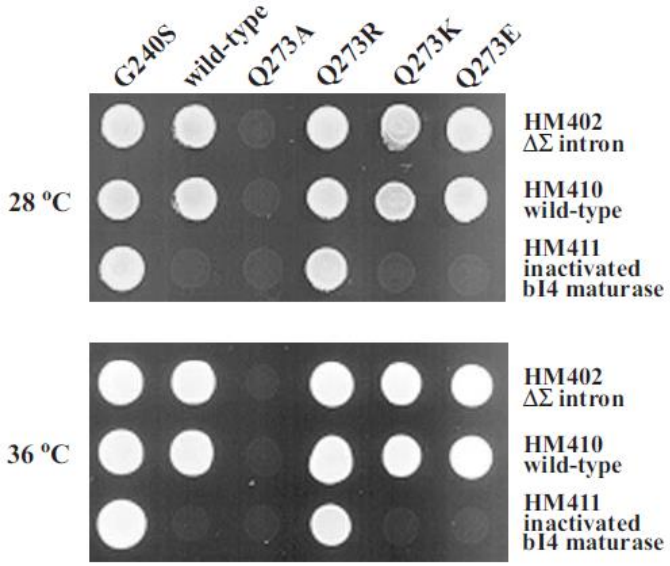

Figure 3.3 Complementation of yeast null strains that contain mitochondrial genome variations. Each of the three null strains have a deletion in the *nam2* allele. The upper row of each plate tested complementation activity of a yeast mitochondrial null strain (HM402) that completely lacks mitochondrial introns (ΔΣ introns). The middle row of each plate represents a null strain (HM410) with a wild-type mitochondrial genome that contains each of the 13 introns. The lower row of each plate tests a null strain that also has a mutant bI4 maturase (V328), which is defective in splicing activity. The plates were incubated on glycerol medium at either 28ºC (upper plate) or 36ºC (lower plate) as described previously (G. Y. Li et al., 1996). This work was carried out by S.B. Rho.

3.3.3 The Gln273 suppressor site modulates RNA binding

We purified the splicing suppressor Q273R LeuRS, as well as the

splicing inactive Q273A LeuRS to test their splicing activity *in vitro*. Similar to *in vivo* complementation results, Q273A mutant exhibited significantly reduced processing of the bI4Δ1168 pre-RNA. The extent of formation of the splicing products bI4 intron and B4-B5 ligated exons was greatly decreased, as compared with the WT *ym*LeuRS. In contrast, the Q273R mutant showed similar intron splicing activity as WT *ym*LeuRS (Figure 3.4 and Figure 3.9).

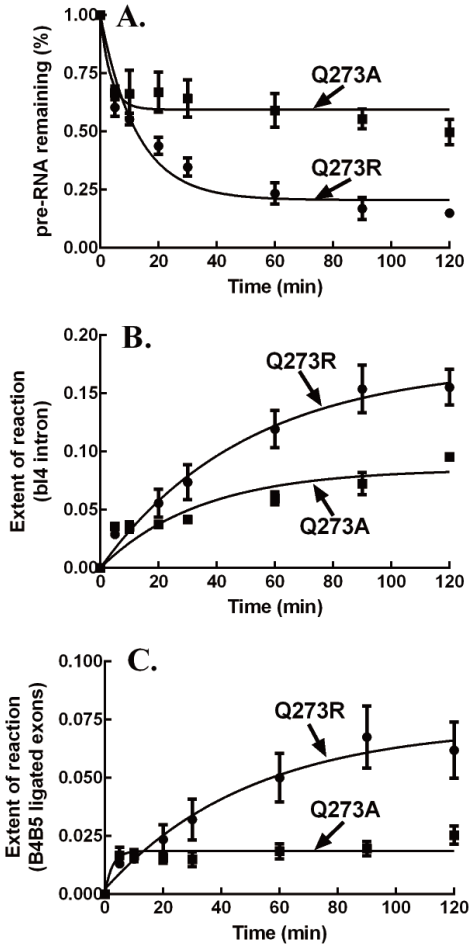

Figure 3.4 Reaction extent for *in vitro* bI4Δ1168 splicing activity of *ym*LeuRS Gln273 mutants. The processing of the bI4Δ1168 pre-RNA was evaluated with respect to substrate pre-RNA processing (A.), fraction of bI4 excised intron (B.), and fraction of the ligated B4-B5 exons (C.). Calculations were based on the intensity of the phosphorimaged bands for the substrate and products bI4 and B4-B5 as well as other alternate bands that emerged during the reaction. Splicing reactions incorporated 1 μM substrate pre-RNA and 1 μM LeuRS and were initiated with 1 mM guanosine. Symbols are: (●), Q273R; (■), Q273A. Error bars for each time point result from each reaction repeated in triplicate.

We also determined binding interactions of LeuRS mutants Q273R and Q273A with the bI4 intron using nitrocellulose binding assay. As would be expected from previously published three-hybrid assays (Rho et al., 2002), the Q273A LeuRS mutant yielded a higher K_D than WT *ym*LeuRS for its interactions with bI4Δ1168 pre-RNA. In contrast, the Q273R LeuRS mutant yielded a similar K_D as WT LeuRS (Table 3.1). In three-hybrid analysis, each of the Q273R, Q273K, and Q273E mutant LeuRSs bound likewise to the bI4 intron (Figure 3.5A).

To confirm the *in vitro* splicing assay results, we isolated RNA from the yeast nucleus of the three-hybrid cells and used RT-PCR to amplify spliced product and the unspliced RNA precursor. In the presence of the Q273R, Q273K, or Q273E mutant LeuRSs, a faint band at 250 bp was produced, supporting that each of these mutant proteins could stimulate bI4 intron splicing in the nucleus (Figure 3.5B). As would be expected, in the absence of LeuRS or the presence of the Q273A mutant LeuRS, spliced product was not detected. We isolated protein from the yeast nucleus of the three-hybrid cells and showed that the Q273A LeuRS mutant is expressed and imported into the yeast nucleus at similar levels to the wild-type protein (Figure 3.5C). Thus, we propose that splicing deficiency of Q273A mutant is the result, at least in part, of compromised binding between the protein and the intron, and that the Q273 site within the CP1 domain of LeuRS is important to splicing activity of the enzyme.

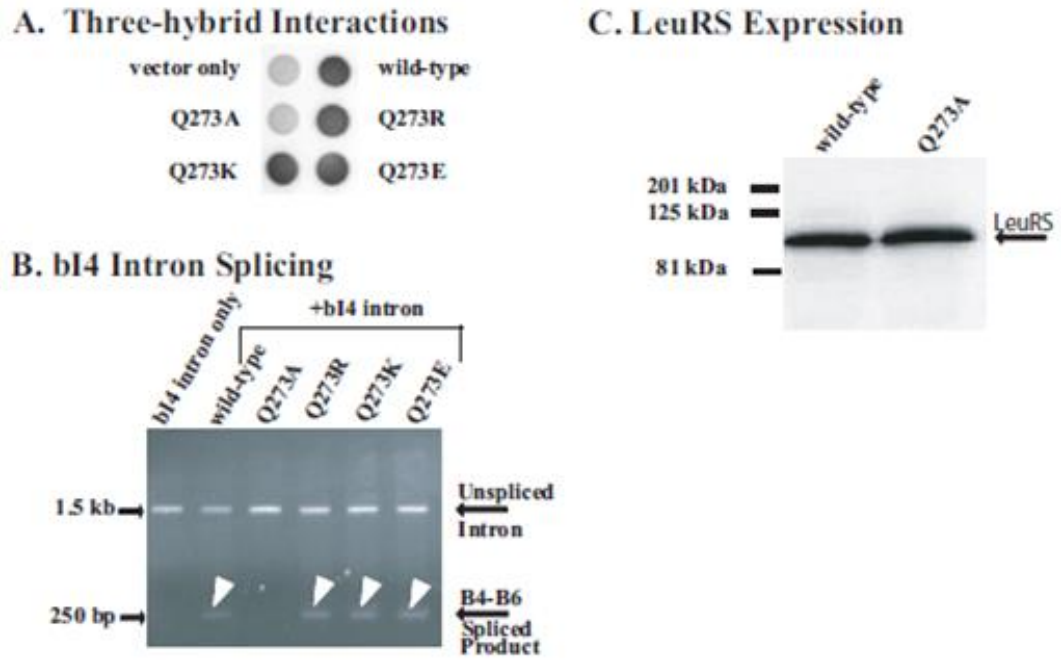

Figure 3.5 Three-hybrid analysis of LeuRS Gln273 mutant-dependent binding and splicing activity of the bI4 intron. A. Three-hybrid binding interactions between the bait bI4 intron fused to the MS2 RNA and wild-type and mutant LeuRS prey that are fused to the B42 activation domain (Rho & Martinis, 2000). Blue color (dark circle in the figure) developed in each case, except when the parent vector control or the Q273A LeuRS were introduced as prey. B. RT-PCR analysis of bI4 intron spliced product. RNA isolated from the nucleus of the L40*ura*MS2 yeast host was amplified by RT-PCR and separated on 1% agarose gels. DNA markers (not shown) identified bands at about 1.5 kb representing unspliced bI4 intron and faint bands at 250 base pairs, marked by white triangles that indicate spliced product. C. Western blot of B42 fused wild-type and Q273A mutant LeuRS. Nuclear proteins were extracted from the L40*ura*MS2 host cells used in the three-hybrid analysis. Anti-V5 antibody was used to detect a 14 amino acid

V5 epitope that is present in each of the prey proteins. A series of protein standards (data not shown) identified the yeast mitochondrial LeuRS band at approximately 120 kDa. This work was carried out by S.B. Rho.

Table 3.1 RNA equilibrium binding constants for wild type and *ym*LeuRS mutants with bI4Δ1168

***ym*LeuRS**	K_D **(nM)**[a]
WT	17 ± 11
Q273R	15 ± 10
Q273A	35 ± 23
L277A	36 ± 23

[a]Standard error is based on measurements that were repeated at least in triplicate.

3.3.4 Alanine scan of the Gln273 splicing suppressor region identifies a second splicing-sensitive site

A LeuRS primary sequence alignment of the neighboring amino acid sites of Gln273 show that it is not conserved (Figure 3.6). Indeed, the glutamine residue is only found in the mitochondrial enzyme from another fungus, *Neurospora crassa*. Upstream is a threonine-rich region that has been shown to be important for the amino acid specificity in LeuRS's hydrolytic editing activity (Mursinna, Lincecum, & Martinis, 2001).

Further downstream (not shown) is another conserved region that comprises a portion of the enzyme's editing active site.

We performed alanine-scanning mutagenesis of the region containing Q273, as indicated in Figure 3.6, to screen for other sites in proximity to this amino acid editing region that might also affect bI4 splicing. The five non-alanine residues were individually mutated to alanine and tested for complementation using the QBY320*Δmsl* strain that lacked yeast mitochondrial LeuRS (Figure 3.7). Only one mutation, L277A, blocked complementation. We also tested each of these LeuRS alanine mutants for protein-RNA interactions with the bI4 intron via three-hybrid assays. With the exception of the L277A LeuRS mutant, each of the mutant LeuRSs bound to the bI4 intron and stimulated splicing activity based on RT-PCR analysis. We analyzed protein expression and import levels for the L277A LeuRS in this system and determined that the L277A mutant LeuRS was present at a level that approximates that of the wild-type LeuRS (Figure 3.8). This supports that the structural integrity of the LeuRS mutant is largely intact. It also supports that the Leu277 site influences the bI4 interaction.

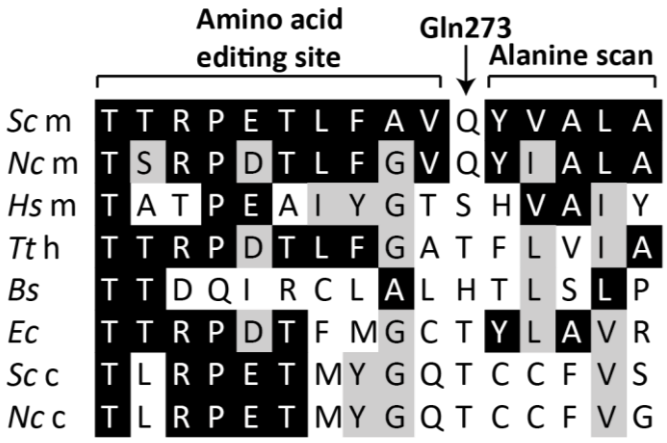

Figure 3.6 Primary sequence alignment of the Gln273 splicing suppressor region within the CP1 domain of LeuRS proteins. Yeast mitochondrial LeuRS (*Sc*m) is shown at the top. Amino acid residues that are conserved or homologous to the yeast mitochondrial LeuRS sequence are highlighted in black or grey, respectively. An upstream threonine-rich region is critical to the enzyme's hydrolytic editing activity (Mursinna et al., 2001; Mursinna & Martinis, 2002). The abbreviations are as follows: *Sc*, *S. cerevisiae*; *Nc*, *N. crassa*; *Hs*, *Homo sapiens*; *Tth*, *Thermus thermophilus*; *Bs*, *Bacillus subtilis*; *Ec*, *Escherichia coli*; c, cytoplasmic; and m, mitochondrial.

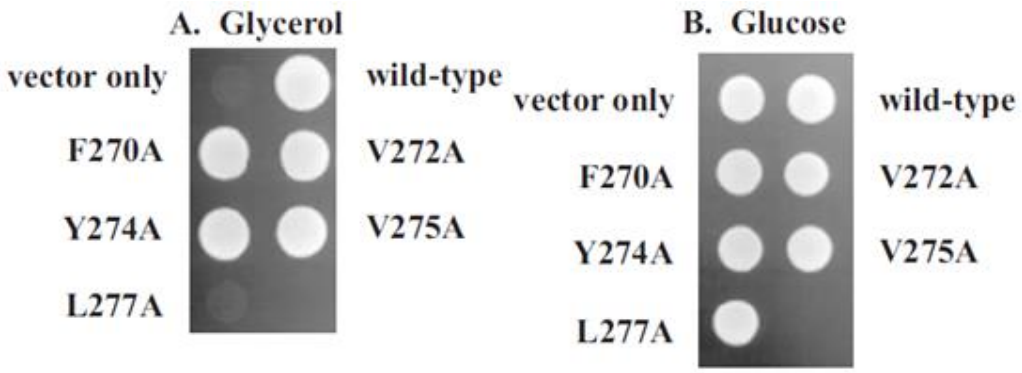

Figure 3.7 Complementation of QBY320 by alanine-scanned mutations in the Gln273 splicing suppressor region. The experiments were carried out as described in Figure 3.2. The null strain was tested for growth on media that contained glycerol (A.) or glucose (B.). This work was carried out by S.B. Rho.

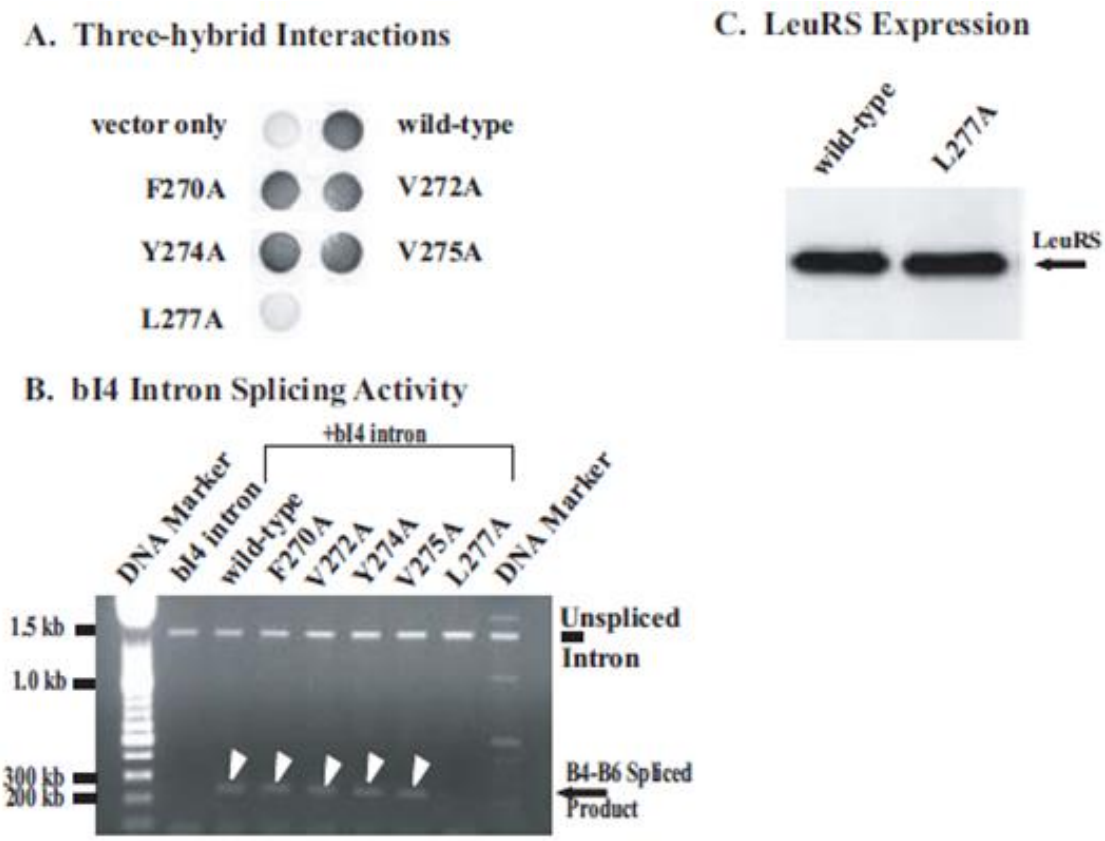

Figure 3.8 Three-hybrid analysis and splicing activity of the alanine-scanned mutation in the Gln273 splicing suppressor region. Experiments were carried out as described in Figure 3.5. A. Cells that exhibit β-galactosidase reporter activity are blue (or dark) colored indicating that the mutant LeuRS prey protein interacts with the bI4 intron. B. RT-PCR analysis. A faint band highlighted by a white triangle represents the spliced product at 250 base pairs. Unspliced bI4 intron is represented by a band at about 1.5 kb. A diffuse band near the bottom of the gel is due to excess primers. Band sizes were determined by two different sets of DNA markers shown in the outside lanes. C. Western blot of B42 fused wild-type and L277A mutant LeuRS. This work was carried out by S.B. Rho.

As would be expected from *in vivo* experiments, affinity-purified L277A LeuRS mutant exhibited significantly reduced processing of the bI4Δ1168 pre-RNA. The extent of formations of the bI4 intron and B4-B5 ligated exons products *in vitro* was greatly decreased compared with WT *ym*LeuRS (Figure 3.9). In addition, nitrocellulose binding assay showed that binding between the L277A mutant and the bI4 intron is compromised compared with WT *ym*LeuRS (Table 3.1). The two-fold change of K_D in binding has dramatic effects on splicing activity *in vivo*.

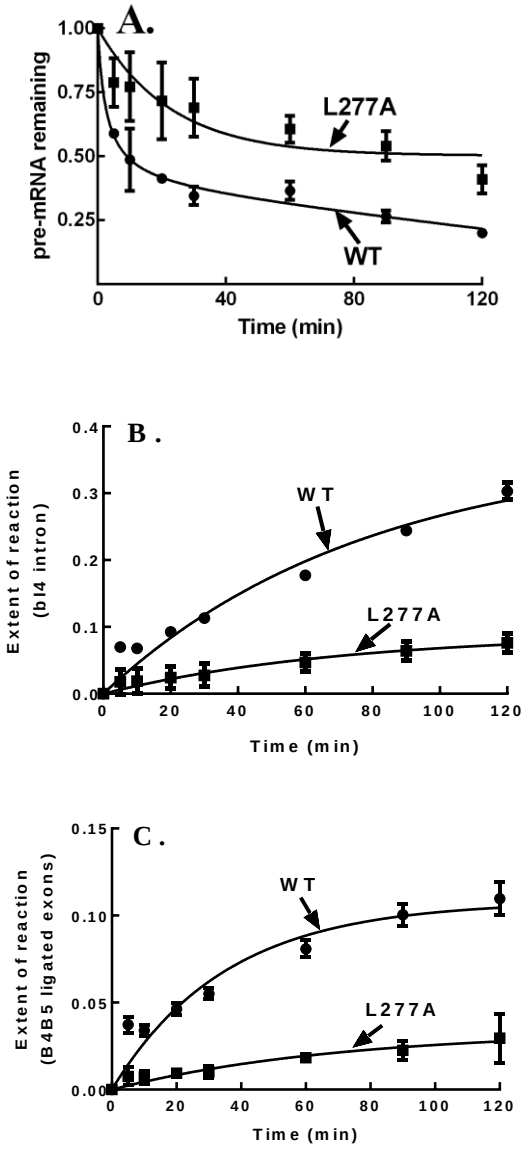

Figure 3.9 Reaction extent for *in vitro* bI4Δ1168 splicing activity of *ym*LeuRS L277A mutant. The processing of bI4Δ1168 pre-RNA was evaluated with respect to substrate pre-RNA processing (A.), fraction of bI4 excised intron (B.), and fraction of the ligated B4-B5 exons (C.). Splicing reactions incorporated 1 μM substrate pre-RNA as well as 1 μM LeuRS and were initiated with 1 mM guanosine. Symbols are: (●), WT; (■), L277A. Error bars for each time point result from each reaction repeated in triplicate.

3.4 Discussion

The bifunctional LeuRS is not only required for protein synthesis (Ibba & Söll, 2000; Pang et al., 2014; Ribas de Pouplana & Schimmel, 2001a), but also in excision of bI4 and aI4α group I introns of the *cob* and *coxIα* pre-mRNAs respectively in yeast mitochondria (Slonimski et al., 1978). The mitochondria-encoded bI4 maturase and the nuclear-encoded LeuRS work in concert as a ternary complex onto the bI4 intron to promote splicing (M. T. Boniecki et al., 2009; Herbert et al., 1988; Labouesse, 1990; Labouesse et al., 1985; Rho & Martinis, 2000). A direct role of LeuRS in splicing has been established, where LeuRS independently binds to the bI4 intron and facilitates splicing both *in vivo* and *in vitro* (M. T. Boniecki et al., 2009; Rho & Martinis, 2000). Here we show that intron binding is modulated, at least in part, by a discrete region of the CP1 domain that is distinct from its editing active sites.

The structure of *ym*LeuRS was modeled based on the X-ray structure of *Ec*LeuRS (Palencia et al., 2012; Rho et al., 2002). The splicing sensitive Gln273 and Leu277 sites in the structure are located on the two ends of the β3 strand in the CP1 domain. The Gln273 site is located on the surface while Leu277 is buried (Figure 3.10). We hypothesized that Gln273 provides critical direct contact with the intron via its polar group. Thus, substitution of charged arginine (Q273R) rescued splicing deficient bI4 maturase by stabilizing *ym*LeuRS interaction with the bI4 intron. We

hypothesized that Leu277 impacts splicing by sterically positioning the β3 strand along an orientation to optimize Gln273-dependent splicing. In proximity to Gln273, potential intron binding sites are identified on the surface of the CP1 domain, including two positively-charged residues as well as several polar but uncharged residues. These amino acids are proposed to comprise the intron face of the CP1 domain. Interestingly, this intron face is distinct from the tRNA face where tRNA binding sites are centralized on the CP1 domain, and suggests that at least a portion of the intron binding face has evolved independent of the LeuRS tRNA binding face. This is similar to TyrRS from *N. crassa*, which also has the intron and tRNA binding sites on two distinct sides of the protein (Paukstelis et al., 2008).

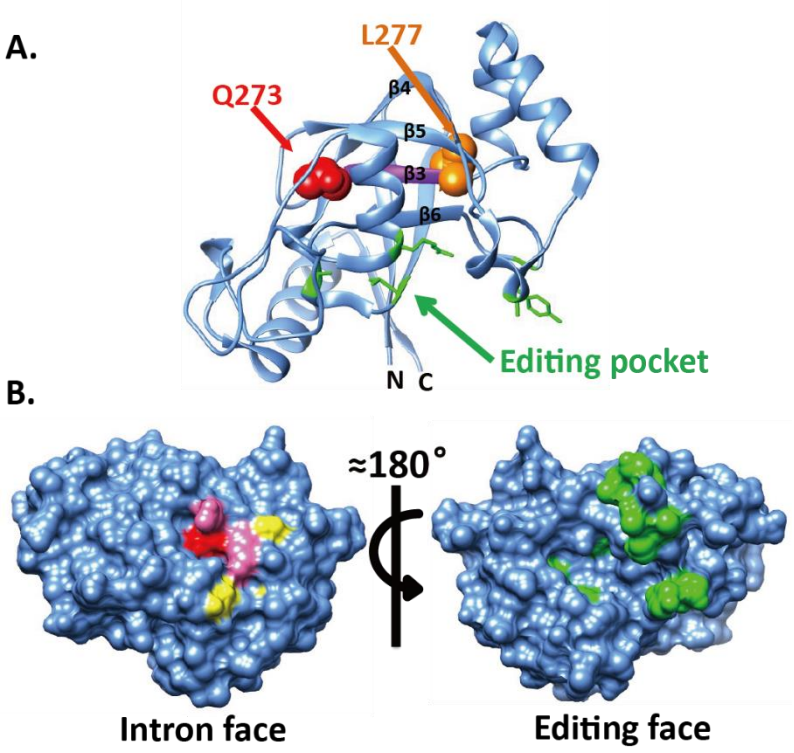

Figure 3.10 bI4 intron face is distinct from the editing face of the LeuRS CP1 domain. The *ym*LeuRS structure is modeled from the X-ray structure of *Ec*LeuRS. A. Gln273 (red) and Leu277A (orange) are located at the two ends of the β3 strand (purple). Editing sensitive sites are colored in green. B. Intron face and editing face are located on opposite sides of the LeuRS CP1 domain. The intron face is composed of Gln273 (red), positively charged K371 and H369 (pink) and polar but uncharged T372, S413 and T324 (yellow). The editing face is colored in green.

Although LeuRSs from different origins could facilitate bI4 intron splicing (Houman et al., 2000), the CP1 domain of *ym*LeuRS has diverged to optimize splicing of the bI4 intron in yeast mitochondria. The CP1 domain along with its two connecting β-strands (*ym*CP1-βext) stimulates

intron splicing both *in vivo* and *in vitro*, whereas compromised in deacylation activity (Sarkar et al., 2012). It is curious that the robust post-transfer editing activity of *ym*LeuRS appears to be dispensable to cell survival. Significantly, human mitochondrial LeuRS has completely lost its editing function (Lue & Kelley, 2007). It is possible that yeast mitochondria has evolved to tolerate increased translational infidelity or alternatively has acquired specificity in the aminoacylation site to increase fidelity via a different mechanism. It is implicated that the *ym*LeuRS has devoted its CP1 domain more to facilitate intron splicing than tRNA editing.

Chapter 4. Identification of splicing sensitive sites in non-splicing *E. coli* leucyl-tRNA synthetase

4.1 Introduction

Yeast mitochondrial leucy-tRNA synthetase (*ym*LeuRS) has two essential functions: aminoacylation and splicing of bI4 and aI4α introns (Pang et al., 2014). *Escherichia coli* (Ec), *Mycobacterium tuberculosis* (*Mtb*) and human mitochondrial (*hm*) LeuRS have been shown to substitute in both functions for *ym*LeuRS *in vivo* (Houman et al., 2000). Among them, EcLeuRS has been shown to have comparable bI4 intron splicing activity as *ym*LeuRS in *in vitro* splicing assay (Sarkar et al., 2012). The above discoveries indicate that features responsible for splicing function of *ym*LeuRS is broadly conserved in different organisms. Furthermore, the CP1 domain as well as the C-terminal domain have been identified to be involved in *ym*LeuRS splicing (Hsu et al., 2006; Rho et al., 2002; Sarkar et al., 2012). The *ym*LeuRS CP1 domain alone is sufficient to perform bI4 intron splicing function *in vivo* (Rho & Martinis, 2000) and *in vitro* (Sarkar et al., 2012). In contrast, the CP1 domain of *Ec*LeuRS lacks splicing function (Sarkar et al., 2012). This infers that not only universal sites but also unique sites on *ym*LeuRS and *Ec*LeuRS respectively are utilized to aid

intron splicing. For *ym*LeuRS, one of those unique sites is a Q273 region on the CP1 domain, which lacks corresponding conserved sites in *Ec*LeuRS. This Q273 region of *ym*LeuRS has been identified to be splicing sensitive both *in vivo* and *in vitro* (Chapter 3).

On *Ec*LeuRS CP1 domain, there is a highly conserved threonine-rich region that contributes to editing activity of LeuRS (Figure 4.1). Within this region a conserved T252 residue acts as a key amino acid discriminator to block cognate leucine from binding (Mursinna et al., 2001), but allows binding and hydrolytic editing of other non-cognate amino acids. Within the *Ec*LeuRS CP1 domain, a second less conserved region downstream of the threonine-rich region also appears to influence editing activity. In this less conserved region, A293 residue's role in aminoacylation and fidelity was discovered by mutational and computational characterization of *Ec*LeuRS (J. F. Chen, Li, Wang, & Wang, 2001; Du & Wang, 2002, 2003; Lee & Briggs, 2004; T. Li, Guo, Xia, Wang, & Wang, 1999). Specifically, the A293D mutation rescues post-transfer editing deficiency in T252Y mutant presumably by activating a pre-transfer editing pathway (Williams & Martinis, 2006). Herein, we demonstrate that A293 is also a splicing sensitive site for *Ec*LeuRS.

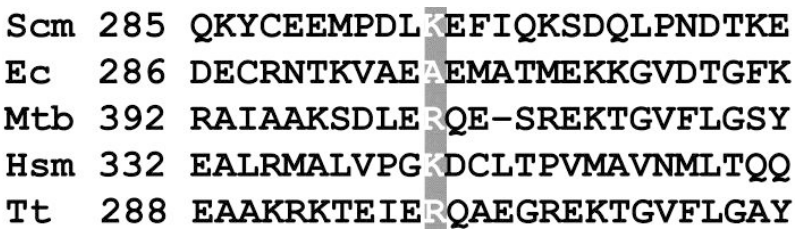

Figure 4.1 Multiple sequence alignments of LeuRSs from diverse origins spanning the semi-conserved alanine. Grey shading indicates the semi-conserved site. Abbreviations are as follows: Yeast mitochondria (Scm), *E. coli* (Ec), *M. tuberculosis (Mtb*), human mitochondria (Hm) and *T. thermophilus* (Tt). This figure is cited from (Poruri, 2007).

4.2 Materials and methods

4.2.1 Cloning and PCR mutagenesis

The *E. coli* LeuRS (*Ec*LeuRS) gene in the resultant clone pRicE1, was out of frame with respect to the mitochondrial import sequence (MIS) and a stop codon was generated after the MIS (Figure 4.3A). The plasmid clone pRicE1 was used as a template to generate mutant clones using site directed mutagenesis by PCR. Denaturation was carried out at 95°C for 30 s followed by annealing at 55 °C for 30 s and then extension at 68 °C for 20 min. After 16 cycles, the PCR reaction was incubated at 68 °C for 20 min. Each mutation was confirmed by DNA sequencing (Seqwright, Houston, USA). The PCR mutagenesis was used to generate the plasmids pMPA293D*e, pMPA293K*e and pMPA293R*e that contained A293D, A293K and A293R mutations in *Ec*LeuRS respectively. The frame shift

within the pRicE1 was corrected to generate the plasmid pKIRAN (Karkhanis, Boniecki, Poruri, & Martinis, 2006) that expressed *Ec*LeuRS gene in-frame with MIS. The plasmid pKIRAN was utilized in PCR mutagenesis to generate pMPA293D, pMPA293K and pMPA293R plasmids that expressed A293D, A293K and A293R *Ec*LeuRS mutant proteins in-frame with MIS.

4.2.2 Yeast complementation assays.

Complementation assays used two yeast null strains, HM410 and HM402 that had a defective ymLeuRS. Competent cells for the null strains HM410 and HM402 were transformed with plasmids pKIRAN, pMPA293D, pMPA293K and pMPA293R encoding wild type *Ec*LeuRS, A239D, A293K and A293R mutant *Ec*LeuRSs respectively or with pMPA293D*e, pMPA293K*e and pMPA293R*e encoding the mutant proteins that were expressed out-of-frame with respect to the MIS.

4.2.3 Plasmids used in protein purification and RNA *in vitro* transcription

The following plasmids are used to express proteins and transcribe RNAs for the *in vitro* splicing assays.

Table 4.1 Plamids used in protein expression and RNA *in vitro* transcription

Protein/RNA encoded	Plasmid name	Reference
*Ec*LeuRS-WT	p14MB-*Ec*LeuRS-WT	(M.T. Boniecki, 2007)
*Ec*LeuRS-A293D	p14MB-*Ec*LeuRS-A293D	(M.T. Boniecki, 2007)
*Ec*LeuRS-A293K	p14MB-*Ec*LeuRS-A293K	(M.T. Boniecki, 2007)
*Ec*LeuRS-A293R	p14MB-*Ec*LeuRS-A293R	(M.T. Boniecki, 2007)
bI4Δ1168 pre-mRNA	pM96Δhj1-3	(M. T. Boniecki et al., 2009)

4.2.4 Protein purification

Plasmids expressing the desired proteins (Table 4.1) were used to transform *E. coli* BL21 (DE3) codon plus strain (Agilent Technologies, Santa Clara, CA). Bacteria cultures were grown at 37°C and were induced with 1 mM isopropyl β-D-1-thiogalactopyranoside (IPTG) for protein expression at room temperature overnight. The N-terminal six-histidine-tagged fusion protein was purified and quantified as described in Chapter 2.

4.2.5 Circular Dichroism (CD)

CD measurements were carried out using a Jasco J-720 spectropolarimeter. A sample containing 0.8 μM protein in 5 mM KPi, pH 7.5, was measured in the far-ultraviolet region using a 0.1 cm path cell. Background signals from the cell and the buffer were subtracted from each spectrum.

4.2.6 Transcription of tRNAs *in vitro*

About 500 µg of the plasmid DNA was digested for 6 h at 60°C with 25 U of with *Bst*NI to linearize the plasmid. The digested plasmid was used as a template for an *in vitro* transcription reaction containing 40 mM Tris (pH 8.0), 30 mM $MgCl_2$, 5 mM DTT, 0.01% Triton-X 100, 50 pg/ml BSA, 7.5 mM each of ATP, GTP, CTP and UTP, 80 mg/ml polyethylene glycol 8000 (PEG 8000), 5 mM spermidine, 40 U/ml RNAase inhibitor (Eppendorf, Hamburg, Germany), 8 µg/ml inorganic pyrophosphatase (PPiase), and 800 nM T7 RNA polymerase (Milligan, Groebe, Witherell, & Uhlenbeck, 1987; Sampson & Uhlenbeck, 1988). The reaction mixture was incubated for 3 h at 42°C, followed by a second addition of 800 nM T7 RNA polymerase, which was then incubated for an additional 3 h at 42°C.

The tRNA was purified on a 10 % polyacrylamide (19:1), 8 M urea denaturing gel. The tRNA band was detected via UV shadowing, excised from the gel followed by extraction in 500 mM ammonium acetate and 1 mM ethylenediaminetetraacetic acid (EDTA), pH 8.0 at 37 °C overnight. The supernatant was collected and the extraction repeated two more times. It was then combined and filtered through a 0.2 µm syringe filter. Butanol extractions were used to concentrate the RNA solution to 500 µl followed by addition of 10 µl of 25 mg/ml glycogen and 1 ml ethanol for an overnight precipitation at -80°C. The tRNA pellet was washed twice with

70% ethanol and precipitated. Purified $tRNA^{Leu}$ was denatured at 80°C for 1 min, followed by addition of 1 mM $MgCl_2$ and quick-cooling on ice to re-fold. The concentration of tRNA was measured by absorbance at 260 nm.

4.2.7 Aminoacylation assays

Leucylation of *in vitro* transcribed $ymtRNA^{Leu}$ and $EctRNA^{Leu}$ was carried out with 50 nM or 1 μM of the wild type and mutant proteins and 4 μM $tRNA^{Leu}$. The aminoacylation reactions also contained 60 mM Tris (pH 7.4), 10 mM $MgCl_2$, 1 mM dithiothreitol (DTT), and 20 μM [^{3}H]-leucine (152 Ci/mmol). The reactions were initiated with 4 mM ATP. Subsequently, 5 μl aliquots were quenched on Whatman grade 3 filter pads (Kent, UK) that were pre-wet with 5 % TCA. The pads were then washed three times for 10 min in cold 5 % TCA, 10 min in cold 70 % ethanol followed by drying with ethyl ether (anhydrous). The radioactivity of the dried pads was quantitated using an LS 6000SC scintillation counter (Beckman).

4.3 Results

4.3.1 Substitutions at A293 in *E. coli* LeuRS do not alter yeast mitochondrial function.

It has been shown that *Ec*LeuRS, *Mtb*LeuRS and *hm*LeuRS compensated for the absence of the endogenous *ym*LeuRS in its bi-

functional roles protein synthesis and group I intron splicing (Houman et al., 2000; Sarkar et al., 2012). We further screened for molecular determinants that govern group I intron splicing in the non-splicing *Ec*LeuRS.

The CP1 domain is responsible for both amino acid editing (Betha et al., 2007; Lincecum et al., 2003; Mursinna et al., 2004; Mursinna et al., 2001) and RNA splicing activity (Rho et al., 2002; Sarkar et al., 2012). A CP1 based key residue, A293, in *Ec*LeuRS was identified to be important for rescue of alternate editing pathway (Williams & Martinis, 2006). It is a semi-conserved amino acid which occurs across various LeuRSs either as an alanine or a positively charged residue (Figure 4.1). However, in *ym*LeuRS there is very little homology within this region when compared to other LeuRSs.

Mutants at the A293 position were also analyzed for their bi-functional roles in the null strains of yeast. We introduced positive and negative charged substitutions at the A293 position in *Ec*LeuRS. The A293K, A293R and A293D LeuRS mutants were tested in complementation assays to determine their effect on yeast mitochondrial protein synthesis and intron splicing. All of these *Ec*LeuRS mutants compensated for the dual roles of the endogenous *ym*LeuRS (Figure 4.2A). Nevertheless, *in vitro* leucylation of *ym*tRNA^{Leu} demonstrated that the A293D substitution had a significant decrease of aminoacylation activity when compared to the

A293K and A293R mutant enzymes which exhibited similar activity to the wild type enzyme (Figure 4.2B).

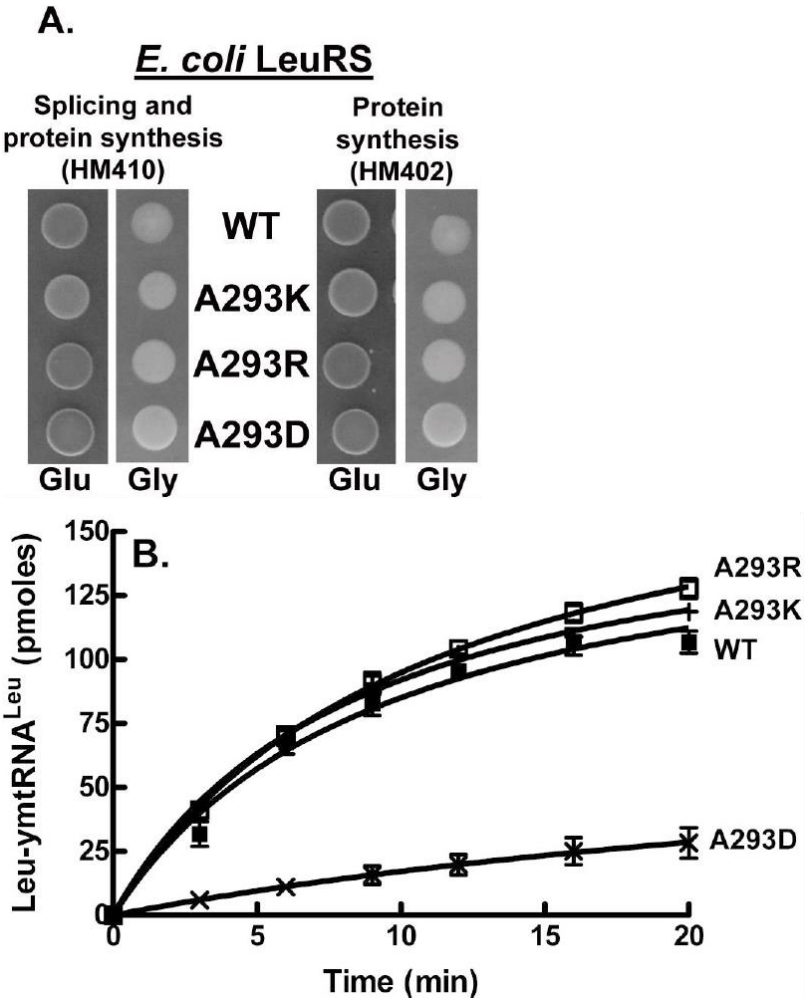

Figure 4.2 Complementation and aminoacylation activities of EcLeuRS semi-conserved alanine mutants. A. Complementation of the yeast null strains by the A293K, A293R and A293D *Ec*LeuRS mutants. Growth on glycerol media is due to mitochondrial function, which is indicated by red color (dark in the figure) on glucose media (due to an *ade*-

2 mutation (Strathem, 1982)). B. Leucylation of *ym*tRNA^{Leu} by the A293 mutant EcLeuRSs. Aminoacylation of *ym*tRNA^{Leu} was carried out with 50 nM of the enzyme and 4 μM *in vitro* transcribed tRNA. The *Ec*LeuRSs used in the assay were: wild type (■); A293K (+); A293R (□) and A293D (×). This figure is cited from (Poruri, 2007).

4.3.2 Low expression levels of *Ec*LeuRS in yeast mitochondria fail to support splicing activity.

A clone containing the *Ec*LeuRS gene was isolated that failed to complement the HM410 yeast null strain that requires both of the LeuRS protein synthesis and splicing functions. DNA sequence determined that the upstream mitochondrial import sequence (Houman et al., 2000) was frame shifted due to the presence of a stop codon after the mitochondrial import sequence (Figure 4.3A). We hypothesized that the *Ec*LeuRS was produced at reduced levels when this clone was allowed to express in the yeast mitochondria, but were unable to isolate the protein from mitochondrial extracts for quantitation. The frame shift clone is represented by *Ec*LeuRS*. When tested in complementation assays involving the yeast null strains, *Ec*LeuRS* complemented the intronless strain (HM402) but were unable to facilitate growth of the wild type (HM410) strain on glycerol media (Figure 4.3B). Thus *Ec*LeuRS was expressed at amounts that were imported into the mitochondria that were

just sufficient enough to support protein synthesis activity, but not the alternate functions.

Since the A293D *Ec*LeuRS mutant had low levels of leucylation activity *in vitro,* we utilized the same mutant in the *Ec*LeuRS* expression system to detect its effect on mitochondrial viability. When the A293 was mutated to aspartic acid (A293D*) and expressed from the *Ec*LeuRS* clone, it failed to complement both the intron containing (HM410) and also the intronless (HM402) strain on glycerol media (Figure 4.3B). Thus, the mutant was unable to aid in mitochondrial protein synthesis at reduced levels of protein expression.

We further tested the importance of this CP1-based semi-conserved site of *Ec*LeuRS by introducing positively charged lysine and arginine at the A293 residue. The positively charged substitutions A293K and A293R that were hypothesized to be expressed at low levels from the *Ec*LeuRS* clone rescued complementation activity in the strain that lacked mitochondrial introns showing that it could aid in protein synthesis. Surprisingly, these also complemented the wild type yeast null strain, suggesting that this site can adapt to support RNA splicing as well as protein synthesis. RNA analysis by northern hybridization revealed spliced B4-B5 exon products in the presence of the A293K and A293R mutant LeuRS enzymes but not for *Ec*LeuRS* wild type or EcLeuRS* A293D mutant (Figure 4.3C).

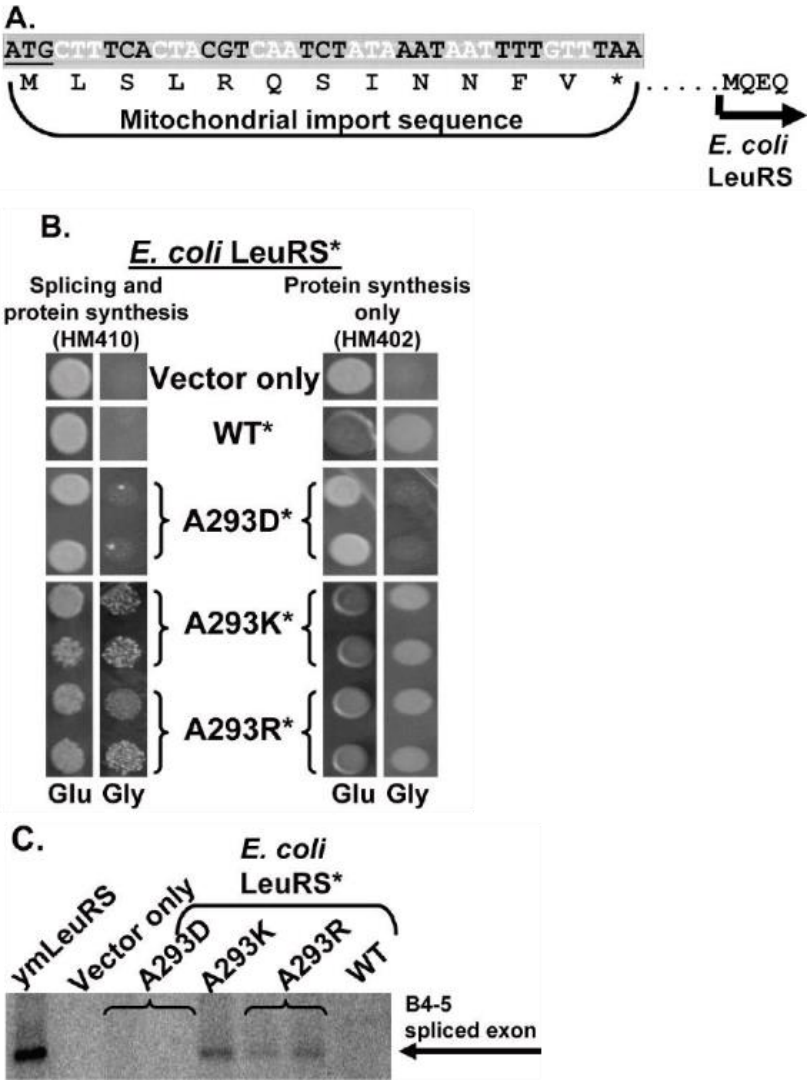

Figure 4.3 Expression of reduced levels of EcLeuRS wild type and mutant proteins in yeast mitochondria. A. Mitochondrial import sequence of *Ec*LeuRS* represented in grey shading. Black and white letters indicate alternate triplet codons. The stop codon is represented by an asterisk (*). The arrow represents the beginning of the *Ec*LeuRS gene. B. Complementation activity of *Ec*LeuRS mutants in yeast null strains. Growth on glycerol media indicates functional mitochondria, which is also represented by dark colored colony on glucose media (due to an *ade-2* mutation (Strathem, 1982)). C. Northern hybridization of yeast total

cellular RNA. RNA extracted from the yeast null strain HM410 cells expressing wild type *Ec*LeuRS* and A293D, A293K and A293R mutant enzymes was separated on 1% formaldehyde agarose gel and hybridized with a probe that represented the B4-B5 exon junction. This figure is cited from (Poruri, 2007).

4.3.3 The A293 residue of *Ec*LeuRS is splicing sensitive *in vitro*

To confirm the *in vivo* complementation results, A293D, A293K and A293R *Ec*LeuRS mutants were affinity-purified and tested in *in vitro* splicing assay. WT *Ec*LeuRS was already tested in a previous publication and exhibited comparable splicing activity as WT *ym*LeuRS. Here the A293D mutant demonstrated decreased splicing activity compared with wild-type *Ec*LeuRS, whereas A293K maintains the same activity (Figure 4.4). A293R has significantly lower splicing activity than A293K, but still higher than A293D. These results are in accordance with the northern hybridization results in Figure 4.3C, in which A293D yielded no spliced exon, whereas one of the A293R duplicated results showed less amount of spliced exon compared with A293K. The kinetics of the splicing reactions is summarized in Table 4.2. This figure is cited from (Poruri, 2007).

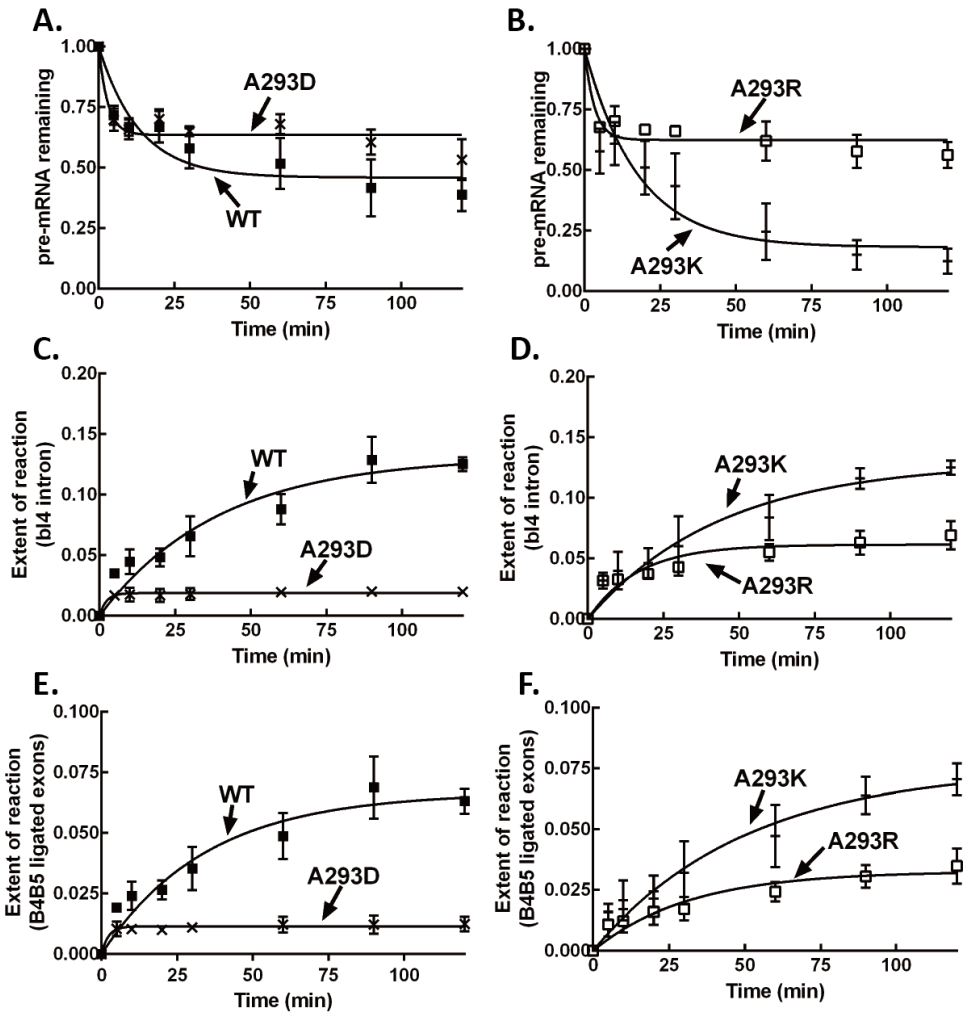

Figure 4.4 splicing activity of EcLeuRS mutants *in vitro*. Evaluation of *in vitro* bI4Δ1168 pre-RNA splicing with respect to (A & B) processing of substrate pre-RNA, (C & D) fraction of bI4 excised intron, and (E & F) fraction of the ligated B4-B5 exons is shown. Splicing reactions incorporated 1μM concentrations of substrate pre-RNA and 1μM LeuRS and were initiated with 1 mM guanosine. The *E. coli* LeuRSs used were: wild type (■); A293K (+); A293R (□) and A293D (×). Error bars for each time point result from each reaction repeated in triplicate.

Table 4.2 Observed (k_{obs}) values for bI4 intron splicing[a]

***Ec*LeuRS**	**Pre-RNA**	**B4-B5**	**bI4 intron**
	$k_{obs} \times 10^{-3}\ min^{-1}$	$k_{obs} \times 10^{-3}\ min^{-1}$	$k_{obs} \times 10^{-3}\ min^{-1}$
WT	74 ± 16	29 ± 6	25 ± 5
A293D	334 ± 111	444 ± 225	451 ± 235
A293K	57 ± 11	20 ± 5	23 ± 5
A293R	306 ± 86	32 ± 7	61 ± 11

[a]Standard error is based on measurements that were repeated at least in triplicate.

Circular dichroism (CD) was carried out to check whether the aminoacylation or splicing deficiencies in the mutants were caused by structural change. Figure 4.5 reveals that all of the mutations minimally affect secondary structure of the protein, as their CD spectra overlap with the wild-type LeuRS. Therefore, low splicing activity in A293R and splicing deficiency in A293D mutant are not caused by structural disruption.

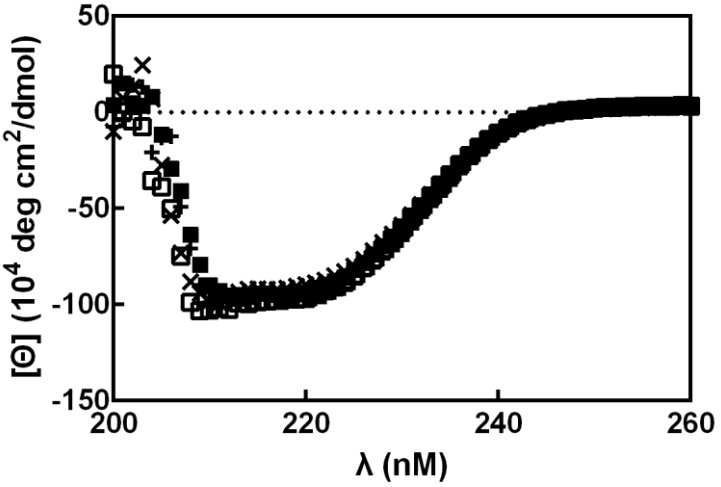

Figure 4.5 CD spectra of the *Ec*LeuRS wild-type and mutant proteins. Protein samples were prepared in 5 mM KPi, pH 7.5. The *E. coli* LeuRSs used were: wild type (■); A293K (+); A293R (□) and A293D (×).

4.4 Discussion

We have shown that when expression level is high, all of the mutants (A293D, A293K and A293R) as well as the wild-type *Ec*LeuRS compensated for splicing function of yeast mitochondrial LeuRS *in vivo*. When expression level is low, only A293K and A293R but not A293D or WT EcLeuRS complemented for splicing. In *in vitro* splicing results and northern hybrid analysis, A293K has similarly high splicing activity as wild-type *Ec*LeuRS, A293R has lower but still significant activity, and A293D has minimum activity. The results indicate that other characteristics instead of their own splicing activity reflected in the *in vitro* assay contribute to their *in vivo* compensation ability of the splicing deficient

yeast strain. One possibility is that the *in vitro* splicing assay was carried out using a truncated intron bI4Δ1168, and A293 site happens to interact with the truncated region, so that the splicing activity of the mutants were not completely reflected in the splicing assay. Another explanation is that positive charge on the A293 site dynamically influenced interaction between the bI4 intron and its other splicing partner, bI4 maturase, considering LeuRS, bI4-maturase and the bI4 intron have been found to form a complex. In another word, mutations on the A293 site might affect intron splicing indirectly through improving splicing activity of the bI4 maturase.

It was shown previously that A293 is also an editing sensitive site of *Ec*LeuRS. Introduction of aspartic acid mutation on the A293 site (A293D) rescues post-transfer editing deficiency of the T252 mutant by presumably activating a pre-transfer editing pathway, whereas A293K and A293R failed to. In summary, A293D mutation enhances pre-transfer editing, while abolishing splicing activity of *Ec*LeuRS. This coincides with previous reports that editing function and splicing function are in a "yin-yang" balance in LeuRS.

Apart from *Ec*LeuRS, *Mtb*LeuRS can also substitute *ym*LeuRS in intron splicing (Houman et al., 2000). Interestingly, the corresponding site of A293 of *Ec*LeuRS on *Mtb*LeuRS, R399, is also splicing sensitive (Poruri, 2007). The alanine substitution (R399A) did not have any effect on

mitochondrial protein synthesis and RNA splicing. The introduction of negatively charged aspartic acid (R399D) resulted in loss of both functions, while the *Mtb*LeuRS R399E mutant supported protein synthesis, but did not assist in bI4 intron splicing. These results demonstrate that either an alanine or an arginine on the conserved A293 (or R399) site of *Ec*LeuRS (or *Mtb*LeuRS) can support their splicing function, which coincides with the semi-conserveness of this site across various LeuRSs either as an alanine or a positively charged residue. This indicates that splicing function of these non-splicing LeuRSs is dependent on conserved features of LeuRS. However, splicing sensitive sites failed to be identified in the A293 corresponding region of *ym*LeuRS (Poruri, 2007). In addition, the CP1 domain of *Ec*LeuRS where the Ala293 residue located failed to exhibit bI4 intron splicing activity, in contrast to its counterpart in *ym*LeuRS. This indicates that at least on the CP1 domain, *Ec*LeuRS and *Mtb*LeuRS aid intron splicing in yeast mitochondria with a completely different mechanism than *ym*LeuRS, which might represent an alternative evolutionary pathway for LeuRS to acquire the splicing function that the nature happened not to choose.

Chapter 5. Leucyl-tRNA synthetase facilitates group I intron remodeling

5.1 Introduction

In yeast mitochondria, the bI4 and aI4α group I introns are located within the genes encoding cytochrome b (*cob*) and cytochrome oxidase α subunit (*coxIα*) (Slonimski et al., 1978). Splicing of these two introns is facilitated by nuclear-encoded mitochondrial leucyl-tRNA synthetase (LeuRS) and mitochondria-encoded bI4 maturase (Herbert et al., 1988; Labouesse, 1990; Labouesse et al., 1985). The LeuRS and bI4 maturase bind independently to the bI4 intron and stimulate RNA splicing (M. T. Boniecki et al., 2009; Rho & Martinis, 2000).

Along with other group I introns, the bI4 and aI4α introns share a conserved catalytic core, which is comprised of two sets of coaxial helices P4-P6 and P3-P9 (Adams et al., 2004; Golden, Kim, & Chase, 2005; F. Guo, Gooding, & Cech, 2004; Michel & Westhof, 1990) (Figure 5.1A, B). Both introns also possess a long (>700 nucleotides) extended P8 loop insert, which is part of the open reading frame for the genes encoding bI4 maturase and DNA aI4α endonuclease, respectively. The 31-nucleotide P6 loop at the end of the bI4 intron P6 stem is distinct compared to the much smaller loop of the aI4α intron. The P5 helix of the bI4 intron contains two inserts that are missing in the aI4α intron. The first 21-nucleotide insert is

predicted to form a hairpin that has a long-range interaction with the P9 loop. The second 120-nucleotide insert called “hj” is proposed to fold into an isolated domain and seems to be stabilized independently by a self-contained long-distance interaction (M. T. Boniecki et al., 2009; Hsu, 2006).

Based on comparative analysis of bI4 and aI4α introns, deletion mutagenesis was carried out to construct minimum bI4 intron that is bound and processed in a LeuRS-dependent manner (M. T. Boniecki et al., 2009). A small derivative of the bI4 intron canonical core of just 380 nucleotides (bI4Δ1168) was generated, in which the P5 “hj” insertion is deleted and the P6 and P8 loop replaced with highly stable tetraloops (Jaeger, Michel, & Westhof, 1994; Murphy & Cech, 1994) (Figure 5.1C). This minimum bI4 intron construct bI4Δ1168 has similar LeuRS-binding affinity as the full-length intron and is stimulated for splicing by LeuRS *in vitro* (M. T. Boniecki et al., 2009).

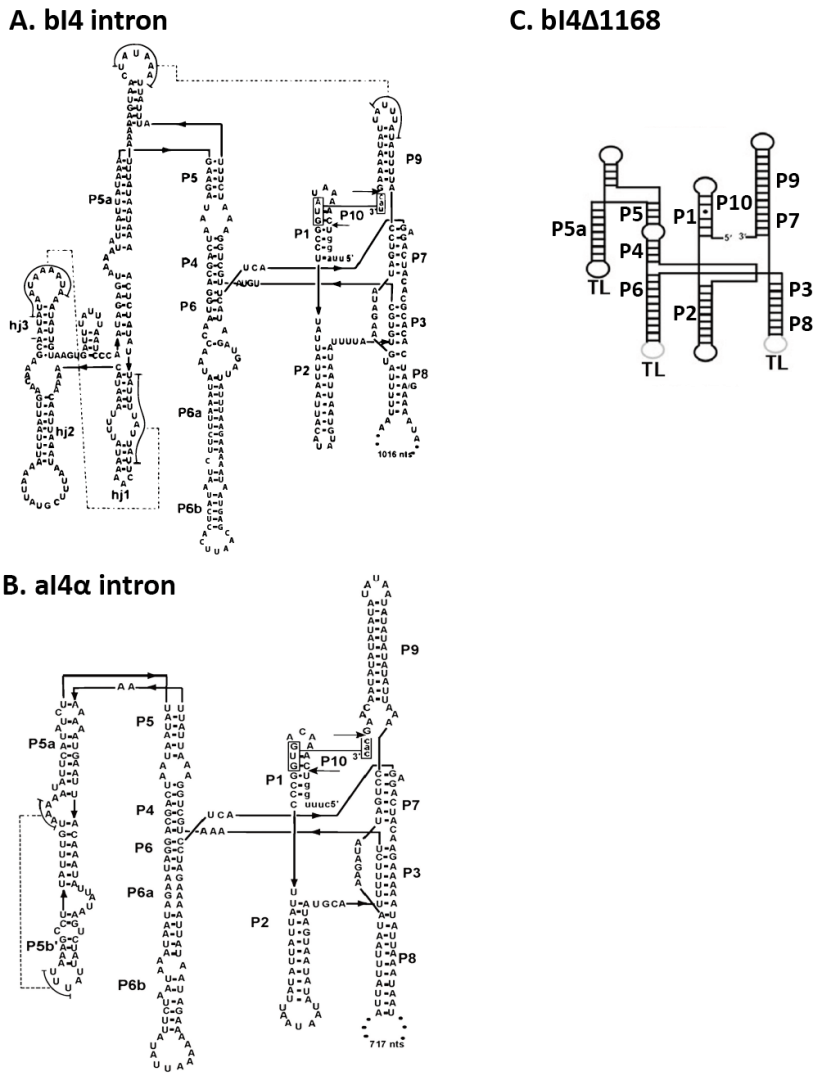

Figure 5.1 Predicted secondary structures of the group I introns. The secondary structure of the bI4 intron (A) and aI4α intron (B) canonical core was based on previous predictions (M. T. Boniecki et al., 2009; Michel & Westhof, 1990). Solid bold lines indicate linear connectivities of the nucleic acid strand with arrowheads oriented in the 5' to 3' direction. The dashed lines represent proposed tertiary interactions. Arrows in the P1 and P9 domain show splice sites, where boxed nucleotides are paired regions. (C) bI4Δ1168 deletion mutant. The abbreviation *TL* indicates loops where a GAAA (P6 and P5) or GUAA (P8) tetraloop was introduced.

In addition to LeuRS and maturases, other group I intron splicing factors that have been extensively characterized include Mss116p in yeast mitochondria, tyrosyl-tRNA synthetase (TyrRS or CYT-18) and CYT-19 in *Neurospora crasssa* mitocohondria. The Mss116p and CYT-19 proteins are DEAD-box RNA helicases that facilitate folding and splicing of mitochondrial group I and group II introns, primarily by unwinding RNA duplexes to disrupt stable but inactive RNA structures in an ATP-dependent manner (Halls et al., 2007; S. Mohr et al., 2006; S. Mohr et al., 2002; Solem et al., 2006; Tijerina et al., 2006).

CYT-18 recognizes highly conserved secondary and tertiary features of the catalytic core of the intron RNA, one of which is a transient P4-P6 structure that is stabilized by CYT-18 in an early step in the group I intron folding process (Caprara, Lehnert, Lambowitz, & Westhof, 1996; Myers, Kuhla, Cusack, & Lambowitz, 2002; Myers et al., 1996; Webb, Jones, & Dodd, 2001). The solved crystalized structure combined with biochemical data suggest that CYT-18 does not rely on its tRNA binding face. Rather, CYT-18 uses a distinct intron-binding surface which is absent from non-splicing bacterial TyrRSs (Paukstelis et al., 2008).

It is known that LeuRS alone can facilitate splicing of the bI4 intron in the absence of the other splicing factor bI4-maturase (M. T. Boniecki et al., 2009), and the editing domain and the C-terminal domain of LeuRS are involved in its splicing activity (Hsu et al., 2006; Rho et al., 2002; Sarkar

et al., 2012). The mechanism of splicing stimulation by yeast mitochondrial LeuRS (*ym*LeuRS) still needs to be further elucidated. Herein, we identified novel LeuRS-dependent annealing of P6 duplex mimetics. We hypothesized that LeuRS facilitates bI4 intron folding to stimulate splicing.

5.2 Experimental methods

5.2.1 Plasmid construction and mutagenesis

Plasmids in Table 5.1 and Table 5.2 were used to transcribe RNAs for *in vitro* assays, and to express wild-type and mutant proteins, respectively.

Table 5.1 Plasmids used for *in vitro* transcription of RNAs

RNA encoded	Plasmid name	Reference
bI4Δ1168	pM96Δhj1-3	(M. T. Boniecki et al., 2009)
*ym*tRNA$^{Leu}_{UAA}$	pGP1-2	Gift from Dr. T. Palmer, University of East Anglia, UK

Table 5.2 Plasmids used for protein expression

Protein encoded	Plasmid name	Reference
*ym*LeuRS	p14MB-*ym*LeuRS-WT	(Rho & Martinis, 2000)
*ym*LeuRSΔC	p32MB-*ym*LeuRS-ΔC	(Hsu et al., 2006)
*ym*LeuRSΔC5	p32MB-*ym*LeuRS-ΔC5	(Hsu et al., 2006)
*ym*LeuRSΔCP1	p32MB-*ym*LeuRS-dCP1(2A)	(M. T. Boniecki et al., 2008)
*ym*LeuRS-CP1	p14MB-*ym*CP1-N-C	(Sarkar et al., 2012)
*ym*LeuRS-CP1-βext	p14MB-*ym*CP1+N+C	(Sarkar et al., 2012)
*Ec*LeuRS	p14MB-EcLeuRS-WT	(M.T. Boniecki, 2007)
Human mt (*hm*) LeuRS	P32MB-hmLeuRS-WT	(M.T. Boniecki, 2007)
*Ec*IleRS	p14MB-*Ec*IleRS-WT	(M.T. Boniecki, 2007)

5.2.2 Construction of tRNA genes

The genes for the mutants of yeast mitochondrial $tRNA^{Leu}_{UAA}$ (*ym*$tRNA^{Leu}_{UAA}$) and *E. coli* $tRNA^{Leu}_{UAA}$ (*Ec*$tRNA^{Leu}_{UAA}$) with an upstream T7 RNA polymerase promoter and a downstream *Bst*NI restriction site were constructed by ligation of seven or eight overlapping DNA oligonucleotides (Table 5.3). Each DNA oligonucleotide at 1 μM concentration was first phosphorylated with 1.7 μM [γ-^{32}P]-ATP (6000Ci/mmol 10mCi/ml), 10 U T4 polynucleotide kinase (New England Biolabs Inc., Beverly, MA) in commercial buffer for 2 hrs. The phosphorylation reaction was subsequently inactivated at 65 °C for 10 min. All seven oligonucleotides were directly mixed without addition of water or buffer and annealed by being heated in a 95 °C water bath for 3 min and then gradually cooled down to room temperature still in the water bath for approximately 45 min, to form the annealed insert with overhangs suitable for cloning into the *Eco*RI and *Pst*I restriction sites.

The plasmid pUC18 (4 μg) was digested with 80 U *Eco*RI and *Pst*I in commercial buffer, followed by purification using a QIAquick PCR purification kit. A 20 μl ligation reaction containing 0.02 μM digested pUC18, 0.1 μM insert and 400 U T4 ligase in commercial buffer was incubated for 30 min at room temperature. The ligase was inactivated at 65 °C for 20 min.

The 2 μl ligation mixture was added to 50 μl DH5α competent *E.*

coli cells for transformation using heat shock. The transformed cells were cultured overnight on Luria broth (LB) plate containing 100 μg/ml ampicillin antibiotic. To select the colonies that contain the tRNA genes, ten colonies were chosen and screened by colony PCR reactions for each tRNA gene. Colony suspensions were prepared by resuspending individual colonies with sterile pipette tip in 50 μl water. The tips were also dropped into 3 ml LB media individually, which were cultured overnight to create stocks for each colony.

The 25 μl colony PCR reaction contained 5 μl of the colony suspension, 200 μM dNTPs, 2 μM primers (seq3A: 5'-GCTCGCCGCAGCCGAACGACCGAGCG-3', FOR88: 5'-GCTGGCGAAAGGGGGATGTGCTG-3'), 250 μg/ml bovine serum albumin (BSA), 0.5 U Vent polymerase (New England Biolabs Inc., Beverly, MA) in commercial buffer. Under the following conditions, 30 cycles of PCR were carried out: 94 °C for 1 min, 55 °C for 30 sec, and 72 °C for 40 sec. The PCR products were digested with 10 U *Bst*NI at 65 °C for 2 hr and assessed by electrophoresis, where a band ~ 500 bp represents successful construction of the tRNA gene. For colonies that contained the gene encoding the respective tRNA, plasmids were extracted from the corresponding overnight cultures using the Qiagen Spin Miniprep kit. The tRNA gene sequences in the plasmids were confirmed using DNA sequencing (UIUC Core Sequencing Facility, Urbana, IL).

Table 5.3 DNA oligonucleotides used for construction of tRNA genes

tRNA	DNA ligonucleotides	
*ym*tRNA^{Leu}-*Ec*VL	1	5’-CTATAGCTATTTTGGTGGAATT-3’
	2	5’-GGTAGACACGATACTCTTAAGATGTAT-3’
	3	5’-CGGCGTTCGCGCTGTGAA-3’
	4	5’-GGTTCAAGTCCTTTAA-3’
	5	5’-ATAGCACCAGGAGACCCTGCA-3’
	6	5’-GTGTCTACCAATTCCACCAAAATAGC-3’
	7	5’-GAACCTTCACAGCGCGAACGCCGATACATCTTAA GAGTATC-3’
	8	5’-GGGTCGCCTGGTGCTATTTAAAGGACTT-3’
*Ec*tRNA^{Leu}-*ym*VL	1	5’-CTATAGCCCGGATGGTGGAATC-3’
	2	5’-GGTAGACACAAGGGATTTAAAATCCCTT-3’
	3	5’-ACTTTACAGTATGCG-3’
	4	5’-GGGTACCAGGCTGCAG-3’
	5	5’-CGGGTACCAGGAGACCCTGCA-3’
	6	5’-GAACCCGCATACTGTAAAGTAAGGGATTTTAAAT CCCTT-3’
	7	5’-CGGGCCTACCACCTTAGCCATCTGTG-3’

5.2.3 Transcription of tRNAs *in vitro*

The *in vitro* transcription of the tRNAs used in this study was carried out as described in Chapter 2. The primers used in preparation of the templates via PCR amplification are seq3A and FOR88.

5.2.4 Protein expression and purification

Plasmids expressing the desired proteins were used to transform *E. coli* BL21 (DE3) codon plus strain (Agilent Technologies, Santa Clara, CA). Bacteria cultures were grown at 37 °C and induced with 1 mM isopropyl β-D-1-thiogalactopyranoside (IPTG) for protein expression at room temperature overnight. The N-terminal six-histidine-tagged fusion

protein was purified and quantified as described in Chapter 2. Purified *Ec*LeuRS and human mitochondrial LeuRS (*hm*LeuRS) proteins are gifts from A. Banerjee and Dr. K. Poruri, respectively.

5.2.5 Oligonucleotides radioactive labeling and *in vitro* annealing assay

The synthesized RNA or DNA oligonucleotides (Integrated DNA Technologies Corp., Coralville, Iowa) used for *in vitro* annealing assay were phosphorylated at the following reaction condition: 1 μM oligo, 1.7 μM [γ-^{32}P]-ATP (6000Ci/mmol, 10mCi/ml) (Pelkin Elmer, Waltham, MA) and 10 U T4 polynucleotide kinase (New England Biolabs Inc., Beverly, MA) in commercial buffer. All radioactive RNA preparations were purified on Chroma Spin + TE-10 columns (Clontech Laboratories, Inc., Mountain View, CA).

An RNA annealing reaction contained equimolar of the two oligonucleotide strands (typically 0.1 nM), with one oligonucleotide end-labeled with [^{32}P]. A final concentration 20 nM LeuRS was added in 1× annealing buffer (40 mM Tris pH 7.5, 50 mM KCl, 0.5 mM $MgCl_2$, 2 mM DTT and 0.01% NP-40) and incubated for 30 min at room temperature. The reaction was stopped by adding an equivalent volume of 1% (w/v) SDS, 50 mM EDTA, 0.1% (w/v) xylene cyanol, 0.1% (w/v) bromophenol blue, and 20% glycerol and the sample placed on ice.

The annealing reaction was analyzed on a 15% native acrylamide gel at 200 V for 80 min in 1× TBE buffer at 4 °C. The gel was dried with a vacuum gel dryer (Bio-Rad Laboratories, Hercules, CA) and phosphorimaged using a FUJIFILM BAS Cassette 2040 (FUJIFILM Medical Systems, Stanford, CT). Products were visualized by scanning the images using a STORM 840 Molecular Dynamics scanner (Amersham Biosciences Corp., Piscataway, NJ). Specific radioactive bands were quantified using ImageQuant software. Bands representing the annealed duplex and single-strand oligonucleotide were normalized for each time point by determining the fraction of each, relative to the sum intensity of the two bands. In addition, background was subtracted based on the zero time point. Extent of reaction (product/total bands in lane) was calculated using GraphPad Prism 5 via its single exponential function.

5.3 Results

5.3.1 LeuRS facilitates annealing of RNA duplexes.

Previously deletion analysis identified a minimized bI4 intron that was dependent on LeuRS for splicing. It is possible that LeuRS, similar to CYT-18, binds and stabilize conformation of the bI4 intron. We hypothesized that LeuRS might facilitate accurate folding of the bI4 intron. Significantly, measurements that defined LeuRS-dependent splicing indicated the level of completely folded bI4 intron was greatly increased in

the presence of LeuRS (M.T. Boniecki, 2007). We wondered if LeuRS could facilitate annealing of the bI4 intron core. Core regions of minimized bI4 intron (bI4Δ1168) (Figure 5.1C) was shown to directly interact with LeuRS in preliminary RNA footprinting experiment (M.T. Boniecki, 2007). It was hypothesized that LeuRS stabilized these core regions.

A P6 stem-loop mimetic RNA duplex P6n (Figure 5.2A) was designed to probe LeuRS-dependent duplex annealing activity. In conditions that facilitate bI4 intron splicing *in vitro* (M. T. Boniecki et al., 2009), complementary oligonucleotides were introduced at low 0.1 nM concentration to slow protein-independent annealing. Importantly, in the presence of affinity purified LeuRS, nearly all the single-strand oligos annealed into P6n duplexes. In contrast, in the absence of LeuRS, about 1% oligos formed duplexes (Figure 5.2). This result suggests that LeuRS facilitates RNA duplex annealing, which was not boosted by addition of ATP-Mg^{2+} (Figure 5.2C).

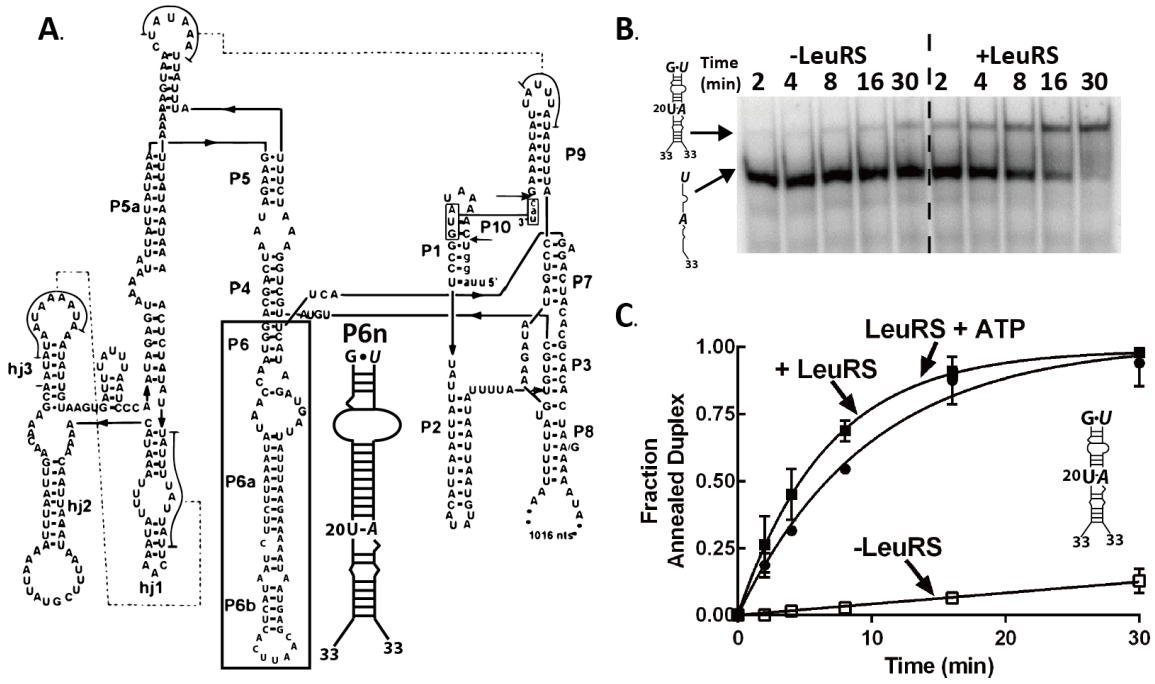

Figure 5.2 Yeast mitochondrial LeuRS facilitates annealing of RNA duplexes. A. Predicted secondary structure of the bI4 intron (M. T. Boniecki et al., 2009). The P6-P6a-P6b region is boxed with the P6n mimetic duplex shown on the right. B. Gel shift assay on a native 15% acrylamide gel displays 1 nM [^{32}P]-labeled 3' strand (lower band) annealed to 10 nM unlabeled 5' strand to form the P6n duplex (upper band) in the absence (□) or presence (■) of 100nM LeuRS in 1 × annealing buffer (40 mM Tris pH 7.5, 50 mM KCl, 0.5 mM $MgCl_2$, 2 mM DTT and 0.01% NP-40). C. Time course of P6n duplex formation in the absence or presence of 100 nM LeuRS or 2 mM ATP-Mg^{2+}. Error bars are the result of experiments repeated triplicate.

5.3.2 Magnesium inhibits LeuRS-dependent duplex annealing

Cations, especially Mg^{2+}, are typically incorporated into *in vitro*

reactions to shield the negatively charged phosphate backbone and promote folding of RNA. Although Mg^{2+} is required for group I intron splicing, concentrations that were higher than 5 mM impede LeuRS-dependent bI4Δ1168 splicing (M. T. Boniecki et al., 2009). We tested different concentrations of Mg^{2+} to determine optimum Mg^{2+} concentrations for LeuRS-dependent *in vitro* annealing of the P6n duplex (Figure 5.3). Similar to LeuRS-dependent splicing of the bI4 intron, increasing concentration of Mg^{2+} hindered annealing of the P6n duplex. An optimal concentration of 0.5 mM Mg^{2+} promoted LeuRS-dependent annealing, which is similar to LeuRS-dependent splicing *in vitro*. In contrast, RNA annealing of the P6n duplex was enhanced in the presence of Mg^{2+}.

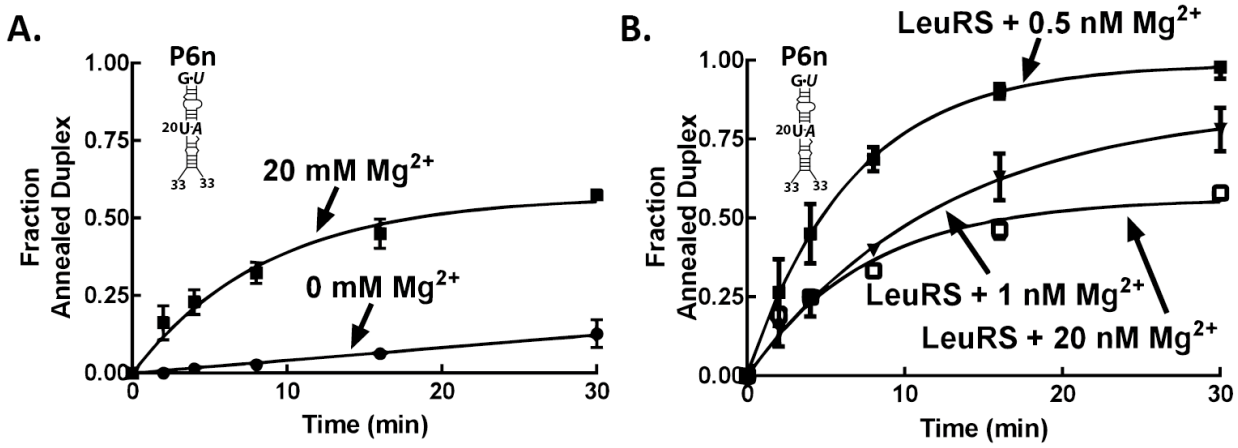

Figure 5.3 Magnesium inhibits LeuRS-dependent annealing. A. In the absence of LeuRS, P6n duplex annealing increased in the presence of 20 mM Mg^{2+}. Error bars are the result of experiments repeated in triplicate. B. Annealing curves of LeuRS-dependent P6n duplex annealing in the presence of 0.5 mM (□), 1 mM (▼) and 20 mM Mg^{2+} (■).

5.3.3 Yeast mitochondrial LeuRS has evolved to anneal RNA duplexes.

Our lab has previously shown that in addition to *ym*LeuRS, prokaryote and human LeuRSs also suppress splicing defects when the bI4 maturase is inactivated (Houman et al., 2000; Sarkar et al., 2012). This suggests that LeuRS in general contain an ancient core that is responsible for splicing. Nevertheless, the *ym*LeuRS is optimized for efficient splicing. For example, the LeuRS from *E. coli* exhibits lower *in vitro* splicing activity compared with *ym*LeuRS (Sarkar et al., 2012).

In order to determine whether the dependence of bI4 intron P6 region annealing is unique to *ym*LeuRS, we tested other proteins in the P6n duplex annealing assay. Non-LeuRS proteins, including BSA as well as *E. coli* isoleucyl-tRNA synthetase (*Ec*IleRS) failed to significantly stimulate annealing (Figure 5.4A). In addition, LeuRSs from human cytoplasmic (*hc*LeuRS) and *E. coli* (*Ec*LeuRS) exhibited very little annealing activity of the P6n helix (Figure 5.4B). The weak annealing promotion activity of *Ec*LeuRS corresponds with its low bI4 intron splicing activity (Sarkar et al., 2012). It is worth mentioning that the buffer of the annealing reaction is compatible with the aminoacylation activity of the above AARSs (Sarkar et al., 2012), which rules out the possibility that protein folding defect accounts for their lower annealing stimulation activity. Interestingly, only yeast cytoplasmic LeuRS (*yc*LeuRS) showed a significant P6n duplex

annealing activity, although still lower than its yeast mitochondrial counterpart (Figure 5.4B).

We hypothesized that the bulged region on the P6 stem-loop might serve as a sequence specific features for recognition by LeuRS. We designed another P6 stem-loop mimetic duplex P6-33 that eliminates the bulge by creating a series of base-pairs (Figure 5.4C). Interestingly, the annealing activity of the P6-33 duplex was increased in the presence of *Ec*IleRS and *Ec*LeuRS of comparable levels to that promoted by *ym*LeuRS. The activity in *hc*LeuRS was also increased, albeit still at a lower level (Figure 5.4C). These results demonstrate that *ym*LeuRS has uniquely adapted to facilitate duplex annealing of a core region of the bI4 intron. We propose that *ym*LeuRS has specifically evolved to recognize and promote folding of critical bulge in the bI4 intron P6 stem-loop.

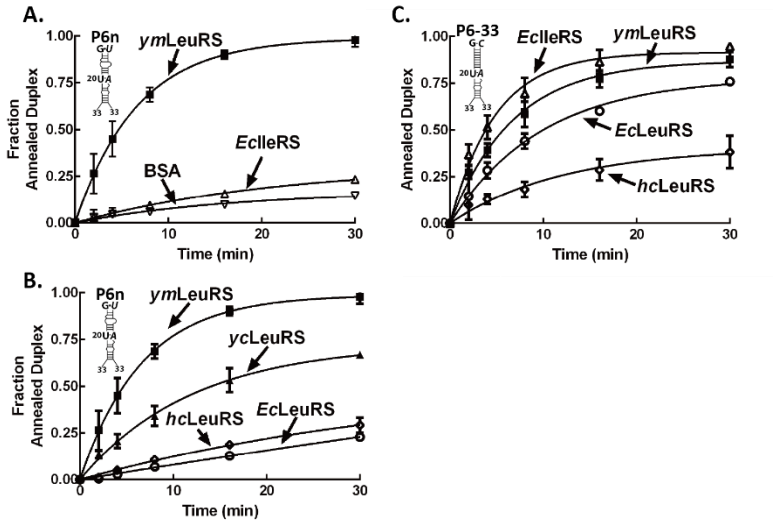

Figure 5.4 Yeast mitochondrial LeuRS has evolved to anneal RNA duplexes. A. Annealing of P6n duplex by *ym*LeuRS, *E. coli* IleRS (*Ec*IleRS) and bovine serum albumin (BSA). Annealing reactions contained 1 nM [^{32}P]-labeled 3' strand and 10 nM unlabeled 5' strand of the P6n duplex in the presence of 100 nM respective proteins in 1× annealing buffer. All of the annealing reactions using the P6n duplex were carried out in this condition. B. Annealing of P6n duplex by *ym*LeuRS, yeast cytoplasmic LeuRS (*yc*LeuRS), human cytoplasmic LeuRS (*hc*LeuRS), *E. coli* LeuRS (*Ec*LeuRS). C. Annealing of P6-33 duplex by *ym*LeuRS, *Ec*IleRS, *Ec*LeuRS, *hc*LeuRS. Annealing reactions contained 0.1 nM [^{32}P]-labeled 3' strand and 0.1 nM unlabeled 5' strand of the P6-33 duplex in the presence of 20 nM respective proteins in 1× annealing buffer. All of the annealing reactions using the P6-33 duplex were carried out in this condition. Symbols are : (▽), BSA; (■), *ym*LeuRS; (△), *Ec*IleRS ; (▲), *yc*LeuRS; (◇), *hc*LeuRS*;* (○), *Ec*LeuRS. Error bars are the result of experiments repeated triplicate.

Deletion mutants of the *ym*LeuRS were then tested to identify specific domains of LeuRS that contribute to its annealing activity. Similar to other synthetases, N-terminal canonical core of LeuRS is appended to a second domain that is less conserved (Burbaum & Schimmel, 1991; Martinis & Schimmel, 1996). However, unlike other AARSs, this LeuRS domain does not interact with the anticodon for cognate tRNA recognition (Asahara et al., 1993; Larkin et al., 2002). Rather, a C-terminal extension of about 60 amino acids folds into a unique domain (CTD) that is tethered via a flexible linker and interacts with the corner of the L-shaped tRNA (Figure 5.5A) (Palencia et al., 2012; M. J. Yaremchuk, 2005). In the absence of $tRNA^{Leu}$, this small unique CTD is disordered in the LeuRS *apo*-crystal structure (A. Yaremchuk, Cusack, & Tukalo, 2000).

Deletion of the CTD has been shown to abolish aminoacylation of LeuRS (Fukunaga, Ishitani, Nureki, & Yokoyama, 2005; Tukalo et al., 2005; Zheng et al., 2004). In addition, deletion of the last five amino acid or the entire CTD abolished LeuRS suppression activity that rescues splicing activity of an inactive bI4 maturase (Houman et al., 2000; G. Y. Li et al., 1996). It was later confirmed that the five amino acid C-terminal deletion of LeuRS failed to stimulate bI4 intron splicing *in vitro*, although it can form a ternary complex with the intron and the bI4 maturase splicing partner (Hsu et al., 2006). Collectively, these results support than LeuRS CTD is important to intron splicing.

Since CTD is involved in bI4 intron splicing activity of LeuRS, we also hypothesized that it might participate in LeuRS-dependent RNA duplex annealing. Two deletion mutants of LeuRS were constructed (Hsu et al., 2006) and affinity-purified. One has the last five amino acid of the C-terminus truncated (LeuRSΔC5), while the other has the entire C-terminus deleted (LeuRSΔC). Deletion of the five terminal residues or the entire C-terminal lowered annealing of the P6n duplex compared with full-length LeuRS (Figure 5.5B). Since deletions of the CTD failed to completely abolish LeuRS-dependent annealing, it is likely that the LeuRS main body contributes to the remaining moderate annealing activity.

In contrast to the P6n duplex, for the P6-33 duplex, LeuRSΔC5 maintains comparable annealing activity as the full-length LeuRS. Surprisingly, LeuRSΔC annealed the P6-33 duplex with an even faster k_{obs} than the wild-type LeuRS (Figure 5.5C). The high LeuRSΔC and LeuRSΔC5-dependent annealing activity again suggests that other regions of LeuRS also contribute to duplex annealing.

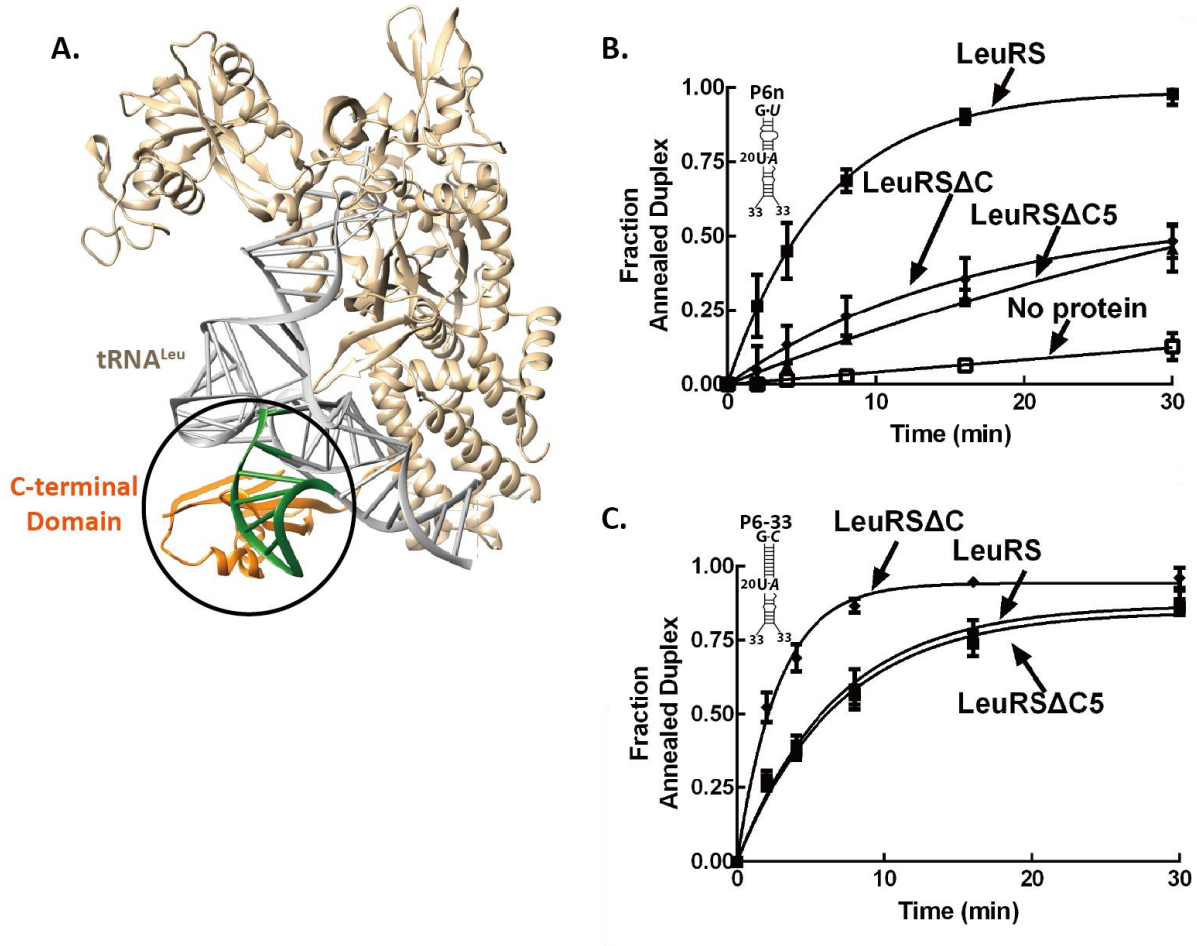

Figure 5.5 The C-terminal domain of LeuRS stimulates RNA duplex annealing. A. Structure of *E. coli* LeuRS-tRNA^{Leu} complex. The C-teriminal domain of LeuRS, tRNA^{Leu} and its variable arm are colored orange, grey and green respectively. Annealing of the P6n (B) and the P6-33 (C) duplex by full-length LeuRS, LeuRSΔC5 and LeuRSΔC. Symbols are: (■), full-length LeuRS ; (▲), LeuRSΔC5; (◆), LeuRSΔC; (▲), LeuRSΔC5; (□), no protein. Error bars are the result of experiments repeated triplicate.

The connective polypeptide 1 (CP1) domain of LeuRS is a 170-amino

acid insertion that splits the ATP binding Rossmann-fold that comprises aminoacylation active site of class I AARSs, folds discretely into a separate domain and is connected to the rest of the enzyme via two flexible β-strands (Figure 5.6A). Although the LeuRS CP1 domain is best known for its role in editing misacylated $tRNA^{Leu}$, it has been found to play a role in group I intron splicing. Splicing sensitive sites were identified within the CP1 domain and its connecting β strands (Figure 5.6A). We have also shown that the isolated CP1 domain from *ym*LeuRS is sufficient in performing bI4 intron RNA splicing *in vivo* and *in vitro* (Rho et al., 2002; Sarkar et al., 2012).

Because the CP1 domain can stimulate bI4 intron splicing, we also hypothesized that it participates in LeuRS-dependent duplex annealing. Moreover, a LeuRS mutant that has the entire CP1 domain deleted (*ym*ΔCP1) significantly enhances annealing activity compared with full-length *ym*LeuRS (Figure 5.6C). On the other hand, the isolated *ym*LeuRS CP1 domain (*ym*CP1-βext and *ym*CP1-β) failed to stimulate P6n duplex annealing. We also tested a deletion of the CP1 domain for *Ec*LeuRS, which also boosted its annealing activity (Figure 5.6D). The results support that the CP1 domain is not involved in RNA annealing activity of LeuRS, and may even impede it.

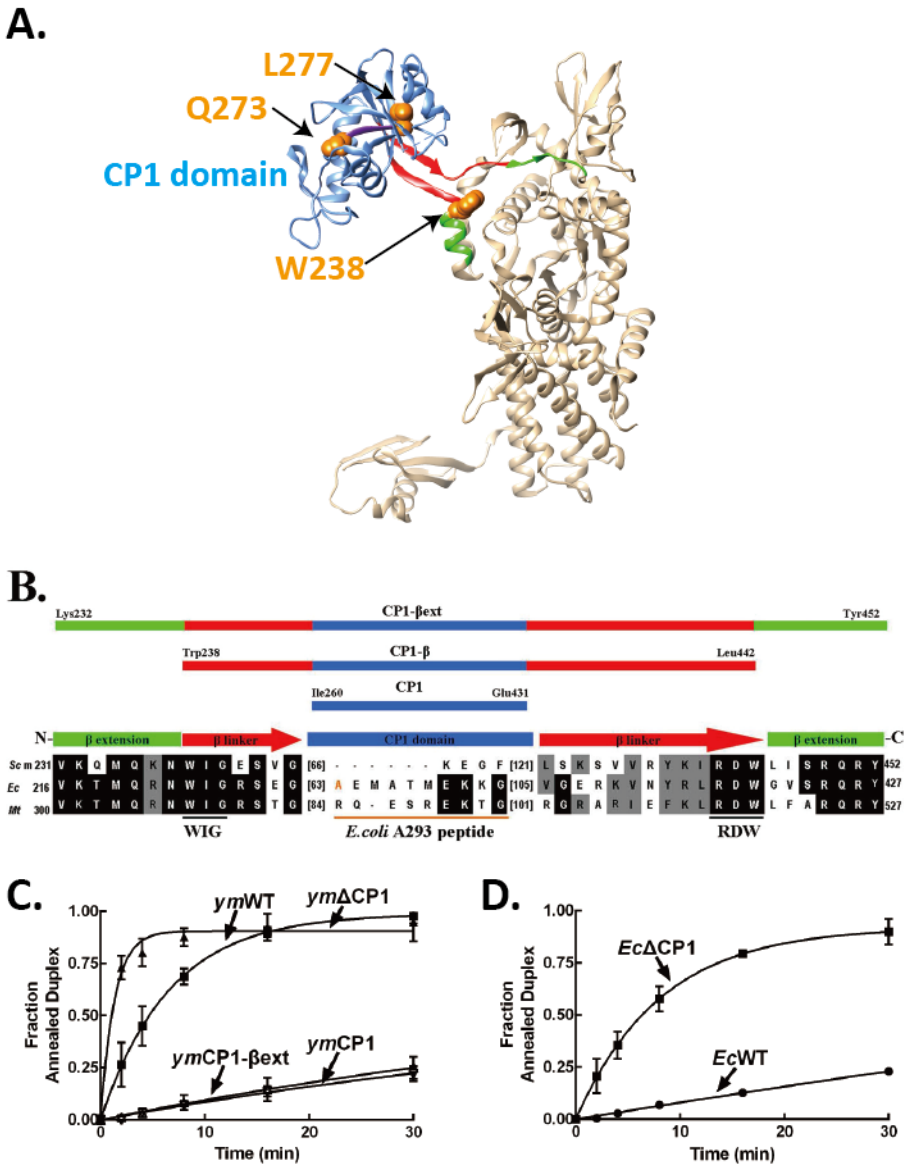

Figure 5.6 Deletion of the CP1 domain stimulates annealing activity of LeuRS. A. Homology model of *ym*LeuRS based on *E. coli* LeuRS (PDB accession code: 4AQ7) (Palencia et al., 2012). The CP1 domain is colored in blue, and splicing sensitive sites are in orange. B. Multiple sequence alignment of LeuRS CP1 domain and flanking regions containing both the N- and C-terminal β-strand linkers and extensions. The CP1 domain, β-strand linkers, and β-strand extensions are shown in blue, red, and green, respectively. Bracketed numbers indicate the number of amino acids within

a peptide insert. The *Ec*LeuRS A293 residue, which is absent in *ym*LeuRS, is highlighted in orange, and the corresponding peptide indicated by an orange line. Each of the yeast mitochondrial CP1 domain constructs is indicated at the top of the figure as follows: CP1 (Ile-260 to Glu-431), CP1-β (Trp-238 to Leu-442), and CP1-βext (Lys-232 to Tyr-452). The N- and C-terminal ends of the CP1-βext construct are also indicated in the homology model. *Scm, S. cerevisiae* mitochondrial; *Ec, Escherichia coli*; *Mt, M. tuberculosis*. C. Annealing of the P6n duplex in the presence of wild-type (*ym*WT) or the following mutant constructs of *ym*LeuRS: *ym*ΔCP1 with CP1 (Ile-260 to Glu-431) deleted, *ym*CP1β-ext, *ym*CP1. D. Annealing of the P6n duplex in the presence of wild-type (*Ec*WT) or a mutant of *Ec*LeuRS that deletes CP1 (Ala-230 to Gly-407) (*Ec*ΔCP1). Symbols are: (■), *ym*WT; (▲), *ym*ΔCP1; (△), *ym*CP1β-ext; (▽), *ym*CP1; (●), *Ec*WT; (■), *Ec*ΔCP1. Error bars are the result of experiments repeated triplicate.

5.3.4 Cognate tRNA competes with RNA duplex for LeuRS-dependent annealing.

Because LeuRS relied on its CTD for annealing, and the CTD interacts with the corner of tRNA for aminoacylation, we wondered if tRNA would inhibit the enzyme RNA annealing activity. When 1 μM excess *ym*tRNA^{Leu} was added to the P6n duplex annealing reaction in the

presence of LeuRS, LeuRS-dependent annealing was abolished (Figure 5.7A). The apparent K_I of *ym*tRNA^{Leu} was determined to be 4.6 ± 0.4 nM (Table 5.4). In contrast, *Ec*tRNA^{Leu} didn't inhibit LeuRS-dependent annealing under the same concentration as *ym*tRNA^{Leu} (Table 5.4). Thus, we hypothesized that binding the bI4 intron to *ym*LeuRS overlaps with the cognate *ym*tRNA^{Leu} in specific ways to facilitate P6n duplex annealing.

Since we have shown that LeuRS CTD is involved in facilitating RNA duplex annealing, also given that the C-terminal interacts with the tRNA^{Leu} variable arm (Palencia et al., 2012), we hypothesized that the binding sites that interact with tRNA^{Leu} variable arm on the LeuRS C-terminal also interact with the annealed RNA duplex. To test that hypothesis, we designed two chimeric tRNAs in which we swapped the variable arms. The *ym*tRNA^{Leu}-*Ec*VL chimera has the *ym*tRNA^{Leu} backbone with the variable stem-loop from *Ec*tRNA^{Leu}, and the *Ec*tRNA^{Leu} -*ym*VL has the *Ec*tRNA^{Leu} backbone with the variable stem-loop from *ym*tRNA^{Leu} (Figure 5.7B). Swap of the The *Ec*tRNA^{Leu} variable arm increased the apparent K_I of *ym*tRNA^{Leu} by 30 fold to 120 ± 27 nM (Table 5.4). This suggests that the variable stem-loop plays a major role in the inhibition of cognate tRNA of LeuRS-dependent annealing. Introduction of the variable arm from *ym*tRNA^{Leu} increased inhibition of *Ec*tRNA^{Leu} in LeuRS-dependent annealing with a K_I of 62 ± 10 nM (Table 5.4). These results emphasized that the tRNA inhibition of RNA annealing is largely influenced by the

variable arm.

Table 5.4 Apparent kinetics of tRNA inhibition of P6n annealing

Standard error is based on measurements that were repeated triplicate[a]

tRNA	K_I^{app} **[nM]**[a]
*ym*tRNA^{Leu}	4.6 ± 0.4
*ym*tRNA^{Leu}-*Ec*VL	120 ± 27
*Ec*tRNA^{Leu}	ND[b]
*Ec*tRNA^{Leu}-*ym*VL	62 ± 10

[b]Not determined because no annealing inhibition observed

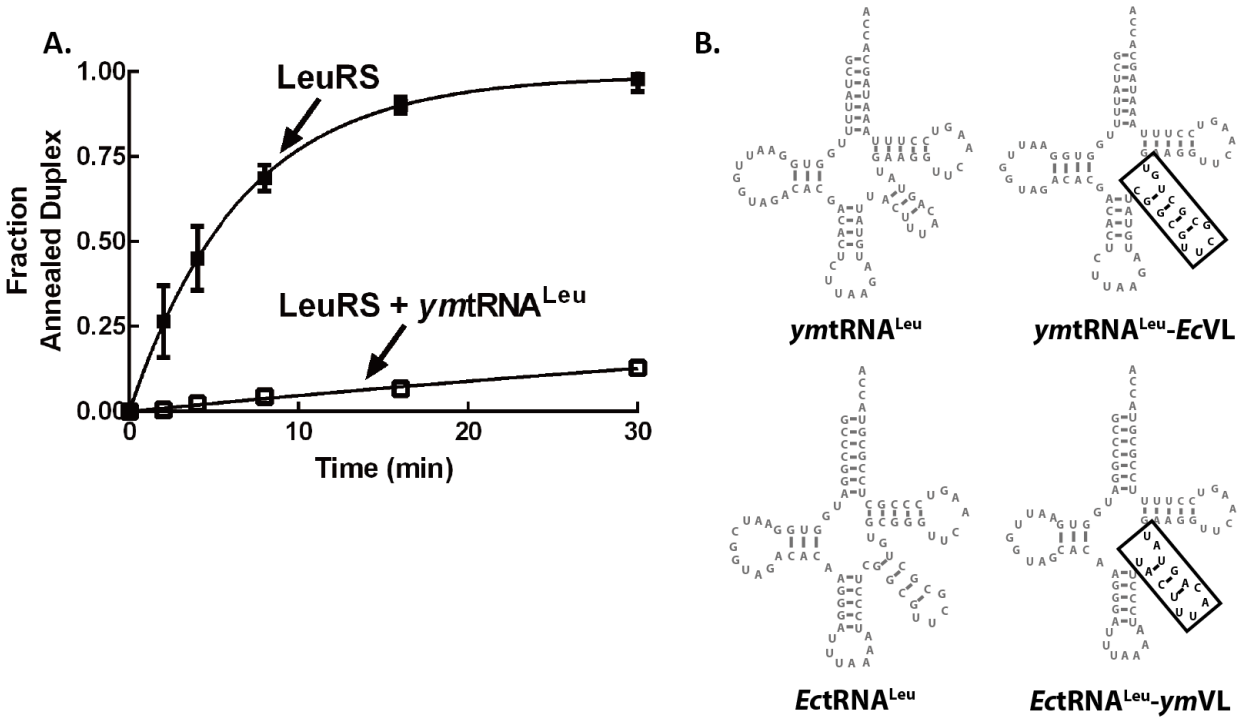

Figure 5.7 Yeast mitochondrial tRNA^{Leu} competes with RNA duplex for LeuRS-dependent annealing. A. LeuRS-dependent P6n duplex annealing in the presence (□) or absence (■) of 1 μM *ym*tRNA^{Leu}. B. The wild-type and chimeric tRNAs used to compete with the duplex in LeuRS-dependent annealing. *ym*tRNA^{Leu}-*Ec*VL chimera: *ym*tRNA^{Leu} backbone with the variable stem-loop from *Ec*tRNA^{Leu}, *Ec*tRNA^{Leu}-*ym*VL chimera: *Ec*tRNA^{Leu} backbone with the variable stem-loop from *ym*tRNA^{Leu}. Error bars are the result of experiments repeated triplicate.

Because the P6n duplex and *ym*tRNA^{Leu} variable arm appear to share binding sites on LeuRS, we sought to identify a region on the P6 stem-loop of bI4 intron that resembles the tRNA^{Leu} variable arm. A three-base-pair region on the P6 stem was identified that matches the *ym*tRNA^{Leu} variable

stem (Figure 5.8A). We designed a P6n duplex mutant (P6n-tMU) which has this three-base-pair swapped to perturb its local structural recognition elements, while preserving its stability (Figure 5.8A). As would be expected based on our results with the P6n duplex, in the absence of LeuRS, P6n-tMU duplex failed to anneal. In the presence of LeuRS, annealing of P6n-tMU was stimulated, but at much less efficiency than the P6n duplex (Figure 5.8B). The result suggests that LeuRS specifically recognizes the P6n duplex via an overlapping region on the protein that interacts with the tRNA variable arm.

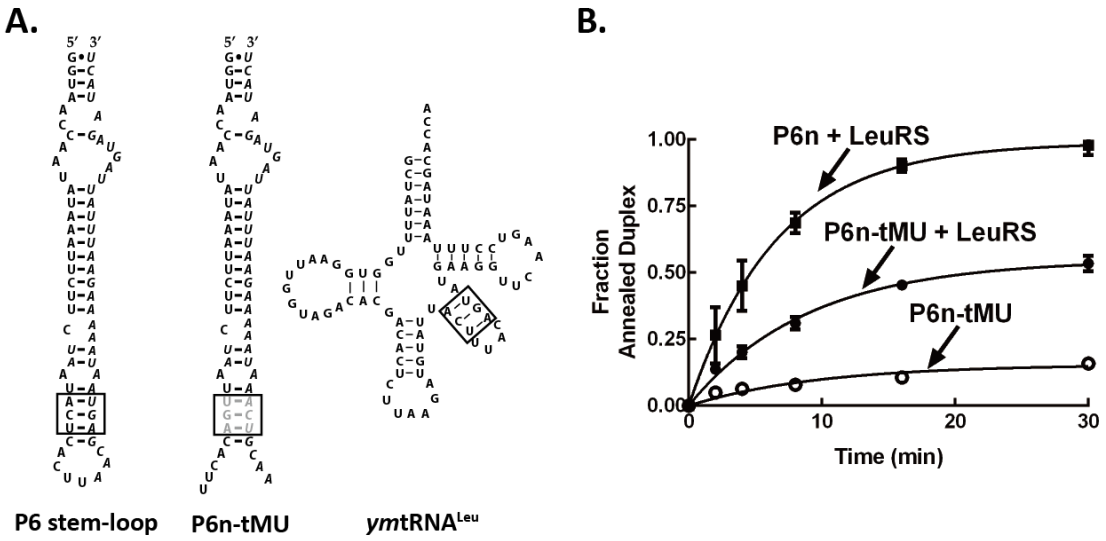

Figure 5.8 The *ym*tRNA^{Leu}-variable-stem-like region on the P6 stem is important for LeuRS recognition. A. Sequence similarity between the P6 stem and *ym*tRNA^{Leu} variable stem. Boxed are the three base pairs in the *ym*tRNA^{Leu}-variable-stem-like region that are reversed in P6-tMU. B. The P6n-tMU shows decreased LeuRS-dependent annealing activity compared with P6n. Symbols are: LeuRS-dependent P6n (■) and P6n-tMU (●) annealing; P6n-tMU annealing in the absence of LeuRS (○). Error bars are the result of experiments repeated triplicate.

5.3.5 Duplex overhangs enhance LeuRS-dependent annealing

We used the P6n and P6-33 duplexes as the template to design several duplexes (Figure 5.11). Similar to tRNA identity, we hypothesized that LeuRS recognized specific sequence such as length and overhang dependency. We first tested the P6n native helix and reduced its length. This resulted in the design of P6n$_{3'13}$, P6n$_{5'13}$, P6ns, all of which failed to

anneal in a LeuRS-dependent way (Figure 5.9). Since no duplex formation was detected, the data is not shown.

The P6-33 helix was used as a template to design P6-$20_{3'13}$ and P6-$20_{5'13}$ and P6-20. In contrast, annealing of P6-$20_{3'13}$ and P6-$20_{5'13}$ was stimulated to a similar level as P6-33. Moreover, annealing of the blunt-ended P6-20 was not increased by LeuRS (Figure. 5.9). The above results suggests that LeuRS is not able to anneal duplexes which cannot self-anneal (P6$n_{3'13}$, P6$n_{5'13}$ and P6ns cannot anneal on their own even at high concentration using heat-up-cool-down annealing method). In another word, a base-pair number threshold exists for duplexes to be recognized by LeuRS. In addition, the blunt-ended P6-20 not recognized by LeuRS indicates that overhangs are critical for LeuRS recognition.

We then further investigate the duplex length and overhang dependency for the P6-33 annealing stimulated by LeuRS. We designed duplexes with different lengths and overhangs originated from P6-33 upper stem region (Figure. S1). From the LeuRS-dependent annealing assay results (Figure 5.9), we can see that there is no stringent duplex length dependency in LeuRS-stimulated annealing. For example, annealing of P6-$19_{5'1}$ is worse than P6-$18_{5'2}$ in the presence of LeuRS, although the former has a longer 5' strand. Nevertheless, we observed LeuRS didn't stimulate annealing of duplexes less than 18 base-pairs.

Overhangs of nucleic acid strands are often critical to RNA helices

that assist annealing (Müller et al., 2001; Yang & Jankowsky, 2005). As such, we designed a series of P6-33 constructs to introduce 5' and 3' overhangs. Results show that annealing of duplexes with longer overhangs was promoted better by LeuRS. For example, the best ones are P6-33, P6-$33_{5'13}$ and P6-$33_{3'13}$, which has the longest 13 nucleotide overhang; the worst one is the blunt-ended P6-20 (Figure 5.9B). Take P6-$18_{5'2}$, P6-$19_{5'1}$ and P6-20 for another example, as the overhang length on the 5' strand ranges from 2 to 0, duplex annealing in the presence of LeuRS also sequentially decreases from around 60% to none (Figure 5.9C).

Moreover, we found that the overhang on the 5' strand is more prone to LeuRS-dependent annealing than if the overhang is on the 3' strand. The P6-19 $_{UP5'1}$, P6-$18_{5'2}$ and P6-$19_{5'1}$ duplexes showed significant activity of LeuRS-dependent annealing (Figure 5.9C). All of them have corresponding duplexes designed with the overhang at the same length on the 3' strand (Figure 5.9D). No duplex formation was observed in the absence or presence of those duplexes. Also, the P6-$19_{3'14}$ duplex which has a 3' overhang has very little LeuRS-dependent annealing activity, similar to the blunt-end P6-20 (Figure 5.9B). Nevertheless, it appears that the number of base-pairs can mask the overhang location bias, as P6-$20_{5'13}$ and P6-$20_{3'13}$ have similarly high LeuRS-dependent annealing activity.

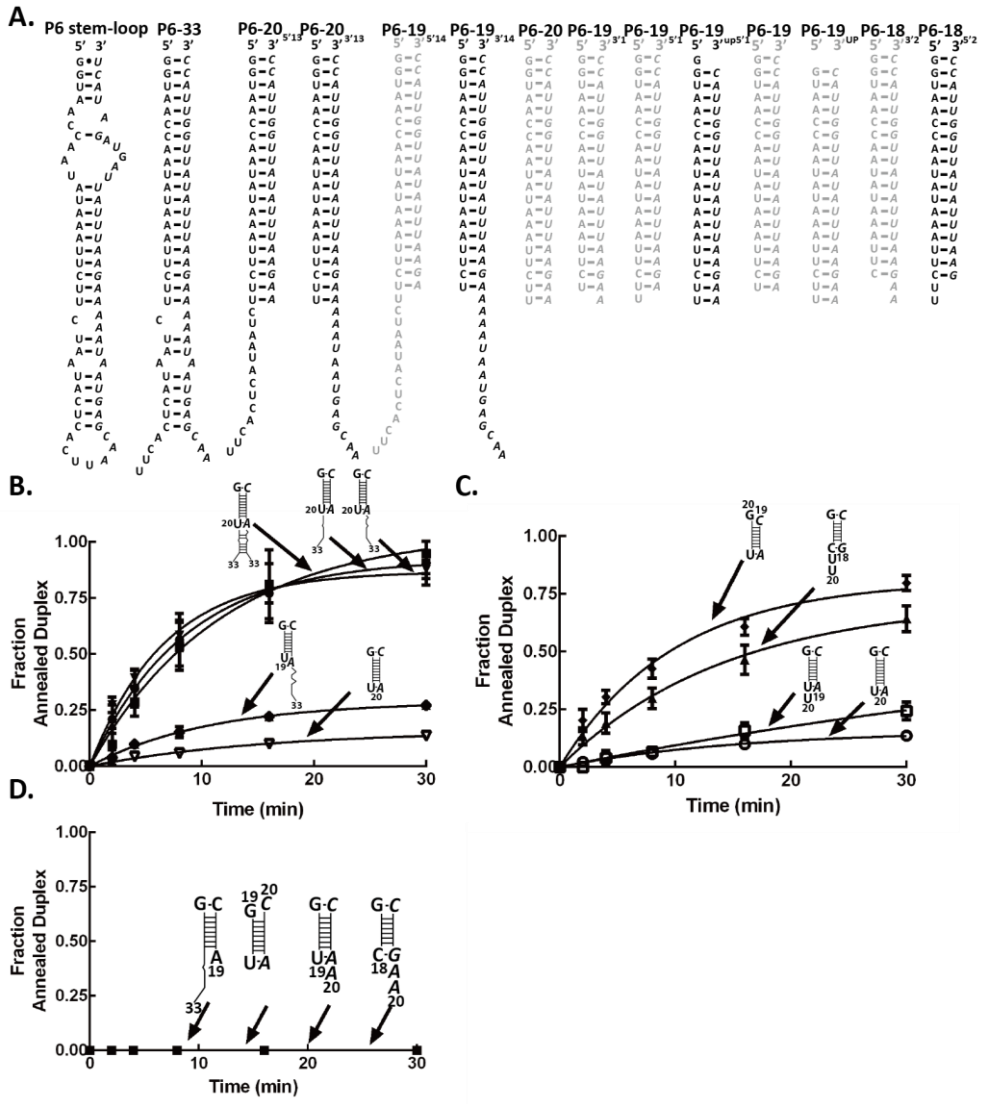

Figure 5.9 Duplex overhangs enhance LeuRS-dependent annealing. A. Duplexes used to test overhang effect on LeuRS-dependent annealing. The bI4 intron P6 stem-loop is shown on the top left as reference. Duplexes colored in grey failed to show significant increase in annealing in the presence of 100 nM LeuRS. B, C, D. All of the curves shown are reactions that carried out in the presence of 100 nM LeuRS. Symbols are: (▼), P6-33; (●), P6-20$_{5',13}$; (■), P6-20$_{3',13}$; (◆), P6-19$_{5',1}$UP; (▲), P6-18$_{5',2}$; (□), P6-19$_{5',1}$; (○), P6-20. Error bars are the result of experiments repeated triplicate.

5.3.6 The LeuRS-dependent P6-33 duplex annealing specificity

We also asked whether LeuRS-dependent duplex annealing is specific to RNA. We designed DNA and RNA-DNA hybrid versions of the P6n and P6-33 duplexes. No annealing was observed in the presence or absence of LeuRS for the P6n DNA and RNA-DNA hybrid duplexes, thus the data is not shown. However, P6-33 duplex annealing of the 5' DNA and the 3' RNA strands was promoted by LeuRS. In contrast, annealing of the 3' DNA and 5' RNA wasn't (Fig. 5.10). These results support that LeuRS binds the 5' RNA strand more directly.

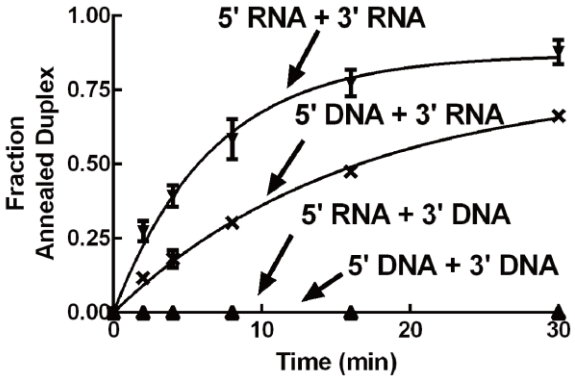

Figure 5.10 The LeuRS-dependent P6-33 duplex annealing specificity. Symbols are: (▼), 5' RNA-3' RNA; (×), 5' DNA-3' RNA; (△), 5' RNA-3' DNA; (▽), 5' DNA-3' DNA. Error bars are the result of experiments repeated triplicate.

Figure 5.11

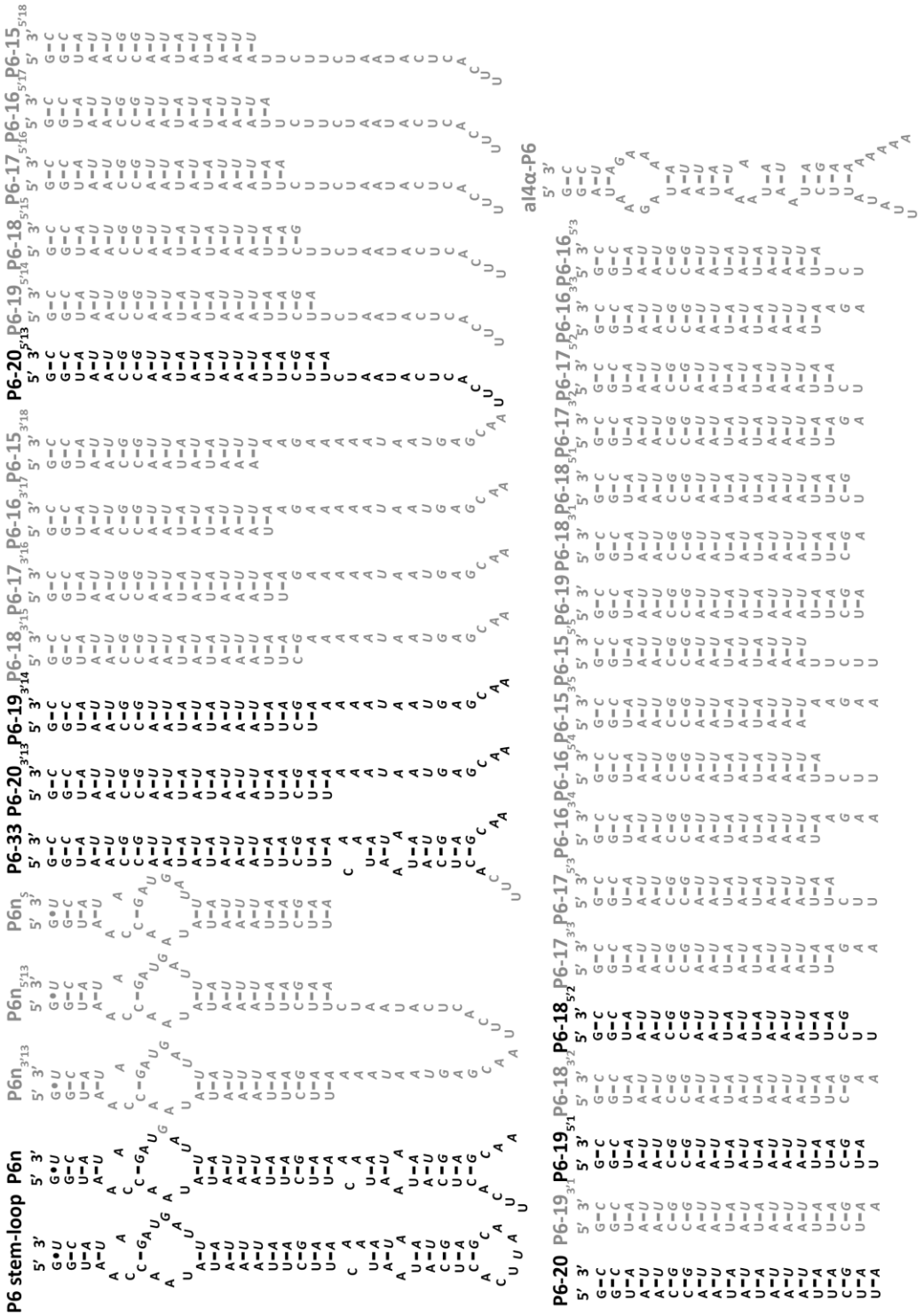

Figure 5.11 P6-stem mimetics. Duplexes colored grey don't show significantly improved annealing in the presence of LeuRS. Boxed are the base pairs that are reversed.

Figure 5.11 (continued)

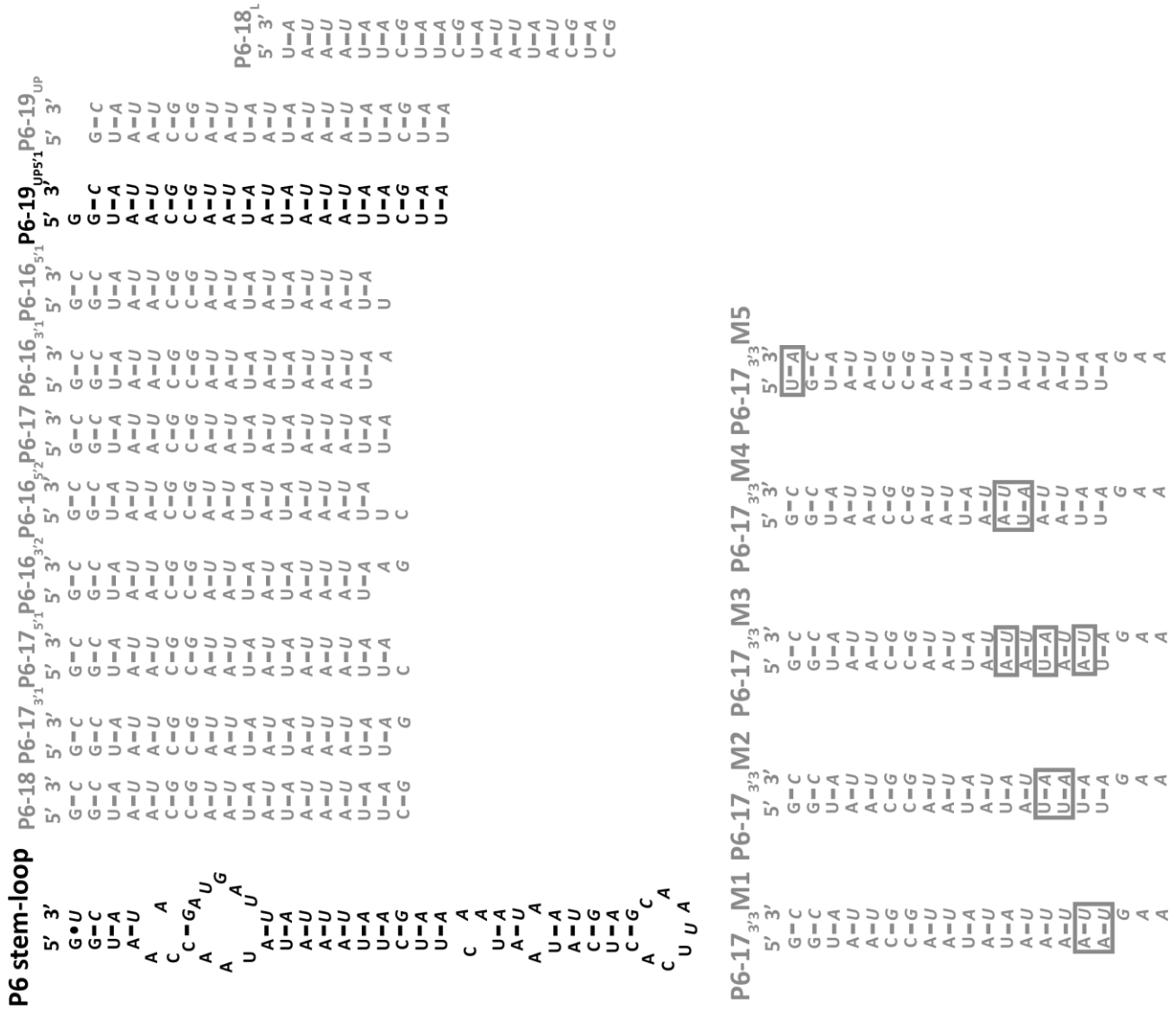

Figure 5.11 P6-stem mimetics (continued). Duplexes colored grey don't show significantly improved annealing in the presence of LeuRS. Boxed are the base pairs that are reversed.

5.4 Discussion

Group I introns use RNA-catalyzed splicing mechanisms (Cech, 1990), but require protein splicing factors *in vivo* to fold into catalytically active structures. The group I intron splicing factors characterized so far

can be divided into three groups (Herschlag, 1995; Rajkowitsch et al., 2007). The first group specifically binds to the intron, inducing the formation of the catalytically active RNA structure. Alternatively, the second group promotes splicing by capturing the native structure. In some cases, group I introns reply on a combination of the two mechanisms. An example of the second group is the CYT-18 in *N. crassa* mitochondria, which binds across one face of the coaxially stacked P4-P6 helix and also makes contacts with P3-P9 helix (Paukstelis et al., 2008). The group I intron P4-P6 and P3-P9 helices form its conserved catalytic core (Adams et al., 2004; Golden et al., 2005; F. Guo et al., 2004; Michel & Westhof, 1990). This intron-binding surface on CYT-18 is distinct from that which binds $tRNA^{Tyr}$, and was proposed to stabilize the P4-P6 and P3-P9 domains in the correct relative orientation (Paukstelis et al., 2008). The third group is non-specific RNA helicases, which function as ATP-dependent chaperone to destabilize non-native RNA structures that constitute kinetic traps in the folding pathway. Examples of the RNA helicases include CYT-19 in *N. crassa* (Tijerina et al., 2006) and Mss116p in *S. cerevisiae* (Halls et al., 2007).

Similar to CYT-18, LeuRS appears to facilitate splicing by recognizing features of the native structure (P6 stem-loop) in a magnesium-inhibitory and ATP-independent manner (M. T. Boniecki et al., 2009). When LeuRS performs its aminoacylation activity *in vitro*, no Mg^{2+}

inhibition effect up to 10 mM Mg^{2+} was observed (Sarkar et al., 2012). Magnesium ion was proposed to be coordinated by amino acids in the aminoacylation catalytic center to help maintain the competent catalytic center conformation (Palencia et al., 2012). The Mg^{2+} inhibition effect in the splicing and annealing on the other hand indicates that bI4 intron splicing and P6n annealing stimulation are not performed by the aminoacylation catalytic center of LeuRS, or if it is, then the conformation of catalytic center to interact with the bI4 intron is different from the conformation to interact with $tRNA^{Leu}$.

Different from CYT-18, which has distinct intron and tRNA binding surfaces, LeuRS employs the tRNA binding sites on the C-terminal domain to interact with the intron. It has been shown that the splicing-sensitive sites identified so far include not only tRNA binding site (Trp238) in the conserved "WIG" region of the editing domain connecting β-strands (Sarkar et al., 2012), but also the Gln273 and Leu277 residues in a less conserved region within the CP1 domain. Collectively, LeuRS uses both tRNA binding sites and splicing-specific inserts to promote group I intron splicing, which is different from CYT18 that has distinct tRNA and intron binding sites.

We found that among LeuRSs ranging from prokaryotes to eukaryotes, LeuRS from yeast mitochondria has the highest activity in annealing the P6n duplex, which has the exactly same sequence as the P6 stem-loop, but

lacks advantage in annealing P6-33 duplex, which has the un-base-paired loops in the P6 stem designed to be base-paired, indicating that *ym*LeuRS is highly adapted in recognition of the P6 domain in the bI4 intron compared with other LeuRSs. Other than the P6n and P6-33 duplexes, LeuRS also supports annealing of a range of duplexes derived from the P6 stem-loop.

It is noteworthy that LeuRS didn't support annealing of duplexes that are recognized by other published RNA annealing proteins (Muller et al., 2001; Yang & Jankowsky, 2005), which supports the selectivity of the introns recognized by LeuRS, in contrast with CYT-18, which recognizes a variety of RNA sequences (Caprara, Lehnert, et al., 1996; Q. Guo & Lambowitz, 1992; G. Mohr, Caprara, Guo, & Lambowitz, 1994; G. Mohr et al., 1992). Also, LeuRS didn't aid annealing of the P6 region in aI4α intron. The P6 stem-loop mimetic of the aI4α intron failed to anneal in the presence or absence of LeuRS (data not shown). This is not surprising because the P6 region of aI4α has only 15 base-pair, lower than the minimum base-pair number (18 base-pair) required in the annealing assay. This suggests that the aI4α intron does not require RNA remodeling in this area.

Intriguingly, we observed a bias in LeuRS recognition of DNA-RNA hybrids: for the same P6-33 duplex sequence, LeuRS facilitates annealing of the 5' DNA-3' RNA version, but not the 5' RNA-3' DNA version. This

implicates other alternative functions of LeuRS, such as regulation of R-loop formation (Thomas, White, & Davis, 1976), which is base-pairing of nascent RNA with its DNA template right after transcription, or mediation of non-coding RNAs interaction with their targets in the chromosome (Mercer, Dinger, & Mattick, 2009), and so on.

Chapter 6. Summary

Aminoacyl-tRNA synthetases (AARSs) were originally discovered as a family of proteins that catalyze the first step of translation via a two-step aminoacylation reaction, which is addition of amino acids onto their cognate tRNAs (Ibba & Söll, 2000). Each amino acid is recognized by one AARS (Pang et al., 2014). AARSs can also prevent or edit tRNAs being mischarged with the wrong amino acid to ensure translational fidelity (A.P. Mascarenhas, Martinis, An, Rosen, & Musier-Forsyth, 2008). In addition to the primary functions of aminoacylation and editing, AARSs have been found to harbor a variety of secondary functions (Martinis et al., 1999), such as group I intron splicing function of mitochondrial LeuRS and TyrRS. My research focuses on unraveling mechanisms of LeuRS splicing function.

The LeuRS in yeast mitochondria catalyzes splicing of the bI4 and aI4α introns in the genes encoding cytochrome *b* (*cob*) and the α subunit of cytochrome oxidase (*cox1α*) (Labouesse, 1990). Our lab has previously shown that the CP1 editing domain catalyzes intron splicing (Rho et al., 2002; Sarkar, Mao, Lincecum, Alley, & Martinis, 2011), and characterized a splicing sensitive site Trp238 on one of the β-strands that connect the CP1 domain to the LeuRS main body (Sarkar et al., 2012). In my first project, in collaboration with Seung Bae Rho, we continued on to

characterize a splicing sensitive site on the CP1 domain, Gln273, and discovered another splicing sensitive site nearby, Leu277. We found that when either the Gln273 or the Leu277 site was mutated to alanine, the LeuRS mutant exhibited a significantly reduced processing of the bI4 intron and formation of the exon, whereas the Q273R LeuRS mutant has similar intron splicing activity as the wild-type LeuRS. In the structural analysis, Gln273 and Leu277 were found to be located at the two ends of the β3 strand in the CP1 domain, Gln273 on the surface while Leu277 was buried. On the surface of *ym*LeuRS, several polar residues including positively charged amino acids were identified in proximity to the Gln273 site, and proposed to comprise the intron face that interacts with the intron RNA. Interestingly, this intron face is distinct from the tRNA face where tRNA binding sites cluster on the CP1 domain, further supporting a previous hypothesis that the CP1 domain is diverged to accommodate both splicing and editing (Sarkar et al., 2011).

Apart from LeuRS in yeast mitochondria, our group has discovered that LeuRSs in other organisms also harbor bI4 intron splicing activity, including LeuRS in *E. coli*, *M. tuberculosis* and human mitochondria, although they never encounter the bI4 intron in the nature (Houman et al., 2000; Poruri, 2007). In my second project, we characterized a splicing sensitive site Ala293 on the CP1 domain of *Ec*LeuRS. The Ala293 residue is located in a relatively non-conserved region and was previously

identified as an aminoacylation and editing sensitive site (Williams & Martinis, 2006). We found that when expressed at a high level, A293D, A293K and A293R *Ec*LeuRS mutants as well as wild-type *Ec*LeuRS complemented a *ym*LeuRS-null yeast strain. In contrast, when expressed at a low level, WT and A293D *Ec*LeuRS failed to complement the splicing function of *ym*LeuRS, whereas A293K and A293R *Ec*LeuRS mutant still rescued growth of the *ym*LeuRS-null yeast strain. The *in vitro* splicing assays confirmed that A293D *Ec*LeuRS indeed lacks splicing activity, and demonstrated that A293R has a compromised but still significant splicing activity, while A293K has similar activity as WT *Ec*LeuRS. These results infer that other factors other than the splicing activity of the *Ec*LeuRS mutants *per se* are responsible for their *in vivo* compensation of *ym*LeuRS splicing function. Combined with the lack of the A293 conserved site in *ym*LeuRS, it is likely that the non-native splicing-active LeuRSs from other organisms facilitate bI4 intron splicing in a completely different mechanism than *ym*LeuRS.

In my third project, the mechanism of *ym*LeuRS-dependent splicing was further elucidated. Based on the preliminary RNA footprinting results that LeuRS interacts with the P6 stem-loop of the bI4 intron, it was hypothesized that LeuRS promotes annealing of the P6 stem so as to facilitate intron folding into a splicing competent conformation. To test that hypothesis, a series of RNA duplexes were designed based on the P6 stem-

loop sequence and were shown to anneal much more rapidly in the presence of LeuRS in a magnesium-inhibitory and ATP-independent manner. The *ym*LeuRS enzyme was exhibited to possess the highest annealing activity and to recognize certain features of the P6 stem-loop, compared with LeuRSs from other organisms. By “dissecting” the LeuRS, we found the C-terminal domain is involved in the annealing activity of LeuRS. Furthermore, it was revealed that the cognate $tRNA^{Leu}$ inhibited LeuRS-facilitated duplex annealing, indicating that the $tRNA^{Leu}$ and the bI4 intron P6 stem share binding sites on LeuRS. In addition, a $tRNA^{Leu}$-variable-arm-like region was identified on P6 stem and was shown to be important for LeuRS-dependent annealing. To further characterize the features on the P6 stem-loop that is recognized by LeuRS, we designed a variety of P6-derived duplexes and found that LeuRS only anneals duplexes longer than 18 bp and prefers duplexes with longer overhangs. LeuRS also demonstrated bias in DNA-RNA hybrid duplex annealing: it only promotes annealing of 5’ DNA-3’ RNA but not 5’ RNA-3’ DNA duplex. The bias in duplex recognition indicates other non-canonical functions that involve DNA-RNA hybrid annealing, such as transcription regulation.

In summary, my studies further unveil the mechanism of LeuRS-dependent annealing. We showed that although group I intron splicing function is universally present in LeuRSs ranging from prokaryotes to

eukaryotes, it seems that those non-native splicing LeuRSs facilitate splicing in a different mechanism than ymLeuRS. For example, splicing sensitive sites Ala293 in *Ec*LeuRS and Arg399 in *Mtb*LeuRS are conserved, but the corresponding conserved residue cannot be identified in *ym*LeuRS. Also, splicing sensitive site Gln273 in *ym*LeuRS lacks corresponding conserved residues in *Ec*LeuRS and *Mtb*LeuRS. In addition, we exhibited that one of the mechanisms LeuRSs employ to facilitate bI4 intron splicing is to promote annealing of the P6-stem. It was shown that *ym*LeuRS is highly adapted to recognize the P6 stem compared with LeuRSs from other organisms. Specifically, one of the key interacting region between *ym*LeuRS and the intron is the $tRNA^{Leu}$-variable-arm-like region on the P6 stem, which *ym*LeuRS binds with its C-terminal domain. Combined with the discovery in the first project that LeuRS evolves new intron binding face on the CP1 domain, and the previous finding that Trp238 on the tRNA binding face of the CP1 domain is splicing sensitive (Sarkar et al., 2011), it seems that LeuRS not only uses tRNA binding sites, but also has developed novel intron binding sites to interact with and facilitate splicing of the group I introns.

References

Adams, P. L., Stahley, M. R., Gill, M. L., Kosek, A. B., Wang, J., & Strobel, S. A. (2004). Crystal structure of a group I intron splicing intermediate. *RNA, 10*(12), 1867-1887.

Afonyushkin, T., Vecerek, B., Moll, I., Blasi, U., & Kaberdin, V. R. (2005). Both RNase E and RNase III control the stability of sodB mRNA upon translational inhibition by the small regulatory RNA RyhB. *Nucleic Acids Res, 33*(5), 1678-1689.

Akins, R. A., & Lambowitz, A. M. (1987). A protein required for splicing group I introns in Neurospora mitochondria is mitochondrial tyrosyl-tRNA synthetase or a derivative thereof. *Cell, 50*(3), 331-345.

Ameres, S. L., Martinez, J., & Schroeder, R. (2007). Molecular basis for target RNA recognition and cleavage by human RISC. *Cell, 130*(1), 101-112.

Antonellis, A., & Green, E. D. (2008). The role of aminoacyl-tRNA synthetases in genetic diseases. *Annu Rev Genomics Hum Genet, 9*, 87-107.

Anziano, P. Q., Hanson, D. K., Mahler, H. R., & Perlman, P. S. (1982). Functional domains in introns: trans-acting and cis-acting regions of intron 4 of the cob gene. *Cell, 30*(3), 925-932.

Arnez, J. G., Harris, D. C., Mitschler, A., Rees, B., Francklyn, C. S., & Moras, D. (1995). Crystal structure of histidyl-tRNA synthetase from Escherichia coli complexed with histidyl-adenylate. *EMBO J, 14*(17), 4143-4155.

Arnez, J. G., & Moras, D. (1997). Structural and functional considerations of the aminoacylation reaction. *Trends Biochem Sci, 22*(6), 211-216.

Arnez, J. G., & Steitz, T. A. (1996). Crystal structures of three misacylating mutants of Escherichia coli glutaminyl-tRNA synthetase complexed with $tRNA^{Gln}$ and ATP. *Biochemistry, 35*(47), 14725-14733.

Asahara, H., Himeno, H., Tamura, K., Hasegawa, T., Watanabe, K., & Shimizu, M. (1993). Recognition nucleotides of Escherichia coli $tRNA^{Leu}$ and its elements facilitating discrimination from $tRNA^{Ser}$ and $tRNA^{Tyr}$. *J Mol Biol, 231*(2), 219-229.

Baldwin, A. N., & Berg, P. (1966). Transfer ribonucleic acid-induced hydrolysis of valyladenylate bound to isoleucyl ribonucleic acid synthetase. *J Biol Chem, 241*(4), 839-845.

Batey, R. T. (2006). Structures of regulatory elements in mRNAs. *Curr Opin Struct Biol, 16*(3), 299-306.

Bear, D. G., Ng, R., Van Derveer, D., Johnson, N. P., Thomas, G., Schleich, T., & Noller, H. F. (1976). Alteration of polynucleotide secondary structure by ribosomal protein S1. *Proc Natl Acad Sci U S A, 73*(6), 1824-1828.

Betha, A. K., Williams, A. M., & Martinis, S. A. (2007). Isolated CP1 domain of Escherichia coli leucyl-tRNA synthetase is dependent on flanking hinge motifs for amino acid editing activity. *Biochemistry, 46*(21), 6258-6267.

Beuning, P. J., & Musier-Forsyth, K. (2000). Hydrolytic editing by a class II

aminoacyl-tRNA synthetase. *Proc. Natl. Acad. Sci. U.S.A., 97*(16), 8916-8920.
Biou, V., Yaremchuk, A., Tukalo, M., & Cusack, S. (1994). The 2.9 Å crystal structure of T. thermophilus seryl-tRNA synthetase complexed with $tRNA^{Ser}$. *Science, 263*(5152), 1404-1410.
Bokinsky, G., Nivon, L. G., Liu, S., Chai, G., Hong, M., Weeks, K. M., & Zhuang, X. (2006). Two distinct binding modes of a protein cofactor with its target RNA. *J Mol Biol, 361*(4), 771-784.
Bonfils, G., Jaquenoud, M., Bontron, S., Ostrowicz, C., Ungermann, C., & De Virgilio, C. (2012). Leucyl-tRNA synthetase controls TORC1 via the EGO complex. *Mol Cell, 46*(1), 105-110.
Boniecki, M. T. (2007). *Enzymatic and splicing activity of class I leucyl-tRNA synthetases from Escherichia coli and Saccharomyces cerevisiae.* (Ph.D.), University of Illinois at Urbana-Champaign, Urbana, IL.
Boniecki, M. T., Rho, S. B., Tukalo, M., Hsu, J. L., Romero, E. P., & Martinis, S. A. (2009). Leucyl-tRNA synthetase-dependent and -independent activation of a group I intron. *J Biol Chem, 284*(39), 26243-26250.
Boniecki, M. T., Vu, M. T., Betha, A. K., & Martinis, S. A. (2008). CP1-dependent partitioning of pretransfer and posttransfer editing in leucyl-tRNA synthetase. *Proc Natl Acad Sci U S A, 105*(49), 19223-19228.
Borel, F., Vincent, C., Leberman, R., & Hartlein, M. (1994). Seryl-tRNA synthetase from Escherichia coli: implication of its N-terminal domain in aminoacylation activity and specificity. *Nucleic Acids Res, 22*(15), 2963-2969.
Brandao, M. M., & Silva-Filho, M. C. (2011). Evolutionary history of Arabidopsis thaliana aminoacyl-tRNA synthetase dual-targeted proteins. *Mol Biol Evol, 28*(1), 79-85.
Breitschopf, K., Achsel, T., Busch, K., & Gross, H. J. (1995). Identity elements of human $tRNA^{Leu}$: structural requirements for converting human $tRNA^{Ser}$ into a leucine acceptor in vitro. *Nucleic Acids Res, 23*(18), 3633-3637.
Brick, P., Bhat, T. N., & Blow, D. M. (1989). Structure of tyrosyl-tRNA synthetase refined at 2.3 Å resolution. Interaction of the enzyme with the tyrosyl adenylate intermediate. *J Mol Biol, 208*(1), 83-98.
Brick, P., & Blow, D. M. (1987). Crystal structure of a deletion mutant of a tyrosyl-tRNA synthetase complexed with tyrosine. *J Mol Biol, 194*(2), 287-297.
Brodersen, D. E., Clemons, W. M., Jr., Carter, A. P., Wimberly, B. T., & Ramakrishnan, V. (2002). Crystal structure of the 30 S ribosomal subunit from Thermus thermophilus: structure of the proteins and their interactions with 16 S RNA. *J Mol Biol, 316*(3), 725-768.
Burbaum, J. J., & Schimmel, P. (1991). Assembly of a class I tRNA synthetase from products of an artificially split gene. *Biochemistry, 30*(2), 319-324.
Burke, J. M. (1988). Molecular genetics of group I introns: RNA structures and protein factors required for splicing--a review. *Gene, 73*(2), 273-294.
Caprara, M. G., Lehnert, V., Lambowitz, A. M., & Westhof, E. (1996). A tyrosyl-tRNA synthetase recognizes a conserved tRNA-like structural motif in the group I intron catalytic core. *Cell, 87*(6), 1135-1145.

Caprara, M. G., Mohr, G., & Lambowitz, A. M. (1996). A tyrosyl-tRNA synthetase protein induces tertiary folding of the group I intron catalytic core. *J Mol Biol, 257*(3), 512-531.

Cavarelli, J., Eriani, G., Rees, B., Ruff, M., Boeglin, M., Mitschler, A., Martin, F., Gangloff, J., Thierry, J. C., & Moras, D. (1994). The active site of yeast aspartyl-tRNA synthetase: structural and functional aspects of the aminoacylation reaction. *EMBO J., 13*(2), 327-337.

Cech, T. R. (1987). The chemistry of self-splicing RNA and RNA enzymes. *Science, 236*(4808), 1532-1539.

Cech, T. R. (1988). Conserved sequences and structures of group I introns: building an active site for RNA catalysis--a review. *Gene, 73*(2), 259-271.

Cech, T. R. (1990). Self-splicing of group I introns. *Annu Rev Biochem, 59*, 543-568.

Chen, J. F., Li, T., Wang, E. D., & Wang, Y. L. (2001). Effect of alanine-293 replacement on the activity, ATP binding, and editing of Escherichia coli leucyl-tRNA synthetase. *Biochemistry, 40*(5), 1144-1149.

Chen, X., Ma, J. J., Tan, M., Yao, P., Hu, Q. H., Eriani, G., & Wang, E. D. (2011). Modular pathways for editing non-cognate amino acids by human cytoplasmic leucyl-tRNA synthetase. *Nucleic Acids Res, 39*(1), 235-247.

Cherniack, A. D., Garriga, G., Kittle, J. D., Jr., Akins, R. A., & Lambowitz, A. M. (1990). Function of Neurospora mitochondrial tyrosyl-tRNA synthetase in RNA splicing requires an idiosyncratic domain not found in other synthetases. *Cell, 62*(4), 745-755.

Clodi, E., Semrad, K., & Schroeder, R. (1999). Assaying RNA chaperone activity in vivo using a novel RNA folding trap. *EMBO J, 18*(13), 3776-3782.

Coetzee, T., Herschlag, D., & Belfort, M. (1994). Escherichia coli proteins, including ribosomal protein S12, facilitate in vitro splicing of phage T4 introns by acting as RNA chaperones. *Genes Dev, 8*(13), 1575-1588.

Cristofari, G., & Darlix, J. L. (2002). The ubiquitous nature of RNA chaperone proteins. *Prog Nucleic Acid Res Mol Biol, 72*, 223-268.

Croitoru, V., Semrad, K., Prenninger, S., Rajkowitsch, L., Vejen, M., Laursen, B. S., Sperling-Petersen, H. U., & Isaksson, L. A. (2006). RNA chaperone activity of translation initiation factor IF1. *Biochimie, 88*(12), 1875-1882.

Cusack, S. (1995). Eleven down and nine to go. *Nature Structural Biology, 2*(10), 824-831.

Cusack, S., Berthet-Colominas, C., Hartlein, M., Nassar, N., & Leberman, R. (1990). A second class of synthetase structure revealed by X-ray analysis of Escherichia coli seryl-tRNA synthetase at 2.5 Å. *Nature, 347*(6290), 249-255.

Cusack, S., Yaremchuk, A., & Tukalo, M. (2000). The 2 Å crystal structure of leucyl-tRNA synthetase and its complex with a leucyl-adenylate analogue. *EMBO J., 19*(10), 2351-2361.

Davies, R. W., Waring, R. B., Ray, J. A., Brown, T. A., & Scazzocchio, C. (1982). Making ends meet: a model for RNA splicing in fungal mitochondria. *Nature, 300*(5894), 719-724.

Davila-Aponte, J. A., Huss, V. A., Sogin, M. L., & Cech, T. R. (1991). A self-splicing

group I intron in the nuclear pre-rRNA of the green alga, Ankistrodesmus stipitatus. *Nucleic Acids Res, 19*(16), 4429-4436.

De La Salle, H., Jacq, C., & Slonimski, P. P. (1982). Critical sequences within mitochondrial introns: pleiotropic mRNA maturase and cis-dominant signals of the box intron controlling reductase and oxidase. *Cell, 28*(4), 721-732.

Dhawale, S., Hanson, D. K., Alexander, N. J., Perlman, P. S., & Mahler, H. R. (1981). Regulatory interactions between mitochondrial genes: interactions between two mosaic genes. *Proc Natl Acad Sci U S A, 78*(3), 1778-1782.

Du, X., & Wang, E. D. (2002). Discrimination of tRNA(Leu) isoacceptors by the mutants of Escherichia coli leucyl-tRNA synthetase in editing. *Biochemistry, 41*(34), 10623-10628.

Du, X., & Wang, E. D. (2003). E292 is important for the aminoacylation activity of Escherichia coli leucyl-tRNA synthetase. *J Protein Chem, 22*(1), 71-76.

Dujardin, G., Pajot, P., Groudinsky, O., & Slonimski, P. P. (1980). Long range control circuits within mitochondria and between nucleus and mitochondria. I. Methodology and phenomenology of suppressors. *Mol Gen Genet, 179*(3), 469-482.

Eriani, G., Delarue, M., Poch, O., Gangloff, J., & Moras, D. (1990). Partition of tRNA synthetases into two classes based on mutually exclusive sets of sequence motifs. *Nature, 347*(6289), 203-206.

Francklyn, C., & Schimmel, P. (1989). Aminoacylation of RNA minihelices with alanine. *Nature, 337*(6206), 478-481.

Fukai, S., Nureki, O., Sekine, S., Shimada, A., Tao, J., Vassylyev, D. G., & Yokoyama, S. (2000). Structural basis for double-sieve discrimination of L-valine from L-isoleucine and L-threonine by the complex of $tRNA^{Val}$ and valyl-tRNA synthetase. *Cell, 103*(5), 793-803.

Fukunaga, R., Ishitani, R., Nureki, O., & Yokoyama, S. (2005). Crystallization of leucyl-tRNA synthetase complexed with tRNALeu from the archaeon Pyrococcus horikoshii. *Acta Crystallogr Sect F Struct Biol Cryst Commun, 61*(Pt 1), 30-32.

Fukunaga, R., & Yokoyama, S. (2005). Crystal structure of leucyl-tRNA synthetase from the archaeon *Pyrococcus horikoshii* reveals a novel editing domain orientation. *J. Mol. Biol., 346*(1), 57-71.

Fukunaga, R., & Yokoyama, S. (2006). Structural basis for substrate recognition by the editing domain of isoleucyl-tRNA synthetase. *J Mol Biol, 359*(4), 901-912.

Gampel, A., Nishikimi, M., & Tzagoloff, A. (1989). CBP2 protein promotes in vitro excision of a yeast mitochondrial group I intron. *Mol Cell Biol, 9*(12), 5424-5433.

Giege, R., Sissler, M., & Florentz, C. (1998). Universal rules and idiosyncratic features in tRNA identity. *Nucleic Acids Res, 26*(22), 5017-5035.

Golden, B. L., Kim, H., & Chase, E. (2005). Crystal structure of a phage Twort group I ribozyme-product complex. *Nat Struct Mol Biol, 12*(1), 82-89.

Goldgur, Y., Mosyak, L., Reshetnikova, L., Ankilova, V., Lavrik, O., Khodyreva, S., & Safro, M. (1997). The crystal structure of phenylalanyl-tRNA synthetase

from thermus thermophilus complexed with cognate tRNAPhe. *Structure, 5*(1), 59-68.

Gruic-Sovulj, I., Rokov-Plavec, J., & Weygand-Durasevic, I. (2007). Hydrolysis of non-cognate aminoacyl-adenylates by a class II aminoacyl-tRNA synthetase lacking an editing domain. *FEBS Lett, 581*(26), 5110-5114.

Guo, F., Gooding, A. R., & Cech, T. R. (2004). Structure of the Tetrahymena ribozyme: base triple sandwich and metal ion at the active site. *Mol Cell, 16*(3), 351-362.

Guo, M., Schimmel, P., & Yang, X. L. (2010). Functional expansion of human tRNA synthetases achieved by structural inventions. *FEBS Lett, 584*(2), 434-442.

Guo, Q., & Lambowitz, A. M. (1992). A tyrosyl-tRNA synthetase binds specifically to the group I intron catalytic core. *Genes Dev, 6*(8), 1357-1372.

Halls, C., Mohr, S., Del Campo, M., Yang, Q., Jankowsky, E., & Lambowitz, A. M. (2007). Involvement of DEAD-box proteins in group I and group II intron splicing. Biochemical characterization of Mss116p, ATP hydrolysis-dependent and -independent mechanisms, and general RNA chaperone activity. *J Mol Biol, 365*(3), 835-855.

Han, J. M., Jeong, S. J., Park, M. C., Kim, G., Kwon, N. H., Kim, H. K., Ha, S. H., Ryu, S. H., & Kim, S. (2012). Leucyl-tRNA synthetase is an intracellular leucine sensor for the mTORC1-signaling pathway. *Cell, 149*(2), 410-424.

Henke, R. M. (2000). *Molecular and biochemical studies on a bifunctional group I intron encoded protein of yeast mitochondria.* University of Texas Southwestern Medical Center at Dallas.

Henke, R. M., Butow, R. A., & Perlman, P. S. (1995). Maturase and endonuclease functions depend on separate conserved domains of the bifunctional protein encoded by the group I intron aI4 alpha of yeast mitochondrial DNA. *EMBO J, 14*(20), 5094-5099.

Henn, A., Cao, W., Licciardello, N., Heitkamp, S. E., Hackney, D. D., & De La Cruz, E. M. (2010). Pathway of ATP utilization and duplex rRNA unwinding by the DEAD-box helicase, DbpA. *Proc Natl Acad Sci U S A, 107*(9), 4046-4050.

Herbert, C. J., Labouesse, M., Dujardin, G., & Slonimski, P. P. (1988). The NAM2 proteins from S. cerevisiae and S. douglasii are mitochondrial leucyl-tRNA synthetases, and are involved in mRNA splicing. *EMBO J, 7*(2), 473-483.

Herschlag, D. (1995). RNA chaperones and the RNA folding problem. *J Biol Chem, 270*(36), 20871-20874.

Herschlag, D., Khosla, M., Tsuchihashi, Z., & Karpel, R. L. (1994). An RNA chaperone activity of non-specific RNA binding proteins in hammerhead ribozyme catalysis. *EMBO J, 13*(12), 2913-2924.

Hitti, E., Neunteufl, A., & Jantsch, M. F. (1998). The double-stranded RNA-binding protein X1rbpa promotes RNA strand annealing. *Nucleic Acids Res, 26*(19), 4382-4388.

Hou, Y. M., Shiba, K., Mottes, C., & Schimmel, P. (1991). Sequence determination and modeling of structural motifs for the smallest monomeric aminoacyl-tRNA synthetase. *Proc. Natl. Acad. Sci. U.S.A., 88*(3), 976-980.

Houman, F., Rho, S. B., Zhang, J., Shen, X., Wang, C. C., Schimmel, P., & Martinis, S. A. (2000). A prokaryote and human tRNA synthetase provide an essential RNA splicing function in yeast mitochondria. *Proc Natl Acad Sci U S A, 97*(25), 13743-13748.

Hountondji, C., Dessen, P., & Blanquet, S. (1986). Sequence similarities among the family of aminoacyl-tRNA synthetases. *Biochimie, 68*(9), 1071-1078.

Hsu, J. L. (2006). *Characterization of leucyl-tRNA synthetase from Escherichia coli and Saccharomyces cerevisiae in aminoacylation, amino Acid editing, and protein-dependent RNA splicing.* (Ph.D.), University of Illinois at Urbana-Champaign, Urbana, IL.

Hsu, J. L., Rho, S. B., Vannella, K. M., & Martinis, S. A. (2006). Functional divergence of a unique C-terminal domain of leucyl-tRNA synthetase to accommodate its splicing and aminoacylation roles. *J Biol Chem, 281*(32), 23075-23082.

Ibba, M., Morgan, S., Curnow, A. W., Pridmore, D. R., Vothknecht, U. C., Gardner, W., Lin, W., Woese, C. R., & Soll, D. (1997). A euryarchaeal lysyl-tRNA synthetase: resemblance to class I synthetases. *Science, 278*(5340), 1119-1122.

Ibba, M., & Söll, D. (2000). Aminoacyl-tRNA synthesis. *Annu. Rev. Biochem., 69*, 617-650.

Ilyin, V. A., Temple, B., Hu, M., Li, G., Yin, Y., Vachette, P., & Carter, C. W., Jr. (2000). 2.9 Å crystal structure of ligand-free tryptophanyl-tRNA synthetase: domain movements fragment the adenine nucleotide binding site. *Protein Sci, 9*(2), 218-231.

Irimia, M., & Roy, S. W. (2014). Origin of spliceosomal introns and alternative splicing. *Cold Spring Harb Perspect Biol, 6*(6).

Irwin, M. J., Nyborg, J., Reid, B. R., & Blow, D. M. (1976). The crystal structure of tyrosyl-transfer RNA synthetase at 2-7 A resolution. *J Mol Biol, 105*(4), 577-586.

Jaeger, L., Michel, F., & Westhof, E. (1994). Involvement of a GNRA tetraloop in long-range RNA tertiary interactions. *J Mol Biol, 236*(5), 1271-1276.

Jaeger, L., Westhof, E., & Michel, F. (1991). Function of P11, a tertiary base pairing in self-splicing introns of subgroup IA. *J Mol Biol, 221*(4), 1153-1164.

Jankowsky, E., & Fairman, M. E. (2007). RNA helicases--one fold for many functions. *Curr Opin Struct Biol, 17*(3), 316-324.

Jarmoskaite, I., & Russell, R. (2014). RNA helicase proteins as chaperones and remodelers. *Annu Rev Biochem, 83*, 697-725.

Karkhanis, V. A., Boniecki, M. T., Poruri, K., & Martinis, S. A. (2006). A viable amino acid editing activity in the leucyl-tRNA synthetase CP1-splicing domain is not required in the yeast mitochondria. *Journal of Biological Chemistry, 281*(44), 33217-33225.

Kawamoto, H., Koide, Y., Morita, T., & Aiba, H. (2006). Base-pairing requirement for RNA silencing by a bacterial small RNA and acceleration of duplex formation by Hfq. *Mol Microbiol, 61*(4), 1013-1022.

Konovalova, S., & Tyynismaa, H. (2013). Mitochondrial aminoacyl-tRNA synthetases

in human disease. *Mol Genet Metab, 108*(4), 206-211.
Labouesse, M. (1990). The yeast mitochondrial leucyl-tRNA synthetase is a splicing factor for the excision of several group I introns. *Mol Gen Genet, 224*(2), 209-221.
Labouesse, M., Dujardin, G., & Slonimski, P. P. (1985). The yeast nuclear gene NAM2 is essential for mitochondrial DNA integrity and can cure a mitochondrial RNA-maturase deficiency. *Cell, 41*(1), 133-143.
Labouesse, M., Herbert, C. J., Dujardin, G., & Slonimski, P. P. (1987). Three suppressor mutations which cure a mitochondrial RNA maturase deficiency occur at the same codon in the open reading frame of the nuclear NAM2 gene. *EMBO J, 6*(3), 713-721.
Lambowitz, A. M., Caprara, M. G., Zimmerly, S., & Perlman, P. S. (1999). Group I and group II ribozymes as RNPs: Clues to the past and guides to the future. In R. F. Gesteland, T. Cech, & J. F. Atkins (Eds.), *The RNA world the nature of modern RNA suggests a prebiotic RNA* (2nd ed., pp. 451-485). Cold Spring Harbor, N.Y.: Cold Spring Harbor Laboratory Press,.
Lambowitz, A. M., & Perlman, P. S. (1990). Involvement of aminoacyl-tRNA synthetases and other proteins in group I and group II intron splicing. *Trends Biochem Sci, 15*(11), 440-444.
Landes, C., Perona, J. J., Brunie, S., Rould, M. A., Zelwer, C., Steitz, T. A., & Risler, J. L. (1995). A structure-based multiple sequence alignment of all class I aminoacyl-tRNA synthetases. *Biochimie, 77*(3), 194-203.
LaRiviere, F. J., Wolfson, A. D., & Uhlenbeck, O. C. (2001). Uniform binding of aminoacyl-tRNAs to elongation factor Tu by thermodynamic compensation. *Science, 294*(5540), 165-168.
Larkin, D. C., Williams, A. M., Martinis, S. A., & Fox, G. E. (2002). Identification of essential domains for Escherichia coli $tRNA^{Leu}$ aminoacylation and amino acid editing using minimalist RNA molecules. *Nucleic Acids Res, 30*(10), 2103-2113.
Lazowska, J., Jacq, C., & Slonimski, P. P. (1980). Sequence of introns and flanking exons in wild-type and box3 mutants of cytochrome b reveals an interlaced splicing protein coded by an intron. *Cell, 22*(2 Pt 2), 333-348.
Lee, K. W., & Briggs, J. M. (2004). Molecular modeling study of the editing active site of Escherichia coli leucyl-tRNA synthetase: two amino acid binding sites in the editing domain. *Proteins, 54*(4), 693-704.
Leveque, F., Plateau, P., Dessen, P., & Blanquet, S. (1990). Homology of lysS and lysU, the two Escherichia coli genes encoding distinct lysyl-tRNA synthetase species. *Nucleic Acids Res, 18*(2), 305-312.
Li, G. Y., Becam, A. M., Slonimski, P. P., & Herbert, C. J. (1996). In vitro mutagenesis of the mitochondrial leucyl tRNA synthetase of Saccharomyces cerevisiae shows that the suppressor activity of the mutant proteins is related to the splicing function of the wild-type protein. *Mol Gen Genet, 252*(6), 667-675.
Li, L., Boniecki, M. T., Jaffe, J. D., Imai, B. S., Yau, P. M., Luthey-Schulten, Z. A., &

Martinis, S. A. (2011). Naturally occurring aminoacyl-tRNA synthetases editing-domain mutations that cause mistranslation in Mycoplasma parasites. *Proc Natl Acad Sci U S A, 108*(23), 9378-9383.

Li, T., Guo, N., Xia, X., Wang, E. D., & Wang, Y. L. (1999). The peptide bond between E292-A293 of Escherichia coli leucyl-tRNA synthetase is essential for its activity. *Biochemistry, 38*(40), 13063-13069.

Lincecum, T. L., Tukalo, M., Yaremchuk, A., Mursinna, R. S., Williams, A. M., Sproat, B. S., Van Den Eynde, W., Link, A., Van Calenbergh, S., Grotli, M., Martinis, S. A., & Cusack, S. (2003). Structural and mechanistic basis of pre- and posttransfer editing by leucyl-tRNA synthetase. *Mol. Cell, 11*(4), 951-963.

Lue, S. W., & Kelley, S. O. (2007). A single residue in leucyl-tRNA synthetase affecting amino acid specificity and tRNA aminoacylation. *Biochemistry, 46*(15), 4466-4472.

Müller, U. F., Lambert, L., & Göringer, H. U. (2001). Annealing of RNA editing substrates facilitated by guide RNA-binding protein gBP21. *EMBO J, 20*(6), 1394-1404.

Majumder, A. L., Akins, R. A., Wilkinson, J. G., Kelley, R. L., Snook, A. J., & Lambowitz, A. M. (1989). Involvement of tyrosyl-tRNA synthetase in splicing of group I introns in Neurospora crassa mitochondria: biochemical and immunochemical analyses of splicing activity. *Mol Cell Biol, 9*(5), 2089-2104.

Martinis, S. A., & Boniecki, M. T. (2010). The balance between pre- and post-transfer editing in tRNA synthetases. *FEBS Lett., 584*(2), 455-459.

Martinis, S. A., Plateau, P., Cavarelli, J., & Florentz, C. (1999). Aminoacyl-tRNA synthetases: a family of expanding functions. Mittelwihr, France, October 10-15, 1999. *EMBO J, 18*(17), 4591-4596.

Martinis, S. A., & Schimmel, P. (1996). In F. C. Neidhardt (Ed.), *Escherichia coli and Salmonella Cellular Molecular Biology* (2nd ed., pp. 887-901). Washington D. C.: ASM Press.

Mascarenhas, A. P., An, S., Rosen, A. E., Martinis, S. A., & Musier-Forsyth, K. (2009). Fidelity mechanisms of the aminoacyl-tRNA synthetases *Protein Engineering* (pp. 155-203). Berlin Heidelberg: Springer-Verlag.

Mascarenhas, A. P., Martinis, S. A., An, S., Rosen, A. E., & Musier-Forsyth, K. (2008). Fidelity mechanisms of the aminoacyl-tRNA synthetases. In U. L. Rajbhandary & C. Koehrer (Eds.), *Protein engineering*.

Mayer, O., Rajkowitsch, L., Lorenz, C., Konrat, R., & Schroeder, R. (2007). RNA chaperone activity and RNA-binding properties of the E. coli protein StpA. *Nucleic Acids Res, 35*(4), 1257-1269.

Mayer, R. J. (1995). Symposium: cell stress genes and the nervous system. *Neuropathol Appl Neurobiol, 21*(6), 472-473.

Mercer, T. R., Dinger, M. E., & Mattick, J. S. (2009). Long non-coding RNAs: insights into functions. *Nat Rev Genet, 10*(3), 155-159.

Michel, F., Jaeger, L., Westhof, E., Kuras, R., Tihy, F., Xu, M. Q., & Shub, D. A. (1992). Activation of the catalytic core of a group I intron by a remote 3' splice junction. *Genes Dev, 6*(8), 1373-1385.

Michel, F., & Westhof, E. (1990). Modelling of the three-dimensional architecture of group I catalytic introns based on comparative sequence analysis. *J Mol Biol, 216*(3), 585-610.

Milligan, J. F., Groebe, D. R., Witherell, G. W., & Uhlenbeck, O. C. (1987). Oligoribonucleotide synthesis using T7 RNA polymerase and synthetic DNA templates. *Nucleic Acids Res, 15*(21), 8783-8798.

Minajigi, A., & Francklyn, C. S. (2010). Aminoacyl transfer rate dictates choice of editing pathway in threonyl-tRNA synthetase. *J Biol Chem, 285*(31), 23810-23817.

Mohr, G., Caprara, M. G., Guo, Q., & Lambowitz, A. M. (1994). A tyrosyl-tRNA synthetase can function similarly to an RNA structure in the Tetrahymena ribozyme. *Nature, 370*(6485), 147-150.

Mohr, G., Zhang, A., Gianelos, J. A., Belfort, M., & Lambowitz, A. M. (1992). The neurospora CYT-18 protein suppresses defects in the phage T4 td intron by stabilizing the catalytically active structure of the intron core. *Cell, 69*(3), 483-494.

Mohr, S., Matsuura, M., Perlman, P. S., & Lambowitz, A. M. (2006). A DEAD-box protein alone promotes group II intron splicing and reverse splicing by acting as an RNA chaperone. *Proc Natl Acad Sci U S A, 103*(10), 3569-3574.

Mohr, S., Stryker, J. M., & Lambowitz, A. M. (2002). A DEAD-box protein functions as an ATP-dependent RNA chaperone in group I intron splicing. *Cell, 109*(6), 769-779.

Moller, T., Franch, T., Hojrup, P., Keene, D. R., Bachinger, H. P., Brennan, R. G., & Valentin-Hansen, P. (2002). Hfq: a bacterial Sm-like protein that mediates RNA-RNA interaction. *Mol Cell, 9*(1), 23-30.

Muller, U. F., & Goringer, H. U. (2002). Mechanism of the gBP21-mediated RNA/RNA annealing reaction: matchmaking and charge reduction. *Nucleic Acids Res, 30*(2), 447-455.

Muller, U. F., Lambert, L., & Goringer, H. U. (2001). Annealing of RNA editing substrates facilitated by guide RNA-binding protein gBP21. *EMBO J, 20*(6), 1394-1404.

Munroe, S. H., & Dong, X. F. (1992). Heterogeneous nuclear ribonucleoprotein A1 catalyzes RNA.RNA annealing. *Proc Natl Acad Sci U S A, 89*(3), 895-899.

Murphy, F. L., & Cech, T. R. (1994). GAAA tetraloop and conserved bulge stabilize tertiary structure of a group I intron domain. *J Mol Biol, 236*(1), 49-63.

Mursinna, R. S., Lee, K. W., Briggs, J. M., & Martinis, S. A. (2004). Molecular dissection of a critical specificity determinant within the amino acid editing domain of leucyl-tRNA synthetase. *Biochemistry, 43*(1), 155-165.

Mursinna, R. S., Lincecum, T. L., Jr., & Martinis, S. A. (2001). A conserved threonine within *Escherichia coli* leucyl-tRNA synthetase prevents hydrolytic editing of leucyl-tRNA^{Leu}. *Biochemistry, 40*(18), 5376-5381.

Mursinna, R. S., & Martinis, S. A. (2002). Rational design to block amino acid editing of a tRNA synthetase. *J. Am. Chem. Soc., 124*(25), 7286-7287.

Myers, C. A., Kuhla, B., Cusack, S., & Lambowitz, A. M. (2002). tRNA-like

recognition of group I introns by a tyrosyl-tRNA synthetase. *Proc Natl Acad Sci U S A, 99*(5), 2630-2635.

Myers, C. A., Wallweber, G. J., Rennard, R., Kemel, Y., Caprara, M. G., Mohr, G., & Lambowitz, A. M. (1996). A tyrosyl-tRNA synthetase suppresses structural defects in the two major helical domains of the group I intron catalytic core. *J Mol Biol, 262*(2), 87-104.

Nakama, T., Nureki, O., & Yokoyama, S. (2001). Structural basis for the recognition of isoleucyl-adenylate and an antibiotic, mupirocin, by isoleucyl-tRNA synthetase. *J Biol Chem, 276*(50), 47387-47393.

Nawaz, M. H., Pang, Y. L., & Martinis, S. A. (2007). Molecular and functional dissection of a putative RNA-binding region in yeast mitochondrial leucyl-tRNA synthetase. *J Mol Biol, 367*(2), 384-394.

Nomanbhoy, T. K., Hendrickson, T. L., & Schimmel, P. (1999). Transfer RNA-dependent translocation of misactivated amino acids to prevent errors in protein synthesis. *Mol Cell, 4*(4), 519-528.

O'Donoghue, P., Sethi, A., Woese, C. R., & Luthey-Schulten, Z. A. (2005). The evolutionary history of Cys-tRNACys formation. *Proc Natl Acad Sci U S A, 102*(52), 19003-19008.

Ogle, J. M., Murphy, F. V., Tarry, M. J., & Ramakrishnan, V. (2002). Selection of tRNA by the ribosome requires a transition from an open to a closed form. *Cell, 111*(5), 721-732.

Palencia, A., Crepin, T., Vu, M. T., Lincecum, T. L., Jr., Martinis, S. A., & Cusack, S. (2012). Structural dynamics of the aminoacylation and proofreading functional cycle of bacterial leucyl-tRNA synthetase. *Nat Struct Mol Biol, 19*(7), 677-684.

Pang, Y. L., Poruri, K., & Martinis, S. A. (2014). tRNA synthetase: tRNA aminoacylation and beyond. *Wiley Interdiscip Rev RNA, 5*(4), 461-480.

Patzel, V., & Sczakiel, G. (1999). Length dependence of RNA-RNA annealing. *J Mol Biol, 294*(5), 1127-1134.

Paukstelis, P. J., Chen, J. H., Chase, E., Lambowitz, A. M., & Golden, B. L. (2008). Structure of a tyrosyl-tRNA synthetase splicing factor bound to a group I intron RNA. *Nature, 451*(7174), 94-97.

Paukstelis, P. J., & Lambowitz, A. M. (2008). Identification and evolution of fungal mitochondrial tyrosyl-tRNA synthetases with group I intron splicing activity. *Proc Natl Acad Sci U S A, 105*(16), 6010-6015.

Perona, J. J., Rould, M. A., & Steitz, T. A. (1993). Structural basis for transfer RNA aminoacylation by *Escherichia coli* glutaminyl-tRNA synthetase. *Biochemistry, 32*(34), 8758-8771.

Phadtare, S., Inouye, M., & Severinov, K. (2002). The nucleic acid melting activity of Escherichia coli CspE is critical for transcription antitermination and cold acclimation of cells. *J Biol Chem, 277*(9), 7239-7245.

Polycarpo, C., Ambrogelly, A., Berube, A., Winbush, S. M., McCloskey, J. A., Crain, P. F., Wood, J. L., & Soll, D. (2004). An aminoacyl-tRNA synthetase that specifically activates pyrrolysine. *Proc Natl Acad Sci U S A, 101*(34), 12450-

12454.
Pontius, B. W., & Berg, P. (1992). Rapid assembly and disassembly of complementary DNA strands through an equilibrium intermediate state mediated by A1 hnRNP protein. *J Biol Chem, 267*(20), 13815-13818.
Poruri, K. (2007). *Understanding primary and alternate functions of leucyl-tRNA synthetases from Escherichia coli, Saccharomyces cerevisiae and Mycobacterium tuberculosis.* (Ph.D.), University of Houston, Houston, TX.
Putney, S. D., & Schimmel, P. (1981). An aminoacyl tRNA synthetase binds to a specific DNA sequence and regulates its gene transcription. *Nature, 291*(5817), 632-635.
Rajkowitsch, L., Chen, D., Stampfl, S., Semrad, K., Waldsich, C., Mayer, O., Jantsch, M. F., Konrat, R., Blasi, U., & Schroeder, R. (2007). RNA chaperones, RNA annealers and RNA helicases. *RNA Biol, 4*(3), 118-130.
Rajkowitsch, L., & Schroeder, R. (2007a). Coupling RNA annealing and strand displacement: a FRET-based microplate reader assay for RNA chaperone activity. *Biotechniques, 43*(3), 304, 306, 308 passim.
Rajkowitsch, L., & Schroeder, R. (2007b). Dissecting RNA chaperone activity. *RNA, 13*(12), 2053-2060.
Rho, S. B., Lincecum, T. L., Jr., & Martinis, S. A. (2002). An inserted region of leucyl-tRNA synthetase plays a critical role in group I intron splicing. *EMBO J, 21*(24), 6874-6881.
Rho, S. B., & Martinis, S. A. (2000). The bI4 group I intron binds directly to both its protein splicing partners, a tRNA synthetase and maturase, to facilitate RNA splicing activity. *RNA, 6*(12), 1882-1894.
Ribas de Pouplana, L., & Schimmel, P. (2001a). Aminoacyl-tRNA synthetases: potential markers of genetic code development. *Trends Biochem Sci, 26*(10), 591-596.
Ribas de Pouplana, L., & Schimmel, P. (2001b). Two classes of tRNA synthetases suggested by sterically compatible dockings on tRNA acceptor stem. *Cell, 104*(2), 191-193.
Riesner, D., Henco, K., Rokohl, U., Klotz, G., Kleinschmidt, A. K., Domdey, H., Jank, P., Gross, H. J., & Sanger, H. L. (1979). Structure and structure formation of viroids. *J Mol Biol, 133*(1), 85-115.
Rock, F. L., Mao, W., Yaremchuk, A., Tukalo, M., Crepin, T., Zhou, H., Zhang, Y. K., Hernandez, V., Akama, T., Baker, S. J., Plattner, J. J., Shapiro, L., Martinis, S. A., Benkovic, S. J., Cusack, S., & Alley, M. R. (2007). An antifungal agent inhibits an aminoacyl-tRNA synthetase by trapping tRNA in the editing site. *Science, 316*(5832), 1759-1761.
Romby, P., Caillet, J., Ebel, C., Sacerdot, C., Graffe, M., Eyermann, F., Brunel, C., Moine, H., Ehresmann, C., Ehresmann, B., & Springer, M. (1996). The expression of E. coli threonyl-tRNA synthetase is regulated at the translational level by symmetrical operator-repressor interactions. *EMBO J., 15*(21), 5976-5987.
Rossmann, M. G., Moras, D., & Olsen, K. W. (1974). Chemical and biological

evolution of nucleotide-binding protein. *Nature, 250*(463), 194-199.
Rould, M. A., Perona, J. J., Soll, D., & Steitz, T. A. (1989). Structure of E. coli glutaminyl-tRNA synthetase complexed with tRNA(Gln) and ATP at 2.8 Å resolution. *Science, 246*(4934), 1135-1142.
Ruff, M., Krishnaswamy, S., Boeglin, M., Poterszman, A., Mitschler, A., Podjarny, A., Rees, B., Thierry, J. C., & Moras, D. (1991). Class II aminoacyl transfer RNA synthetases: crystal structure of yeast aspartyl-tRNA synthetase complexed with tRNA(Asp). *Science, 252*(5013), 1682-1689.
Russell, R., & Herschlag, D. (2001). Probing the folding landscape of the Tetrahymena ribozyme: commitment to form the native conformation is late in the folding pathway. *J Mol Biol, 308*(5), 839-851.
Sajish, M., Zhou, Q., Kishi, S., Valdez, D. M., Jr., Kapoor, M., Guo, M., Lee, S., Kim, S., Yang, X. L., & Schimmel, P. (2012). Trp-tRNA synthetase bridges DNA-PKcs to PARP-1 to link IFN-gamma and p53 signaling. *Nat Chem Biol, 8*(6), 547-554.
Sampson, J. R., & Uhlenbeck, O. C. (1988). Biochemical and physical characterization of an unmodified yeast phenylalanine transfer RNA transcribed in vitro. *Proc Natl Acad Sci U S A, 85*(4), 1033-1037.
Sankaranarayanan, R., Dock-Bregeon, A. C., Romby, P., Caillet, J., Springer, M., Rees, B., Ehresmann, C., Ehresmann, B., & Moras, D. (1999). The structure of threonyl-tRNA synthetase-tRNA^{Thr} complex enlightens its repressor activity and reveals an essential zinc ion in the active site. *Cell, 97*(3), 371-381.
Sarkar, J., Mao, W., Lincecum, T. L., Jr., Alley, M. R., & Martinis, S. A. (2011). Characterization of benzoxaborole-based antifungal resistance mutations demonstrates that editing depends on electrostatic stabilization of the leucyl-tRNA synthetase editing cap. *FEBS Lett., 585*(19), 2986-2991.
Sarkar, J., & Martinis, S. A. (2011). Amino-acid-dependent shift in tRNA synthetase editing mechanisms. *J. Am. Chem. Soc., 133*(46), 18510-18513.
Sarkar, J., Poruri, K., Boniecki, M. T., McTavish, K. K., & Martinis, S. A. (2012). Yeast mitochondrial leucyl-tRNA synthetase CP1 domain has functionally diverged to accommodate RNA splicing at expense of hydrolytic editing. *J Biol Chem, 287*(18), 14772-14781.
Schimmel, P. (1987). Aminoacyl tRNA synthetases: general scheme of structure-function relationships in the polypeptides and recognition of transfer RNAs. *Annu Rev Biochem, 56*, 125-158.
Schmitt, E., Meinnel, T., Blanquet, S., & Mechulam, Y. (1994). Methionyl-tRNA synthetase needs an intact and mobile 332KMSKS336 motif in catalysis of methionyl adenylate formation. *J Mol Biol, 242*(4), 566-576.
Schroeder, R., Barta, A., & Semrad, K. (2004). Strategies for RNA folding and assembly. *Nat Rev Mol Cell Biol, 5*(11), 908-919.
Schumacher, M. A., Pearson, R. F., Moller, T., Valentin-Hansen, P., & Brennan, R. G. (2002). Structures of the pleiotropic translational regulator Hfq and an Hfq-RNA complex: a bacterial Sm-like protein. *EMBO J, 21*(13), 3546-3556.
Seiradake, E., Mao, W., Hernandez, V., Baker, S. J., Plattner, J. J., Alley, M. R. K., &

Cusack, S. (2009). Crystal structures of the human and fungal cytosolic leucyl-tRNA synthetase editing domains: A structural basis for the rational design of antifungal benzoxaboroles. *J. Mol. Biol., 390*(2), 196-207.

Semrad, K., Green, R., & Schroeder, R. (2004). RNA chaperone activity of large ribosomal subunit proteins from Escherichia coli. *RNA, 10*(12), 1855-1860.

Seraphin, B., Boulet, A., Simon, M., & Faye, G. (1987). Construction of a yeast strain devoid of mitochondrial introns and its use to screen nuclear genes involved in mitochondrial splicing. *Proc Natl Acad Sci U S A, 84*(19), 6810-6814.

Silvian, L. F., Wang, J., & Steitz, T. A. (1999). Insights into editing from an Ile-tRNA synthetase structure with tRNAile and mupirocin. *Science, 285*(5430), 1074-1077.

Singh, R. N., Saldanha, R. J., D'Souza, L. M., & Lambowitz, A. M. (2002). Binding of a group II intron-encoded reverse transcriptase/maturase to its high affinity intron RNA binding site involves sequence-specific recognition and autoregulates translation. *J Mol Biol, 318*(2), 287-303.

Slonimski, P. P., Claisse, M., M., F., Jacq, C., Kochko, A., Lamouroux, A., Pajot, P., Perrodin, G., Spyridakis, A., & WambierKluppel, M. L. (1978). Mosaic organization and expression of the mitochondrial DNA region controlling cytochrome c reductase and oxidase. Ill. A model of structure and function. In M. Bacila, B. L. Horecker, A. O. M. Stoppani, & Academia Brasileira de Ciências. (Eds.), *Biochemistry and genetics of yeasts pure and applied aspects : proceedings of the symposium held at the Universidade de São Paulo, Brazil, December 4-10, 1977* (pp. 1 online resource (xx, 594 pages)). New York: Academic Press,.

Solem, A., Zingler, N., & Pyle, A. M. (2006). A DEAD protein that activates intron self-splicing without unwinding RNA. *Mol Cell, 24*(4), 611-617.

Soma, A., Kumagai, R., Nishikawa, K., & Himeno, H. (1996). The anticodon loop is a major identity determinant of Saccharomyces cerevisiae $tRNA^{Leu}$. *J Mol Biol, 263*(5), 707-714.

Splan, K. E., Ignatov, M. E., & Musier-Forsyth, K. (2008). Transfer RNA modulates the editing mechanism used by class II prolyl-tRNA synthetase. *J Biol Chem, 283*(11), 7128-7134.

Sprinzl, M., & Cramer, F. (1975). Site of aminoacylation of tRNAs from Escherichia coli with respect to the 2'- or 3'-hydroxyl group of the terminal adenosine. *Proc Natl Acad Sci U S A, 72*(8), 3049-3053.

Starzyk, R. M., Webster, T. A., & Schimmel, P. (1987). Evidence for dispensable sequences inserted into a nucleotide fold. *Science, 237*(4822), 1614-1618.

Strathem, J. N. (1982). *The Molecular Biology of the Yeast Saccharomyces: Metabolism and Gene Expression*. Plainview, NY: Cold Spring Harbor Lab. Press.

Subramanian, A. R. (1983). Structure and functions of ribosomal protein S1. *Prog Nucleic Acid Res Mol Biol, 28*, 101-142.

Sugino, A., & Gietz, R. D. (1988). New yeast-*Escherichia coli* shuttle vectors constructed with *in vitro* mutagenized yeast genes lacking six-base pair

restriction sites. *Gene, 74*, 527-534.
Sukhodolets, M. V., & Garges, S. (2003). Interaction of Escherichia coli RNA polymerase with the ribosomal protein S1 and the Sm-like ATPase Hfq. *Biochemistry, 42*(26), 8022-8034.
Szostak, W. B., & Sekula, W. (1991). Nutritional implications of political and economic changes in eastern Europe. *Proc Nutr Soc, 50*(3), 687-693.
Talkington, M. W., Siuzdak, G., & Williamson, J. R. (2005). An assembly landscape for the 30S ribosomal subunit. *Nature, 438*(7068), 628-632.
Tanner, N. K., & Cech, T. R. (1985). Self-catalyzed cyclization of the intervening sequence RNA of Tetrahymena: inhibition by intercalating dyes. *Nucleic Acids Res, 13*(21), 7741-7758.
Thomas, M., White, R. L., & Davis, R. W. (1976). Hybridization of RNA to double-stranded DNA: formation of R-loops. *Proc Natl Acad Sci U S A, 73*(7), 2294-2298.
Tijerina, P., Bhaskaran, H., & Russell, R. (2006). Nonspecific binding to structured RNA and preferential unwinding of an exposed helix by the CYT-19 protein, a DEAD-box RNA chaperone. *Proc Natl Acad Sci U S A, 103*(45), 16698-16703.
Tinoco, I., Jr., & Bustamante, C. (1999). How RNA folds. *J Mol Biol, 293*(2), 271-281.
Tukalo, M., Yaremchuk, A., Fukunaga, R., Yokoyama, S., & Cusack, S. (2005). The crystal structure of leucyl-tRNA synthetase complexed with $tRNA^{Leu}$ in the post-transfer-editing conformation. *Nat Struct Mol Biol, 12*(10), 923-930.
Wakasugi, K., & Schimmel, P. (1999). Two distinct cytokines released from a human aminoacyl-tRNA synthetase. *Science, 284*(5411), 147-151.
Wakasugi, K., Slike, B. M., Hood, J., Otani, A., Ewalt, K. L., Friedlander, M., Cheresh, D. A., & Schimmel, P. (2002). A human aminoacyl-tRNA synthetase as a regulator of angiogenesis. *Proc. Natl. Acad. Sci. U.S.A., 99*(1), 173-177.
Waldsich, C., Grossberger, R., & Schroeder, R. (2002). RNA chaperone StpA loosens interactions of the tertiary structure in the td group I intron in vivo. *Genes Dev, 16*(17), 2300-2312.
Walstrum, S. A., & Uhlenbeck, O. C. (1990). The self-splicing RNA of Tetrahymena is trapped in a less active conformation by gel purification. *Biochemistry, 29*(46), 10573-10576.
Webb, A. K., Jones, A. W., & Dodd, M. E. (2001). Transition from paediatric to adult care: problems that arise in the adult cystic fibrosis clinic. *J R Soc Med, 94 Suppl 40*, 8-11.
Webster, T., Tsai, H., Kula, M., Mackie, G. A., & Schimmel, P. (1984). Specific sequence homology and three-dimensional structure of an aminoacyl transfer RNA synthetase. *Science, 226*(4680), 1315-1317.
Weeks, K. M. (1997). Protein-facilitated RNA folding. *Curr Opin Struct Biol, 7*(3), 336-342.
Williams, A. M., & Martinis, S. A. (2006). Mutational unmasking of a tRNA-dependent pathway for preventing genetic code ambiguity. *Proc. Natl. Acad.*

Sci. U.S.A., 103(10), 3586-3591.

Wong, F. C., Beuning, P. J., Nagan, M., Shiba, K., & Musier-Forsyth, K. (2002). Functional role of the prokaryotic proline-tRNA synthetase insertion domain in amino acid editing. *Biochemistry, 41*(22), 7108-7115.

Xu, X., Shi, Y., Zhang, H. M., Swindell, E. C., Marshall, A. G., Guo, M., Kishi, S., & Yang, X. L. (2012). Unique domain appended to vertebrate tRNA synthetase is essential for vascular development. *Nat Commun, 3*, 681.

Yang, Q., & Jankowsky, E. (2005). ATP- and ADP-dependent modulation of RNA unwinding and strand annealing activities by the DEAD-box protein DED1. *Biochemistry, 44*(41), 13591-13601.

Yaremchuk, A., Cusack, S., & Tukalo, M. (2000). Crystal structure of a eukaryote/archaeon-like protyl-tRNA synthetase and its complex with $tRNA^{Pro}$(CGG). *EMBO J, 19*(17), 4745-4758.

Yaremchuk, M. J. (2005). Making concave faces convex. *Aesthetic Plast Surg, 29*(3), 141-147; discussion 148.

You, J. C., & McHenry, C. S. (1994). Human immunodeficiency virus nucleocapsid protein accelerates strand transfer of the terminally redundant sequences involved in reverse transcription. *J Biol Chem, 269*(50), 31491-31495.

Zaher, H. S., & Green, R. (2009). Quality control by the ribosome following peptide bond formation. *Nature, 457*(7226), 161-166.

Zaug, A. J., Grabowski, P. J., & Cech, T. R. (1983). Autocatalytic cyclization of an excised intervening sequence RNA is a cleavage-ligation reaction. *Nature, 301*(5901), 578-583.

Zhang, A., Wassarman, K. M., Ortega, J., Steven, A. C., & Storz, G. (2002). The Sm-like Hfq protein increases OxyS RNA interaction with target mRNAs. *Mol Cell, 9*(1), 11-22.

Zhao, Z., Hashiguchi, A., Hu, J., Sakiyama, Y., Okamoto, Y., Tokunaga, S., Zhu, L., Shen, H., & Takashima, H. (2012). Alanyl-tRNA synthetase mutation in a family with dominant distal hereditary motor neuropathy. *Neurology, 78*(21), 1644-1649.

Zheng, Y. G., Wei, H., Ling, C., Martin, F., Eriani, G., & Wang, E. D. (2004). Two distinct domains of the beta subunit of Aquifex aeolicus leucyl-tRNA synthetase are involved in tRNA binding as revealed by a three-hybrid selection. *Nucleic Acids Res, 32*(11), 3294-3303.

Zhou, Q., Kapoor, M., Guo, M., Belani, R., Xu, X., Kiosses, W. B., Hanan, M., Park, C., Armour, E., Do, M. H., Nangle, L. A., Schimmel, P., & Yang, X. L. (2010). Orthogonal use of a human tRNA synthetase active site to achieve multifunctionality. *Nat Struct Mol Biol, 17*(1), 57-61.

Appendix. Plasmid constructs

Plasmid name	**Parent vector**	**Description**
p14ZL-*ym*LeuRS-Q273A	p14MB-*ym*LeuRS-WT	Gln273 mutated to Ala
p14ZL-*ym*LeuRS-Q273R	p14MB-*ym*LeuRS-WT	Gln273 mutated to Arg
p14ZL-*ym*LeuRS-L277A	p14MB-*ym*LeuRS-WT	Leu277 mutated to Ala
pGP1-2-*Ec*tRNA^{Leu}-VL	pGP1-2	Replace *ym*tRNA^{Leu} variable arm with *Ec*tRNA^{Leu} variable arm
pGFIB-I-*ym*tRNA^{Leu}-VL	pGFIB-I	Replace *Ec*tRNA^{Leu} variable arm with *ym*tRNA^{Leu} variable arm